

To my parents and my wife, Wakana

Studies of The Structure of Cytochrome P450 4A1

by Ming Qi Fan, BSc, MSc

Thesis submitted to the University of Nottingham
for the degree of Doctor of Philosophy

September 2002

Table of Contents

1	INTRODUCTION.....	13
1.1	General background of Cytochrome P450.....	13
1.1.1	Function of cytochrome P450.....	14
1.1.2	Catalytic reaction of cytochrome P450.....	16
1.1.3	Redox partners of cytochrome P450.....	19
1.2	The CYP 4 family.....	20
1.2.1	CYP4A.....	20
1.2.2	CYP4B.....	24
1.2.3	CYP4F.....	25
1.3	Heterologous expression of cytochrome P450.....	26
1.3.1	Mammalian expression system.....	27
1.3.2	Yeast expression system.....	28
1.3.3	Insect cell expression system.....	29
1.3.4	Bacterial expression system.....	30
1.4	Structure and function of cytochrome P450.....	33
1.4.1	The structure of CYP102.....	34
1.4.2	Structure-function relationships of CYP4 family.....	38
1.4.3	Interaction between cytochromes P450 and redox partners.....	40
1.5	Aims of the thesis.....	42
2	MATERIALS AND METHODS	43
2.1	Materials.....	43
2.2	General Methods.....	46
2.2.1	Bacterial culture.....	46
2.2.2	Phenol: chloroform: isoamyl alcohol (25:24:1) extraction of DNA ..	46
2.2.3	Ethanol precipitation of nucleic acids.....	46
2.2.4	Isolation of plasmid DNA.....	47
2.2.4.1	Alkaline lysis method.....	47
2.2.4.2	Qiagen mini-preparation.....	48
2.2.4.3	Qiagen maxi-preparation.....	49
2.2.4.4	Wizard maxi-preparation.....	50
2.2.5	Restriction enzyme digest of plasmid DNA.....	51
2.2.6	Agarose gel electrophoresis.....	51
2.2.7	Photography methods.....	52
2.2.8	Purification of DNA from an agarose gel.....	52
2.2.8.1	GeneClean system.....	52
2.2.8.2	QIAquick gel extraction kit.....	53
2.2.9	Phosphatase treatment of DNA.....	53
2.2.10	Transformation of the plasmid.....	54
2.2.10.1	Preparation of calcium chloride competent cells.....	54
2.2.10.2	Transformation.....	54
2.3	Protein Methodologies.....	55
2.3.1	Bradford protein assay.....	55
2.3.2	SDS-polyacrylamide gel electrophoresis (SDS-PAGE).....	55

2.3.3	Western blotting	57
2.3.4	Nickel affinity chromatography	58
2.3.4.1	His•Bind resins	58
2.3.4.2	Ni-NTA His•Bind Resins	58
2.3.5	Protein Desalting by size exclusive PD-10 columns	59
2.4	Expression of cytochrome b5	59
2.4.1	Spectrophotometric measurement	59
2.4.2	Expression of cytochrome b5	60
2.4.2.1	Transformation and preparation of plasmids	60
2.4.2.2	Optimising expression of cytochrome b5	60
2.4.2.3	The preparation of cytochrome b5 by large-scale culture	61
2.5	Expression of human cytochrome P450 Reductase (CPR)	63
2.5.1	Expression of recombinant CPR	63
2.5.2	Affinity purification of CPR	64
2.5.3	Assay method (reduction of cytochrome c)	64
2.6	Expression of CYP4A1	65
2.6.1	Spectrophotometer measurement	65
2.6.1.1	The P450 assay	65
2.6.1.2	The absolute spectrum and substrate binding difference spectrum	65
2.6.2	Expression of CYP4A1	68
2.6.2.1	Construction of the plasmid pGEM-T.OmpA.4A1.HT	68
2.6.2.2	Subcloning: Construction of pCWori ⁺ /OmpA.4A1.HT plasmid	71
2.6.2.3	Expression and purification of OmpA.CYP4A1.HT	73
2.7	Construction of mutants of CYP4A1	74
2.7.1	Site-directed mutagenesis	74
2.7.2	Subcloning K93E mutant	78
2.7.3	Subcloning F149Y and F149I mutants	81
3	RESULTS	84
3.1	Expression of cytochrome b5	84
3.1.1	Restriction enzyme analysis of pRSET cytochrome b5 sense and anti-sense plasmids	84
3.1.2	Optimising expression of cytochrome b5	86
3.1.2.1	Host strain and media	86
3.1.2.2	Induction time and concentration of IPTG	87
3.1.2.3	Induction temperature	88
3.1.2.4	Recovery of cytochrome b5	89
3.1.3	Preparation of cytochrome b5 by large-scale culture	92
3.2	Expression of recombinant human cytochrome P450 reductase (CPR)	94
3.3	Expression of CYP4A1 (OmpA.4A1.HT)	96
3.3.1	Optimising expression of OmpA.4A1.HT	100
3.3.1.1	Different host strains on expression of cytochrome P450	100
3.3.1.2	Effect of temperature and concentration of IPTG	101
3.3.1.3	Effect of δ -ALA	102
3.3.1.4	Optimal conditions of expressing OmpA.4A1.HT	103
3.3.1.5	Solubilisation of membrane-bound OmpA.4A1.HT	103
3.3.2	Comparison of the expression level of OmpA.4A1.HT and N-terminally modified CYP4A1	104

3.3.3	Expression and purification of CYP4A1 by large-scale culture	105
3.3.4	Spectral characteristics of recombinant OmpA.CYP4A1.HT.....	108
3.4	Study in structure-function relationships of CYP4A1	109
3.4.1	Substrate binding residues	109
3.4.1.1	K93	109
3.4.1.1.1	Prediction	109
3.4.1.1.2	Expression and purification of the K93E mutant.....	112
3.4.1.1.3	Substrate binding assay of K93E	113
3.4.1.2	R87	120
3.4.1.2.1	R87E and R87E/K93E mutants.....	121
3.4.1.2.2	R87W/K93E mutant.....	130
3.4.1.3	N116.....	136
3.4.2	The C-helix region in CYP4A1.....	141
3.4.2.1	H141	142
3.4.2.2	F149	146
3.4.2.3	R142 and R143.....	150
4	DISCUSSION	153
4.1	Expression of cytochrome b5.....	153
4.2	Expression of CPR.....	158
4.3	Expression of CYP4A1	159
4.4	Structure-function relationships of CYP4A1	162
4.4.1	Substrate binding sites	162
4.4.1.1	K93	162
4.4.1.2	R87	164
4.4.1.3	N116.....	167
4.4.2	The C-helix region	171
4.4.2.1	H141	171
4.4.2.2	F149	172
4.4.2.3	R142 and R143.....	173
4.5	Future direction	173
5	REFERENCES.....	175

List of Figures

Figure 1-1. Catalytic cycle for cytochrome P450 reactions (adapted from Guengerich, Hosea <i>et al.</i> 1998).	17
Figure 1-2. Structures of lauric acid and its analogos.	39
Figure 2-1. Structures of lauric acid and dodecyltrimethylammonium bromide.	66
Figure 2-2. Measurement of difference spectra of substrate binding.	67
Figure 2-3. Construction of plasmid pGEM-T.OmpA.4A1.HT.	70
Figure 2-4. Construction of pCWori ⁺ .OmpA.4A1.HT plasmid.	72
Figure 2-5. Construction of K93E mutant expression plasmid.	80
Figure 2-6. Construction of F149I mutant expression plasmid.	82
Figure 2-7. Construction of F149Y mutant expression plasmid.	83
Figure 3-1. Sequence of cytochrome b5 fusion.	85
Figure 3-2. Maps of plasmids pRSET-b b5 Sense and Anti-Sense.	85
Figure 3-3. Restriction enzyme analysis of plasmid pRSET-b5 sense and anti sense.	86
Figure 3-4. Effect of strains and media on expression of cytochrome b5.	87
Figure 3-5. Effect of time and IPTG on expression of cytochrome b5.	88
Figure 3-6. Effect of temperature on expression of cytochrome b5.	89
Figure 3-7. SDS-PAGE evaluation of the process of cytochrome b5 purification. ...	93
Figure 3-8. Difference spectrum of cytochrome b5.	94
Figure 3-9. SDS-PAGE evaluation of CPR purification process.	96
Figure 3-10. Nucleotide sequences for <i>OmpA.4A1.HT</i>	99
Figure 3-11. Comparison of construction of <i>OmpA.4A1.HT</i> and N-terminally modified CYP4A1.	100
Figure 3-12. Different host strains on expression of P450.	101
Figure 3-13. Effect of temperature and IPTG on expression of P450.	102
Figure 3-14. Effect of δ -ALA on expression of cytochrome P450.	103
Figure 3-15. Expression level of <i>OmpA.4A1.HT</i> and modified CYP4A1 (n=3). ...	105
Figure 3-16. Purification of <i>OmpA.4A1.HT</i>	106
Figure 3-17. PAGE of <i>OmpA.4A1.HT</i> during purification.	107
Figure 3-18. Western analysis of recombinant CYP4A1.	108
Figure 3-19. The spectrum of <i>OmpA.4A1.HT</i>	109
Figure 3-20. Alignment of CYP4As and CYPBM3.	110
Figure 3-21. Homologous model of CYP4A1.	112
Figure 3-22. DNA Sequence of K93E mutant and deduced amino acids.	112
Figure 3-23. The purified K93E mutant protein.	113
Figure 3-24. Interaction of lauric acid and CYP4A1.	115
Figure 3-25. Interaction of lauric acid and K93E.	116
Figure 3-26. Interaction of dodecyltrimethylammonium bromide and CYP4A1. ...	118
Figure 3-27. Interaction of dodecyltrimethylammonium bromide and K93E.	119
Figure 3-28. R87 and K93 in CYP4A1 model.	120
Figure 3-29. DNA sequences of R87E/K93E and R87E mutants and deduced amino acids.	121
Figure 3-30. Purified R87E, R87E/K93E and R87W/K93E mutants protein.	122

Figure 3-31. The difference spectra of (A) R87E and (B) R87E/K93E mutants.	123
Figure 3-32. Interaction of lauric acid and R87E.....	125
Figure 3-33. Interaction of lauric acid and R87E/K93E mutant.....	126
Figure 3-34. Interaction of dodecyltrimethylammonium bromide and R87E.....	127
Figure 3-35. Interaction of dodecyltrimethylammonium bromide and R87E/K93E.	129
Figure 3-36. DNA Sequence of R87W/K93E and deduced amino acids.	130
Figure 3-37. The CO-difference spectrum of R87W/K93E.....	131
Figure 3-38. Interaction of lauric acid and R87W/K93E.....	132
Figure 3-39. Interaction of dodecyltrimethylammonium bromide and R87W/K93E.	134
Figure 3-40. Alignment of CYP4A proteins.....	137
Figure 3-41. The position of N116 in CYP4A1 model.....	137
Figure 3-42. DNA sequence of N116E and N116E/K93E and deduced amino acids.	138
Figure 3-43. The purified N116E mutant protein.	139
Figure 3-44. Interaction of N116E and lauric acid.	140
Figure 3-45. Interaction of N116E and dodecyltrimethylammonium bromide.	141
Figure 3-46. Alignment of the C-helix region in CYP4 proteins.....	142
Figure 3-47. The position of H141 in the model of CYP4A1.....	143
Figure 3-48. DNA sequences of H141R, H141L and H141F and deduced amino acids.....	144
Figure 3-49. The purified H141R, H141F and H141L proteins.	144
Figure 3-50. The CO-difference spectrum of purified H141R mutant.	145
Figure 3-51. The CO-difference spectrum of purified H141F.....	145
Figure 3-52. The CO-difference spectrum of purified H141L.....	146
Figure 3-53. The F149 residue in the model of CYP4A1.....	147
Figure 3-54. DNA Sequences of F149Y and F149I and deduced amino acids.	147
Figure 3-55. The purified F149I and F149Y protein.	148
Figure 3-56. The CO-difference spectrum of F149Y.....	149
Figure 3-57. The CO-difference spectrum of F149I.....	150
Figure 3-58. The position of R142 and R143 in CYP4A1 model.....	151
Figure 3-59. DNA Sequences of R142A and R143A and deduced amino acids.....	151
Figure 3-60. The R143A mutant protein.....	152
Figure 4-1. Y95 residue in CYP4A1 model.....	170
Figure 4-2. Alignment of CYP4As protein sequence.	171
Figure 4-3. Alignment of 4A1 with 2B4 and 2B1.	173

List of Tables

Table 1-1. CYP4A subfamily.....	21
Table 1-2. Activity of ω -hydroxylation in Rat, Rabbit and Human CYP4A forms ..	24
Table 1-3. CYP4F subfamily and its substrate profile.....	26
Table 2-1. The component of separating gel (50ml).....	56
Table 2-2. The components of buffer for purifying cytochrome b5	62
Table 2-3. Substrates dissolved in solvents	66
Table 2-4. The components of buffer of purification by His•Bind resin	74
Table 2-5. The components of buffer of purification by Ni-NTA His•Bind resin.....	74
Table 2-6. Templates for mutants	75
Table 2-7. Denaturation of the plasmids	75
Table 2-8. The hybridisation reaction	76
Table 2-9. The oligonucleotides for mutagenesis	77
Table 2-10. The synthesis reaction of mutants.....	77
Table 3-1. Recovering membrane-bound cytochrome b5 from cells.....	90
Table 3-2. Recovering membrane-bound cytochrome b5 from cells.....	91
Table 3-3. The isolation and purification of cytochrome b5.....	92
Table 3-4. Improvement of recovery of cytochrome b5 purification.....	93
Table 3-5. Purification of cytochrome P450 reductase.....	94
Table 3-6. Effect of detergent on recovery of membrane-bound OmpA.4A1.HT...	104
Table 3-7. Extraction and Purification of OmpA.4A1.HT.	105
Table 3-8. Binding of substrate to CYP4A1 and K93E.....	120
Table 3-9. Binding of substrate to R87E, R87E/K93E and R87W/K93E.	135
Table 3-10. Binding of substrate to N116E and CYP4A1.....	139
Table 4-1. Expression of cytochrome b5 in the different systems.....	155

Abstract

Cytochrome P450 4A1 (CYP4A1) is involved in ω -hydroxylation of fatty acids and eicosanoids. The resulting metabolites may have physiological activities such as regulation of blood pressure.

In order to identify structural determinants of substrate binding, site-directed mutagenesis was used. According to a model of CYP4A1, the residues K93, R87 and N116 were predicted to respond to substrate binding. To test the hypothesis, we designed a series of mutants, K93E, R87E, R87E/K93E, R87W/K93E, N116E and N116E/K93E, which would change the substrate specificity of CYP4A1 from a fatty acid to a fatty amine ω -hydroxylase.

To reconstitute CYP4A1 activity *in vitro*, cytochrome b5 and cytochrome P450 reductase were expressed in *E.coli* and purified. Recombinant CYP4A1 and mutants were expressed in *E.coli* with an OmpA signal peptide. The conditions of expression were optimised; the enzyme was purified by Ni²⁺-chelate affinity chromatography. Under optimal conditions, the expression level of CYP4A1 was approximately 60-100nmol/l; mutants were expressed at various levels. The purified enzymes were used in a spectral substrate-binding assay. The K93E mutation did not induce a major change in the substrate specificity from fatty acid to amine; however, K93E showed weak binding to dodecyltrimethylammonium bromide and the K_s (Spectral dissociation constant) value for binding lauric acid increased about three times. R87E mutants had low affinity for lauric acid, but did not show increased affinity for dodecyltrimethylammonium bromide. N116E is similar to wild type CYP4A1 in substrate affinity and specificity. N116/K93E could not be examined owing to the low expression level. These results suggest that K93 is not the principle residue for

substrate binding but could be involved in transient contact with substrate; that R87 is crucial for keeping the substrate binding but might not directly contribute to binding of substrate and that N116 does not contribute directly to substrate contact.

The residues, H141, R142, R143 and F149, which are located in the conserved C-helix in CYP4A1, were also investigated. We hypothesised that H141 and F149 bind to conserved residues in the I-helix. R142 and R143 may be involved in contacts with electron donors of CYP. Seven mutants including H141R, H141F, H141L, R142A, R143A, F149I and F149Y were constructed. All mutants were expressed and purified as for CYP4A1. R142A was expressed in low level and not further purified. F149I yielded proteins of the expected size, but these proteins did not support a 450nm peak in a reduced CO-difference spectrum, demonstrating an improperly folded enzyme. The enzyme activity of other mutants for lauric acid metabolism is variable; preliminary data showed that the H141L, H141F, R143A and F149Y had very poor enzyme activity, whereas the H141R retained enzyme activity. The results suggest that certain C-helix: I-helix contacts are not required for correct folding of the haem-environment, but are required for function of the P450 enzyme.

Acknowledgements

I would like to acknowledge my supervisor Dr. David R. Bell for his scientific guidance, great enthusiasm, patience and encouragement throughout my PhD studies. I especially appreciate that he has shown me the importance of having critical views in science in many ways. This has been and will be extremely influential in all my scientific work.

My special thanks go to Dr. Neill J. Horley, who has always been kind, generous and made lab works more enjoyable with his great sense of humour. I sincerely appreciate his great deal of help during my first year study, which was the hardest time in my three years. For improving the level of my writing and all DNA sequencing works, I would like to express my sincere thanks to Mrs Ingrid Davies Gibbs, who also kindly agreed to be one of witnesses at our wedding.

I also wish to thank all past and present members in David's group, including Dr. Simon Tomlison, Dr. Munium Choudhury who kindly helped me to find an accommodation, Dr. Brett Jefferies, Sunny (I realise how quiet our labs become after he left), Dr. Chris Mee, Paul Clarke, Dr. Helen Sims, Tao Jiang and our technician Declan who helped me to order all "weird stuffs". The British drinking customs that they showed me is also very appreciated.

I am also very grateful to my parents who have given me the opportunity to study for my Ph.D in the U.K. Finally, my thanks go to my wife Wakana, who has lightened the road and always been there for me when I felt depressed, lonely and frustrated during my studies. This thesis is dedicated to my parents and my wife.

Abbreviations

4A1	Cytochrome P450 4A1
A	Adenine
AA	Arachidonic Acid
AhR	Arylhydrocarbon receptor
ALA	δ -Amino Levulinic Acid
AMP	Adenosine monophosphate
Amp	Ampicillin
APS	Ammonium Persulphate
ATP	Adenosine triphosphate
b5	Cytochrome b5
BSA	Bovine Serum Albumin
bp	base pair
C	Cytosine
Chl	Chloramphenicol
CPR	Cytochrome P450 Reductase
CYP	Cytochrome P450
DNA	Deoxyribonucleic acid
cDNA	Complementary DNA
DMSO	Dimethyl sulphoxide
DTT	Dithiothreitol
EDTA	Ethylene diamine tetra acetic acid (disodium salt)
EET	Epoxyeicosatetraenoic acid

ER	Endoplasmic Reticulum
FAD	Flavin Adenine Dinucleotide
FMN	Flavin Mononucleotide
G	Guanine
HETE	Hydroxyeicosatetraenoic acid
HT	Histidine Tag
IPTG	Isopropyl- β -D-thiogalactopyranoside
kb	kilobase
kDa	kiloDalton
Ks	Spectral dissociation constant
LB	Luria-Bertani broth
LPH	Latrophilin
LTB	Leukotriene
Ni ²⁺ -NTA	Nickel-nitriloacetic acid
OmpA	OmpA leader peptide
OmpA.4A1.HT	CYP4A1 with OmpA leader peptide at N-terminus and Histidine Tag at C-terminus
P450	Cytochrome P450
PA	Palmitoleic Acid
PAH	Polycyclic aromatic hydrocarbon
PAGE	Polyacrylamide Gel Electrophoresis
PB	Phenobarbital
PBS	Phosphate buffered saline
PCR	Polymerase Chain Reaction

PG	Prostaglandin
PMSF	Phenylmethylsulfonylfluoride
RNA	Ribonucleic acid
mRNA	Messenger RNA
SDS	Sodium Dodecyl Sulphate
SRS	Substrate Recognition Sites
T	Thymine
TAE	Tris-Glacial acetic acid-EDTA buffer
TB	Terrific Broth
TBE	Tris-Boric acid-EDTA buffer
TBS	Tris-buffered saline
TTBS	Tween-TBS
TEMED	N, N, N', N', -tetramethylethylenediamine
Tet	Tetracyclin
TTP	Thymidine triphosphate
UHP	Ultra High Purity

1 Introduction

1.1 General background of Cytochrome P450

The cytochromes P450 (CYPs, P450s) are a superfamily of heme-containing proteins, which produce a unique spectral absorption peak at approximately 450nm after the protein is reduced and reacted with carbon monoxide. This optical characteristic is unusual because most other hemoproteins do not show a similar spectral band. For example, the ferrous-CO complex of myoglobin has a maximum absorption at 423nm (Ortiz de Montellano 1997). Owing to this spectral property, this family of proteins is called cytochrome P-450 (R.Lemberg 1973).

Cytochrome P450 proteins usually contain approximate five hundred amino acids with heme as the prosthetic group (Estabrook 1999). The iron in the heme uses a thiol-group from the cysteine of the protein as the fifth ligand; the other four ligands are from the porphyrin group of heme (Guengerich 1991; Estabrook 1999). Most other hemoproteins have nitrogen from histidine as the ligand (Ortiz de Montellano 1997; Estabrook 1999). Hence, when carbon monoxide binds to the opposite side of thiolate ligand coordinated heme-iron, this Fe^{2+} -CO complex of cytochrome P450 shows a distinctive absorbance band at near 450nm (Ortiz de Montellano 1997). This unique spectrum was also used for measurement of P450 content (Omura and Sato 1964b; Ortiz de Montellano 1997). However, this thiol-ligand is easily destroyed so that the non-functional form (P420) (Omura and Sato 1964a; Omura 1999), whose carbon monoxide-binding compound has an optical absorption peak at 420nm, can be detected. Therefore, the spectral character of maximal absorption at 450nm is necessary for cytochrome P450 activity (Ortiz de Montellano 1997).

Cytochrome P450 was first found as a new kind of pigment in rat liver microsome in 1958 (R.Lemberg 1973; Estabrook 1999). Currently, around 1,000 *CYP* genes have been identified (Estabrook 1999), which are widely present in prokaryotes and eukaryotes. A great variety of cytochromes P450 from bacteria, fungi, plants, insects and animals have been reported (Nelson 1999). Cytochrome P450 is normally bound to a membrane except for some soluble bacterial P450s. Most eukaryotic cytochrome P450s are associated with the endoplasmic reticulum (ER) and are known as microsomal P450; but some P450s are located in mitochondria or mitochondrial P450. Cytochrome P450 can be classified into two types on the basis of the redox partner: Class I, including mitochondrial P450s and some bacterial P450s, use flavoprotein that contains FAD and an iron-sulfur protein as electron transporters. Class II, including microsomal P450s, require the flavoprotein that contains both FAD and FMN for their function (Estabrook 1999).

A nomenclature of cytochrome P450 based on evolution has been widely adopted (Nebert and Nelson 1991). Those P450 proteins that share at least 40% identity belong to the same family, designated by an Arabic number; a letter represents the subfamily, which shares more than 55% identity; and the individual gene is indicated by numbers (Nebert and Nelson 1991; Coon *et al.* 1992). 265 families have now been identified, of which 18 families and 43 subfamilies are from mammals (<http://drnelson.utmem.edu/famcount.html>).

1.1.1 Function of cytochrome P450

The function of P450 has been intensely studied. The typical function of P450 is monooxygenation activity but other atypical functions such as dehydration, isomerization and dehydrogenation have been found (Mansuy 1998).

As a monooxygenase, P450s have two main functions:

1) Metabolism of exogenous compounds

Cytochromes P450 can introduce a polar group, such as hydroxyl, into hydrophobic chemicals, which makes these chemicals more hydrophilic and easier to be excreted or metabolised by other enzymes (Smith *et al.* 1998). In human beings, three CYP families including CYP1, CYP2 and CYP3 are principally involved in the metabolism of “foreign chemicals” (Smith *et al.* 1998). These CYPs play an important role in the metabolism of drugs (Parikh *et al.* 1997; Smith *et al.* 1998; Murray 1999). For example, CYP2D6, 2C19 and 3A4, can metabolise a wide range of clinical drugs (Hasler 1999; van der Weide and Steijns 1999). Therefore, the activity, induction and inhibition of these CYPs controls the elimination rate of drugs and as a result, the therapeutic response, side effects and drug-drug interaction are often related to these CYPs (Farrell 1999; van der Weide and Steijns 1999). Furthermore, it was found that an individual’s response to specific medicines is due to the polymorphism of several *CYP* genes (Hasler 1999; van der Weide and Steijns 1999). *CYP1A1*, *1A2*, *2A6*, *2C9*, *2C19*, *2D6* and *2E1* have already been identified to be polymorphic (Hasler 1999; van der Weide and Steijns 1999). The different alleles of these genes result in higher, lower or even non-functional enzyme activity (van der Weide and Steijns 1999). Thus, “poor metabolisers”, who produce the lower activity drug-metabolising P450 such as CYP2D6, possibly have more risk of the side effect caused by the high concentration of drug (van der Weide and Steijns 1999). By contrast, “extensive metabolisers”, who have high activity drug-metabolising P450, may fail to be treated by the medicine (van der Weide and Steijns 1999). Therefore, studying these CYPs may change our diagnosis methods and lead

us to find new medicine (Boitier and Beaune 1999; Gelboin *et al.* 1999; van der Weide and Steijns 1999).

Human CYPs are also associated with producing carcinogens. The polycyclic aromatic hydrocarbons (PAHs), which are strong carcinogens, can be bioactivated by some members in the CYP1 family such as CYP1A1, 1A2 and 1B1 (Guengerich 1991; Kaminsky and Spivack 1999; Omura 1999). Therefore, these CYPs may provide a novel target enzyme against cancer.

Some insects use CYPs to resist xenobiotics. The relationship between insecticide resistance and P450s has been examined (Scott 1999).

2) Biosynthesis and biotransformation of endogenous chemicals

The role of CYPs in the steroid hormone biosynthesis has been elucidated (Omura 1999; Pikuleva and Waterman 1999). In the synthesis path of cholesterol, one key step is catalysed by the CYP belonging to CYP51 family (Pikuleva and Waterman 1999). Moreover, the production of bile from cholesterol also depends on several CYPs (Pikuleva and Waterman 1999). In insects and plants, CYPs are involved in the biosynthesis of certain hormones (Stegeman and Livingstone 1998). The CYP4 family metabolise fatty acids and arachidonic acid (AA) in mammals (Capdevila *et al.* 1999). The metabolism products are possibly responsible for the regulation of vessel pressure (Capdevila *et al.* 2000; Harder *et al.* 2000; Capdevila and Falck 2001; Holla *et al.* 2001). Therefore, cytochrome P450 also plays an important role in physiological functions.

1.1.2 Catalytic reaction of cytochrome P450

A scheme for the catalytic cycle of cytochrome P450 has been proposed (Guengerich *et al.* 1991; Guengerich and Johnson 1997; Ortiz de Montellano 1997; Guengerich *et*

al. 1998; Mansuy 1998). There are nine steps in the reaction cycle as shown in Figure 1-1. Substrate binding is the first step. The P450-substrate complex then receives the first electron from cytochrome P450 reductase. The Fe^{3+} in the heme is reduced. The reduced P450- Fe^{2+} intermediate binds to O_2 , and then receives the second electron from cytochrome b5. The substrate is oxidised by P450 iron-oxo intermediate. One oxygen atom is transferred to the substrate; another oxygen atom forms H_2O molecule. The oxidised substrate is released from cytochrome P450 and the iron in P450 returns to Fe^{3+} form. Although this catalytic cycle is generally accepted, details of some steps are still poorly understood because some intermediates have a lifespan too short to be detected (Mansuy 1998).

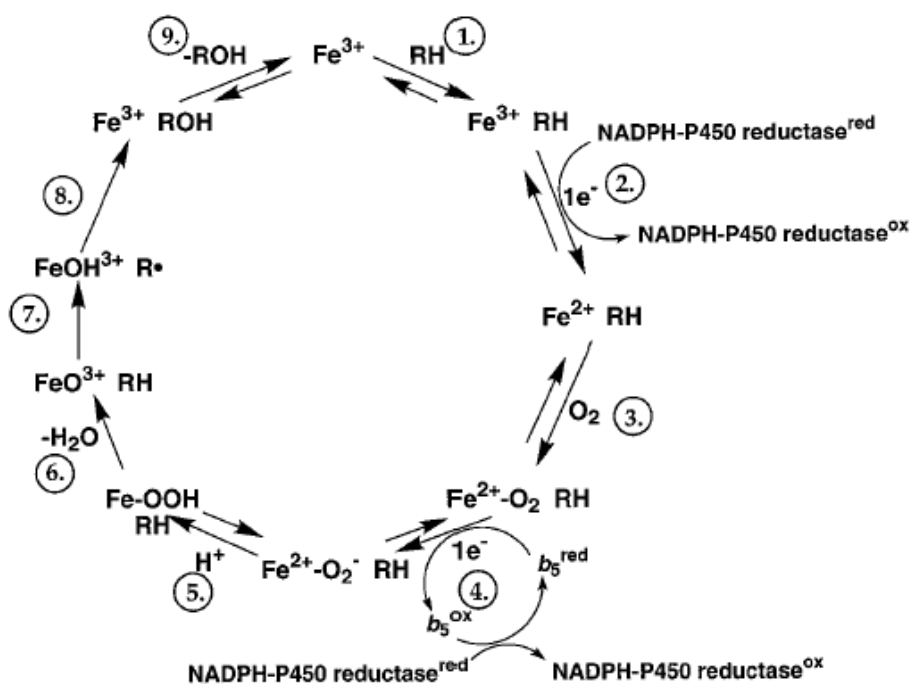


Figure 1-1. Catalytic cycle for cytochrome P450 reactions (adapted from Guengerich, Hosea *et al.* 1998).

Nine steps in cytochrome P450 catalytic reactions are shown by numbers. Fe^{3+} = oxidised cytochrome P450, Fe^{2+} = reduced cytochrome P450, b5= cytochrome b5, RH=substrate, ROH=product, and e^- = electron.

Substrate binding is well studied among these steps. The spin state of iron in the heme is different in the absence and presence of substrate (Jefcoate 1978; Ortiz de

Montellano 1997). Without substrate, the ferric in a heme group has six ligands, nitrogen atoms of porphyrin provide four ligands, cysteine from cytochrome P450 is the fifth ligand and water molecule binds to iron as the sixth ligand (Ortiz de Montellano 1997). This state is called low spin state. After substrate binding to cytochrome P450, the substrate replaces water and as a result, the ferric state changes from hexacoordination to pentacoordination (Ortiz de Montellano 1997). This state is called high spin state.

Spectroscopy can be used to detect a change of the spin state of the haem iron. The change from low spin state to high spin state results in the blue shift of maximal absorption in the optical spectrum (Jefcoate 1978; Ortiz de Montellano 1997); therefore, the difference spectrum can be used to monitor the process of substrate binding. Difference spectra are categorised by three types (Jefcoate 1978; Ortiz de Montellano 1997). Type I difference spectrum, which shows a peak at approximate 385-390nm and a trough at approximate about 420nm. Type II difference spectrum, which shows the maximal absorption at 425-435nm and the minimum at 390-405nm. Finally, Reverse Type I difference spectrum, which is opposite to Type I spectrum, has an absorption peak at approximate 420nm and trough at approximate 388-390nm. Type I difference spectrum is caused by change from low spin to high spin of cytochrome P450 (Jefcoate 1978). However, some substrates such as amine compounds produce Type II spectrum. It has been proposed that this is because the nitrogen from these compounds is coordinating with ferric heme (Jefcoate 1978). In contrast to Type I spectrum, change of low spin to high spin results in a reverse Type I spectrum.

In summary, owing to the large number and various function of cytochrome P450, this superfamily plays a central role in biological world.

1.1.3 Redox partners of cytochrome P450

Cytochrome P450 requires redox partners for its function. Cytochrome P450 reductase (CPR) and cytochrome b5 are the electron donors for microsomal cytochrome P450 (Guengerich 1991).

CPR is a 78k-dalton flavoprotein containing equal molar amount of FMN and FAD (Strobel and Dignam 1978). Natural CPR in mammals is also bound to endoplasmic reticulum (Strobel and Dignam 1978), similar to cytochrome P450. CPR catalyses electron transfer from NADPH to FMN to FAD to cytochrome P450 (Shen *et al.* 1989). Heterologous expression systems, including bacteria and yeast are developed to express CPR at high level (Porter *et al.* 1987; Shen *et al.* 1989; Ohgiya *et al.* 1997). Cytochrome b5 is approximately a 17kDa hemoprotein (Schenkman and Jansson 1999). In animals, cytochrome b5 is associated with the endoplasmic reticulum. This protein comprises of two domains, a hydrophobic C-terminal tail which binds to membrane, and a heme-containing region (Holmans *et al.* 1994). It was once thought that cytochrome b5 helped cytochrome P450 receive the second electron from NADPH in the catalytic reaction of cytochrome P450 (Schenkman and Jansson 1999). However, the role of cytochrome b5 remains in question. Certain observations have shown that catalytic activity of several cytochromes P450 was stimulated by apo-cytochrome b5 without heme group, therefore providing the argument that cytochrome b5 was only a allosteric effector but not an electron donor (Yamazaki *et al.* 1996; Loughran *et al.* 2001; Yamazaki *et al.* 2001). However, it has also been demonstrated that stimulation of CYP3A4 and CYP17A activities by apo-b5 was

caused by heme transfer from P450 to apo-b5 (Gilep *et al.* 2001; Guryev *et al.* 2001). Therefore, it is necessary to further investigate the real function of cytochrome b5 in the P450 reaction cycle.

Originally, cytochrome b5 was purified from liver (Strittmatter *et al.* 1978). More recently, it has been found that recombinant cytochrome b5 can be expressed in high level *E.coli* (Holmans *et al.* 1994; Chudaev and Usanov 1997; Mulrooney and Waskell 2000), and therefore it is easy to obtain a large amount of eukaryotic cytochrome b5 from bacteria.

1.2 The CYP 4 family

The CYP 4 family is one of the oldest cytochrome P450 families, which is approximately one billion years old (Simpson 1997; Okita and Okita 2001). This family contains eighteen subfamilies (<http://drnelson.utm.edu/biblioB.html>). However, in mammals, there are only three subfamilies: CYP4A, 4B and 4F (Nelson *et al.* 1996; Simpson 1997).

1.2.1 CYP4A

Currently, 24 members belonging to CYP4A subfamily have been identified (<http://drnelson.utm.edu/famcount.html>). CYP4As are known for hydroxylation of a series of fatty acids, eicosanoids and prostaglandins (PGs) (Simpson 1997; Capdevila *et al.* 1999; Omura 1999). Furthermore, CYP4A uniquely prefers to hydroxylate the ω position of the substrate, which is not thermodynamically favourable.

Table 1-1. CYP4A subfamily

	Species	GenEMBL	References
CYP4A1	Rat	M14972 M33937 and M57718	(Hardwick <i>et al.</i> 1987; Kimura <i>et al.</i> 1989a)
CYP4A2	Rat	M33938 and M57719	(Kimura <i>et al.</i> 1989a)
CYP4A3	Rat	M33936	(Kimura <i>et al.</i> 1989b)
CYP4A4	Rabbit	J02818	(Matsubara <i>et al.</i> 1987; Palmer <i>et al.</i> 1993)
CYP4A5	Rabbit	L04758 M28655 X57209	(Johnson <i>et al.</i> 1990; Yokotani <i>et al.</i> 1991)
CYP4A6	Rabbit	M28656 L04755	(Johnson <i>et al.</i> 1990; Muerhoff <i>et al.</i> 1992)
CYP4A7	Rabbit	M28657	(Johnson <i>et al.</i> 1990)
CYP4A8	Rat	M37828	(Stromstedt <i>et al.</i> 1990)
Cyp4a10	Mouse	X71478	(Bell <i>et al.</i> 1993)
CYP4A11	Human	S67580	(Imaoka <i>et al.</i> 1993)
Cyp4a12	Mouse	X71479	(Bell <i>et al.</i> 1993)
CYP4A13	Guinea Pig	X71481	(Bell <i>et al.</i> 1993)
Cyp4a14	Mouse	Y11639-Y11642	(Heng <i>et al.</i> 1997)
CYP4A15	Koala	AF252263	(Ngo <i>et al.</i> 2000)
CYP4A16	Cat	U91789	Gebremedhin, Lange <i>et al.</i> , unpublished
CYP4A17	Hamster	No accession number	Bell, unpublished
CYP4A18	Hamster	No accession number	Bell, unpublished
CYP4A19	Hamster	No accession number	Bell, unpublished
CYP4A20*	Human	AC026935 (replaced by AL450996, from genome)	Mclay, unpublished
CYP4A21	Pig	AJ278474	(Lundell <i>et al.</i> 2001)
CYP4A22	Human	AL390073 (from genome)	Mclay, unpublished
CYP4A23	Pig	AF384031	Van Es <i>et al.</i> , unpublished
CYP4A24	Pig	AJ318096	(Lundell 2002)
CYP4A25	Pig	AJ318097	(Lundell 2002)

*Formerly named 4Z1.

Twenty-four CYP4A members are summarised in the Table 1-1. The accession numbers of CYP4A members are also shown in the table. The accession numbers of CYP4A20 and CYP4A22 are from the human genomic sequence.

The function of CYP4A *in vivo* is not well understood. CYP4A could be involved in degrading long or medium fatty acids to short chain dicarboxylic acids in hepatocytes *via* hydroxylation (Okita and Okita 2001). However, CYP4A can also metabolise long chain polyunsaturated fatty acids such as arachidonic acid *in vivo*,

and generate metabolites that have various and significant biological activities (Okita and Okita 2001).

The relationship between CYP4As and hypertension has been extensively studied. CYP4A1, 4A2 and 4A3 were able to catalyse ω and ω -1 hydroxylation of arachidonic acid (AA), and CYP4A1 was thought to be a main enzyme for the synthesis of 20-hydroxyeicosatetraenoic acid (20-HETE), a vasoconstrictor (Nguyen *et al.* 1999). Also, CYP4A2 and 4A3 showed AA 11,12-epoxidation activity, which could convert AA to epoxyeicosatrienoic acids (EETs), a potential vasodilator (Wang *et al.* 1996; Nguyen *et al.* 1999). Specific antisense oligonucleotides (ODNs) of 4A1, 4A2 and 4A3 were used to inhibit the expression of 20-HETE in Sprague-Dawley rats (Wang *et al.* 1999). The ODNs of 4A1 and 4A2 decreased the synthesis of 20-HETE, and the blood pressure of rats which received the CYP4A1 and 4A2 ODNs was reduced (Wang *et al.* 1999). In the spontaneously hypertensive rat, CYP4A1 antisense oligonucleotide reduced 20-HETE synthesis in mesenteric arterial vessels and decreased the blood pressure, but scrambled antisense ODNs had no effect (Wang *et al.* 2001). Furthermore, the mRNA level of CYP4A3 and 4A8 in spontaneous hypertensive rats was higher than that in ordinary Wistar-Kyoto rats (Kroetz *et al.* 1997).

In human beings, CYP4A11 was identified as the dominant lauric acid ω -hydroxylase in human liver (Powell *et al.* 1996), and ω -hydroxylation of AA was mainly catalysed by CYP4F2 and 4A11 in human kidney (Lasker *et al.* 2000). CYP4A11 and CYP4F2 were the major enzymes to generate 20-HETE in human liver. However, CYP4F2 was the more important form based on both kinetic

parameters and the inhibition of 20-HETE formation using antibodies of CYP4A11 and CYP4F2 (Powell *et al.* 1998).

Another important endogenous substrate of CYP4A is prostaglandin (PG), a precursor for the generation of thromboxanes (TXs) (Capdevila *et al.* 1999). CYP4A4 expressed in *E.coli* was able to metabolise PGE1 (Nishimoto *et al.* 1993); CYP4A4 expressed in COS-1 cells exhibited activity of hydroxylation of PGE1 and PGA1 (Roman *et al.* 1993). Therefore, CYP4A is possibly involved in many important physiological activities in mammals.

Although the members of CYP4A show high sequence identity, some of them have distinct substrate profiles. For example, CYP4A4 can metabolise PGs, but fails to use lauric acid as the substrate (Nishimoto *et al.* 1993; Palmer *et al.* 1993; Roman *et al.* 1993). However, CYP4A5, 4A6 and 4A7 can utilize lauric acid but PGs are poor substrates (Roman *et al.* 1993). Although 4A1, 4A2 and 4A3 can metabolise medium to long length of fatty acids, their kinetic parameters, such as K_m and V_{max} , are different (Nguyen *et al.* 1999; Hoch *et al.* 2000a; Hoch *et al.* 2000b). Recently, CYP4A21, a new member of the CYP4A subfamily in pig, was cloned. It showed a unique activity as a taurochenodeoxycholic acid 6 α -hydroxylase but it did not metabolise lauric acid, a common substrate for other CYP4As (Lundell *et al.* 2001).

Table 1-2. Activity of ω -hydroxylation in Rat, Rabbit and Human CYP4A forms

Enzyme	Lauric acid	Palmic acid	Arachidonic acid	PGE1	PGA1
CYP4A1	36 ^a (13.5 ^d)	7.5 ^d	6.3 ^a	0.6 ^d	2.5 ^d
CYP4A2	5 ^a	6 ^e	1.1 ^a	-	-
CYP4A3	8.5 ^a	ND ^e	0.7 ^a	-	-
CYP4A4	ND ^b	13 ^b	30 ^b	145 ^b	80 ^b
CYP4A5	99 ^b	7 ^b	4 ^b	ND ^b	ND ^b
CYP4A6	47 ^b	19 ^b	23 ^b	ND ^b	ND ^b
CYP4A7	250 ^b	54 ^b	114 ^b	ND ^b	29 ^b
CYP4A8	0.4 ^a	-	ND ^a	-	-
CYP4A11	14.7 ^d	0.78 ^d	ND ^d	ND ^d	ND ^d

ND=Not detected

a) (Nguyen *et al.* 1999) (nmol/min/nmol P450)

b) (Roman *et al.* 1993) (nmol/min/mg protein)

c) (Kawashima *et al.* 2000) (nmol/min/nmol P450)

d) (Hardwick 1991) (nmol/min/nmol P450)

e) (Hoch *et al.* 2000b) (min⁻¹)

CYP 4A1, as a member in 4A subfamily, has the important and unique physiological activities described above. Because CYP4A1 is from the rat, one of the most often used animal models, it is easier to study the properties of CYP4A1. Research on CYP4A1 can help us to understand other CYP4A members, such as 4A11 in humans, because of the similar activity among them (Simpson 1997; Okita and Okita 2001).

1.2.2 CYP4B

The CYP4B subfamily contains the least members (4B1) of all the CYP4 subfamilies (Nelson *et al.* 1996). CYP4B1 has been found in human (Nhamburo *et al.* 1989), mouse (Imaoka *et al.* 1995), rats and rabbits (Gasser and Philpot 1989). CYP4B1 mRNA was mainly detected in the lung (Gasser and Philpot 1989; Nhamburo *et al.* 1989). However, CYP4B1 could be induced in rabbit liver by phenobarbital (PB) (Gasser and Philpot 1989). In rat, no or little CYP4B was expressed in liver, irrespective of PB treatment (Gasser and Philpot 1989). The *Cyp4b1* gene in mouse was cloned from kidney cDNA library (Imaoka *et al.* 1995).

The real function of CYP4B *in vivo* is not well understood. In mouse, Cyp4b1 was identified as the activator of 3-methoxy-4-aminoazobenzene (3-MeO-AAB), a potent procarcinogen, and therefore the authors proposed that Cyp4b1 was the main form responsible for carcinogenesis in renal microsomes of male mice (Imaoka *et al.* 1995). CYP4B1 can also ω and ω -1 hydroxylate short-medium fatty acids, which partly overlaps with the fatty acid ω -hydroxylation activity of 4A (Fisher *et al.* 1998; Zheng *et al.* 1998).

1.2.3 CYP4F

CYP4F is a growing subfamily, currently ten members have been identified, in sea bass (Sabourault *et al.* 1999), rat and human (Nelson *et al.* 1996). CYP4F shows hydroxylation activity of a series of eicosanoids including leukotrienes (LTBs), prostaglandins (PGs), lipoxins, arachidonic acid (AA) and HETEs. (Kikuta *et al.* 1993; Kawashima *et al.* 1997; Jin *et al.* 1998; Kikuta *et al.* 1998; Christmas *et al.* 1999; Kikuta *et al.* 1999a; Kikuta *et al.* 1999b; Bylund *et al.* 2000; Bylund *et al.* 2001; Hashizume *et al.* 2001). These metabolites of CYP4Fs contribute to various biological activities. For example, metabolites of AA play an important role in blood pressure (Capdevila and Falck 2001). Moreover, LTB₄, one of most common substrates of CYP4Fs, is a known mediator of inflammation and is also associated with some important physiological activities such as chemotaxis and chemokinesis, cellular aggregation and superoxide generation (Jin *et al.* 1998). Therefore, CYP4Fs possibly play a role in inflammation and other related diseases.

Table 1-3. CYP4F subfamily and its substrate profile

	Species	Tissue	Substrates	References
CYP4F1	Rat	Liver	LTB ₄ , PGA ₁ , lipoxin A ₄ and HETEs	(Chen and Hardwick 1993; Kikuta <i>et al.</i> 1999a)
CYP4F2	Human	Liver	LTB ₄	(Jin <i>et al.</i> 1998; Powell <i>et al.</i> 1998; Kikuta <i>et al.</i> 1999b; Lasker <i>et al.</i> 2000)
CYP4F3	Human	Liver, neutrophil	LTB ₄ , lipoxin A ₄ and B ₄ , HETEs	(Kikuta <i>et al.</i> 1998; Christmas <i>et al.</i> 1999)
CYP4F4	Rat	Brain	PGA ₁ , PGE ₁ and LTB ₄	(Kawashima and Strobel 1995; Kawashima <i>et al.</i> 1997)
CYP4F5	Rat	Brain	LTB ₄	(Kawashima and Strobel 1995; Kawashima <i>et al.</i> 1997)
CYP4F6	Rat	Brain	-	(Kawashima and Strobel 1995)
CYP4F7	Sea Bass	Kidney	-	(Sabourault <i>et al.</i> 1999)
CYP4F8	Human	Seminal vesicles	AA, PGH ₁ and PGH ₂	(Bylund <i>et al.</i> 1999; Bylund <i>et al.</i> 2000)
CYP4F11	Human	Liver, kidney, heart and skeletal	-	(Cui <i>et al.</i> 2000)
CYP4F12	Human	Small intestine and liver	LTB ₄ , AA, ebastine	(Bylund <i>et al.</i> 2001; Hashizume <i>et al.</i> 2001)
	Human	Liver, kidney, colon, small intestine and heart	AA, LTB ₄ , PGH ₂ , PGE ₂ ,PGF _{2α}	

Ten CYP4F members are summarised in Table 1-3. The substrates of CYP4Fs are also described in the table. AA= Arachidonic Acid, HETE= Hydroxyeicosatetraenoic acid, LTB= Leukotriene, PG= Prostaglandin.

1.3 Heterologous expression of cytochrome P450

In order to investigate catalytic activity of cytochrome P450, it is necessary to obtain enough functional protein. However, the traditional purification from animal organs is fairly complicated and time-consuming. Moreover, it is difficult to purify a specific cytochrome P450 from other similar P450s. It is particularly problematic, if cytochrome P450 is expressed in low level. Hence, cDNA-directed heterologous

expression provides an efficient way to obtain a large amount of cytochrome P450. It is also easy to study structure-function relationships of cytochrome P450 by site-directed mutagenesis in a heterologous expression system.

Several expression systems including bacteria, yeast, insect cells and mammalian cells have been successfully developed to produce CYPs in the last twenty years (Gonzalez and Korzekwa 1995; Crespi and Miller 1999). All of the systems have advantages and disadvantages.

1.3.1 Mammalian expression system

Mammal cells offer the native environment such as phospholipid bilayer, which is required for membrane-binding of cytochrome P450. In mammalian cells, the heterologously expressed eukaryotic P450 should fold accurately to keep its function. Furthermore, mammalian cells contain endogenous redox partners, such as P450 reductase and cytochrome b5, which makes it possible to establish the catalytic activity in a single cell. Several mammalian expression systems have been established for expression of CYP. Heterologous cytochrome P450s have been expressed in COS cells (Clark and Waterman 1991), V79 chinese hamster cells (Doehmer and Oesch 1991) and human B lymphoblastoid cells (Crespi 1991). The method of using vaccinia virus to express mammalian cytochromes P450 has also been reported (Gonzalez *et al.* 1991a).

However, heterologous cytochrome P450s are expressed in relatively low level in mammalian cells because excess cytochrome P450 could disturb the growth of host mammalian cell (Crespi and Miller 1999). Another potential problem of the mammalian expression system is the endogenous cytochrome P450. It is important to

choose a mammalian cell line that has low background of endogenous P450 as the host. Proper controls are necessary.

Therefore, the mammalian expression system is ideal for mutagenicity and drug metabolism, which do not require large quantities of enzyme (Doehmer and Oesch 1991; Crespi and Miller 1999). However, this system can have difficulty in providing enough protein for spectral analysis, kinetic study and investigation of function (Clark and Waterman 1991).

1.3.2 Yeast expression system

The yeast was the first system that successfully expressed the mammalian CYP (Gonzalez and Korzekwa 1995). Yeast provides a way to express CYPs in high level with low cost (Gonzalez and Korzekwa 1995).

Special yeast expression vectors have been designed (Guengerich *et al.* 1991). In order to overcome the inefficient activity of endogenous electron donors, the redox partners can either be co-expressed with CYPs in yeast or fused with CYP cDNA (Gonzalez and Korzekwa 1995). However, co-expression and fusion expression systems are not very stable owing to the large size of foreign DNA and therefore genomically modified yeast have been developed to provide the optimal redox environment for expression of cytochrome P450 (Pompon *et al.* 1996).

The defect of this system is the endogenous P450 in yeast. It is important to prevent contamination from the endogenous yeast P450 during extraction and purification (Crespi and Miller 1999).

1.3.3 Insect cell expression system

Insect cells infected by baculovirus are currently one of the most popular systems for expressing CYPs (Crespi and Miller 1999) because of the high expression level (Gonzalez *et al.* 1991b; Lee *et al.* 1996). When expression levels of P450c17 in yeast, mammalian cells, *E.coli* and insect cells were compared, the insect cell expression system produced the most molecules of P450 per cell. The environment in insect cells is relatively closer to mammals, which benefits expression of mammalian proteins (Galleno and Stick 1999).

To express cytochrome P450 in insect cell, the cDNA was firstly cloned in a shuttle vector. The baculovirus, AcMNPV, transfected insect cell such as Sf9 or *T.ni* with the shuttle vector (Gonzalez *et al.* 1991b; Lee *et al.* 1996). The CYP cDNA was integrated into the viral DNA to generate the recombinant baculovirus because the vector and AcMNPV carried the same DNA such as polyhedrin gene promoters and p10 gene (Gonzalez *et al.* 1991b; Lee *et al.* 1996). The use of multiple viral promoters allowed the co-expression of several genes in insect cells at the same time (Lee *et al.* 1996). Therefore, redox partners including cytochrome P450 reductase or cytochrome b5 could be expressed in insect cells with cytochrome P450 under the control of different promoters (Buters *et al.* 1995; Lee *et al.* 1995; Patten and Koch 1995; Chen *et al.* 1997). The co-expression system with redox partners was established, in which the total P450 activity could be recovered (Lee *et al.* 1995).

However, the selection of recombinant virus and the culture of insect cells are time-consuming, and cost of media is expensive (Fernandez and Hoeffler 1999; Galleno and Sick 1999).

1.3.4 Bacterial expression system

The bacterial system is often the first choice for expressing heterologous proteins due to the low cost, high expression level and easy control (Fernandez and Hoeffler 1999). However, it has been a challenge to express mammalian P450s in bacteria because there is a hydrophobic N-terminal tail in mammalian P450s, which possibly inhibits expression. Several strategies have been developed for the expression of P450s.

1) Modification in the N-terminus of the protein (Porter and Larson 1991; Barnes 1996). The high level expression of functional microsomal P450, P45017 α , was obtained by modifying the first seven codons of cDNA (Barnes *et al.* 1991). The modified 5-terminus of cDNA was believed to favour expression in *E.coli* (Barnes *et al.* 1991). This modified N-terminus (MALLLAVF) was widely applied in expressing other mammalian P450s including 1A2 (Fisher *et al.* 1992a), 2D6 (Gillam *et al.* 1995), 2C10 (Sandhu *et al.* 1993), 3A4 (Gillam *et al.* 1993), 4A1 (Dierks *et al.* 1998a) and 4A5 (Hosny *et al.* 1999), which cover CYP 1-4 subfamilies. It seems the modification of the hydrophobic tail at the N-terminus does not seriously affect the activity of the enzyme.

Some similar methods also have been reported. For example, only the second codon was changed to Ala (GCT), which is thought to be the preferred second codon for expression in *E.coli* (Soucek 1999), or the whole hydrophobic area was removed (Guengerich *et al.* 1996). The replacement of the hydrophobic tail by an amphipathic peptide also enhanced the expression level of P450 2a-4 (Sueyoshi *et al.* 1995).

2) Fusion of bacterial signal peptide. Although the signal peptide has been used in expression of mammalian P450 reductase (Shen *et al.* 1989), until recently, this

strategy was not applied in the expression of CYPs (Pritchard *et al.* 1997). There are several advantages to using a bacterial signal peptide fusion. Firstly, the signal peptide is often from a naturally secreted protein such as OmpA (Baneyx 1999), therefore this sequence is easily recognised and expressed in bacteria. The modification of the CYP at the N-terminus can be reduced to minimum by using signal peptide fusion, which could benefit understanding of the function of new P450s. Secondly, the leader sequences help to transport recombinant proteins to the periplasm of *E.coli*, which avoids proteolysis in the cytoplasm (Shen *et al.* 1989).

There are other methods that were developed to enhance expression of eukaryotic cytochromes P450 in bacteria. It was reported that co-expression with chaperone GroEL could help to obtain functional CYP3A7 (Inoue *et al.* 2000). Therefore, the extra molecular chaperones that help proteins fold correctly, such as GroEL and GroES, may benefit expression of CYPs in *E.coli*.

Some antibiotics, which can induce a cold shock response, and ethanol, which induces the heat shock response, were found to improve expression of P450s in *E.coli*. The authors proposed that cold shock proteins induced by antibiotics, could enhance translation of protein; and that ethanol could induce a series of chaperones that assist the folding of protein.

The initial expression of functional CYP3A7 (Inoue *et al.* 2000) and human placental CYP4B1 (Zheng *et al.* 1998) in *E.coli* failed, but when residues, Ser427 in CYP4B1 and Thr485 in CYP3A7, which are near the heme-binding region, were replaced by Pro residue, functional P450s were detected (Zheng *et al.* 1998; Inoue *et al.* 2000). It seems that these Pro residues could be involved in heme incorporation (Zheng *et al.* 1998; Inoue *et al.* 2000).

In order to express P450s in bacteria, only a few specific plasmids have been used including pCWori⁺, pSP19g10L (GIBCO-BRL), pKK233-2 (Amersham Pharmacia biotech) and pTrc99A (Amersham Pharmacia biotech)(Jenkins *et al.* 1998). Recently, another plasmid pLW01 was constructed to express CYP2B4 (Bridges *et al.* 1998; Saribas *et al.* 2001).

The pCWori⁺ plasmid is most widely used. It was originally derived from plasmid pHSe5 (Muchmore *et al.* 1989). The foreign DNA is tightly controlled by the two copies of a *tac* promoter (Barnes 1996). The expression of foreign protein is induced by IPTG (Barnes 1996). The pCWori⁺ plasmid carries the ampicillin resistance gene, which helps select the recombinant bacteria (Barnes 1996). However, this plasmid is not commercially available and as a result the whole length sequence is unknown. Also it does not contain multiple cloning sites that could be used in subcloning.

pSP19g10L, pKK233-2 and pTrc-99A are commercially available. pSP19g10L has a *lac* promoter (Barnes 1996); pKK233-2 and pTrc-99 (pTrc99 is derived from pKK233-2) have a *trc* promoter (Porter and Larson 1991). All of them carry the ampicillin resistance gene. Subcloning CYP cDNA in these plasmids is relatively convenient because there are multiple cloning sites (Porter and Larson 1991; Barnes 1996).

It was reported that a strong promoter such as T7 could cause the formation of inclusion bodies during expression of P450 in *E.coli* (Barnes 1996). However pLW01, based on the T7 promoter, could express functional CYP2B4, which might benefit from the high copy origin of replication in this plasmid (Bridges *et al.* 1998). Therefore, the origin of plasmid replication may also affect heterologous expression of functional P450 in *E.coli*.

Mammalian cytochromes P450 have been expressed in the common *E.coli* strains such as JM105, JM109, DH5 α and XL-1 blue (Porter and Larson 1991; Barnes 1996; Jenkins *et al.* 1998). More recently, special host strains derived from BL21(DE3) were developed to express membrane protein (Miroux and Walker 1996). CYP2B4 was expressed in one of the strains, C41(DE3), and up to 100mg of 2B4 per liter was obtained (Saribas *et al.* 2001). However, the choice of plasmid is limited because these strains are based on the T7 expression system.

Cytochrome P450 was also co-expressed with reductase in *E.coli*. A couple of similar strategies were developed. The cDNA of CYP and reductase carry individual promoters and terminators and could be linked in tandem in the same plasmid (Iwata *et al.* 1998). Alternatively, CYP and reductase cDNA shared the same promoter but there was a stop code after the CYP gene (Dong and Porter 1996). A plasmid containing cytochrome P450 and reductase fusion was also constructed (Fisher *et al.* 1992b; Fisher *et al.* 1996). A CYP4A1-reductase fusion was expressed in *E.coli* and the purified fusion protein showed hydroxylation activity (Shet *et al.* 1996). P450c17-reductase expressed in *E.coli* also showed the full function (Shet *et al.* 1997).

1.4 Structure and function of cytochrome P450

Information about cytochrome P450 structure is essential for understanding enzyme function and new drug design. The direct way to reveal the structure is using X-ray crystallography, however eukaryotic P450s, as membrane proteins, are very difficult to crystallise due to their hydrophobic membrane-bound region (Alberts *et al.* 1994). The soluble bacterial P450s provide the first step to explore the structure of cytochrome P450. Several crystals of soluble bacterial P450s have been obtained.

The crystal structures of CYP101, CYP102, CYP108, CYP107A1 and CYP 35A1 have been elucidated (Graham and Peterson 1999). A great effort has been made to crystallise mammalian P450 and only recently the first eukaryotic P450 crystal, CYP2C5, was obtained by removing the membrane-spanning area in the N-terminus (Cosme and Johnson 2000; Williams *et al.* 2000b; Williams *et al.* 2000a).

At the same time, homology models of mammalian P450s were constructed based on the crystal structure of similar bacterial P450 (Lewis 1995; Lewis and Lake 1995; Modi *et al.* 1996; Lewis and Lake 1999; Lewis *et al.* 1999; Dai *et al.* 2000). However, most of bacterial P450s belong to Class I, and only one bacterial P450, CYP102 (CYPBM3) from *Bacillus megaterium*, belongs to Class II, which is the same as microsomal P450s (Ravichandran *et al.* 1993). Therefore, CYP102 is an ideal model to study the structure of mammalian P450s.

Apart from these approaches, site-directed mutagenesis is also a common and powerful method of deducing structural information of about mammalian P450s (Domanski and Halpert 2001).

1.4.1 The structure of CYP102

CYP102 (CYPBM3) is a natural fusion protein, which contains the heme domain and flavoprotein domain (Li and Poulos 1999). The heme domain is similar to microsomal cytochrome P450 and the flavoprotein is similar to reductase. CYPBM3 has fatty acid hydroxylation catalytic activity, similar to the CYP4A subfamily (Li and Poulos 1999).

The crystal structures of the hemoprotein domain of CYPBM3 with and without the substrate, were published (Ravichandran *et al.* 1993; Li and Poulos 1997; Haines *et al.* 2001; Li *et al.* 2001b). A hydrophobic substrate channel has been identified in

CYPBM3. It is formed by sheet 1, sheet 4, B' and F helices including Phe42, Tyr51, Leu181, Met185, Leu188, Ala328, Ala 330 and Met354 residues (Ravichandran *et al.* 1993). The substrate channel opens near the surface, and ends at the active centre heme (Ravichandran *et al.* 1993). The end of channel is narrower than the open entrance (Ravichandran *et al.* 1993). There is a hydrophobic area at the entrance of the substrate binding channel, which is proposed to initially help dock the substrate (Ravichandran *et al.* 1993). The basic residue R47 flanks the entrance of the substrate channel but was poorly defined in the CYPBM3 crystal structure (Ravichandran *et al.* 1993). It was found that Y51 and F42 were located at the mouth of the substrate channel (Ravichandran *et al.* 1993). The crystal structure of CYPBM3 with palmitoleic acid, the substrate of CYPBM3, showed that Y51 and R47 could form hydrogen and ion pairs with the carboxylate of palmitoleic acid (Li and Poulos 1997). The position of Y51 has been properly determined, but the electron density of R47 has not been well characterised (Li and Poulos 1997). Molecular dynamic simulations of BM3 have shown strong electrostatic interaction between palmitoleic acid and the region near the entrance of the substrate channel (Chang and Loew 1999b). Y51, R47 and S72 in this region are believed to be involved in protein-substrate contact (Chang and Loew 1999b). Moreover, the distance between R47 and S72 is 1.26Å closer after substrate binding, suggesting that this movement could help R47 and S72 to interact well with the substrate (Chang and Loew 1999b). Therefore several residues in CYPBM3, including R47, Y51 and S72 could contribute to substrate binding.

F87 is located at the distal side of heme in CYPBM3. In the presence of substrate, the phenyl group of F87 moves from a perpendicular position to become parallel

with the heme (Li and Poulos 1997). Therefore, F87 could block the substrate access to the heme, explaining why CYPBM3 failed to hydroxylate ω -terminal methyl groups of fatty acids (Li and Poulos 1997).

The conformational change was observed in the crystal structure of CYPBM3 with palmitoleic acid and palmitoylglycine (Li and Poulos 1997; Haines *et al.* 2001). The axial water molecule, serving as the sixth ligand of heme-iron, shifts to the side of the iron and forms hydrogen bonds with Ala264 and Thr268 (Haines *et al.* 2001). This movement creates the space for further oxygen binding, which is important for later catalytic reaction.

Site-directed mutagenesis was also used to identify some key residues, which were related to substrate binding and stereo and regio-selectivity of products. The role of R47 and Y51 has been extensively studied. For examples, an R47E mutant failed to metabolise arachidonic acid (AA), with no difference spectrum induced by arachidonate (Graham-Lorence *et al.* 1997). Another group reported that the R47E mutant changed substrate specificity from C12-C16 fatty acids to corresponding trimethylammonium compounds (Oliver *et al.* 1997). It has also been shown that a R47A mutant decreases the affinity for AA and palmitoleic acid (PA) and the activity of AA and PA hydroxylation also decreases (Coward *et al.* 2001). A Y51F mutant showed a similar k_{cat}/K_m value for laurate to the wild type but it was four times smaller than wild type for AA (Noble *et al.* 1999). The Y51A mutant has also shown as increased spectral dissociation constant (Ks) for binding AA and PA, and a decreased turnover for oxidation of AA and PA (Coward *et al.* 2001). Furthermore, a R47A/Y51A double mutant has shown an even lower substrate affinity than a single

mutant (Coward *et al.* 2001). Therefore, the role of R47 and Y51 in substrate binding was supported by site-directed mutagenesis.

F87G and F87Y mutants had higher K_m and lower k_{cat} for fatty acid than wild type CYPBM3 (Noble *et al.* 1999). The F87V mutant showed a low rate of metabolising AA and PA (Graham-Lorence *et al.* 1997). More interestingly, the F87A mutant has shown ω -hydroxylation activity for laurate and myristate which is not observed in wild type CYPBM3 (Coward *et al.* 2001). F87 mutants have also been shown to affect the stereoselectivity of propylbenzene and 3-chlorostyrene oxidation (Li *et al.* 2001a). Therefore, F87 has been proposed as a key residue that kept the stereo and regio-selectivity of products.

An F42A mutant showed a 9-fold decrease of k_{cat}/K_m value, compared with the wild type, and it has been proposed that F42 helps to keep the hydrophobic environment and improve the electrostatic contact between substrate and enzyme (Noble *et al.* 1999). P25 has been identified to contribute to the initial docking of substrates by random mutagenesis because in previous work a P25Q mutant exhibited approximately 100-fold weaker affinity for palmitate than the wild type (Maves *et al.* 1997).

Mutagenesis of T268 has confirmed that the role of T268 is keeping the substrate in its proper position in the enzyme (Truan and Peterson 1998).

Recently, the role of conserved phenylalanine 393 was elucidated by site-directed mutagenesis (Ost *et al.* 2001a; Ost *et al.* 2001b). This residue is involved in transferring electrons from the redox partner to oxygen in CYPBM3.

1.4.2 Structure-function relationships of CYP4 family

Owing to the progress in understanding the structure of bacterial cytochromes P450, the structure-function relationships of mammalian P450s has been gradually revealed. Compared with some drug metabolising P450s such as CYP2D6 and CYP3A4, the substrate specificity of CYP4A proteins is quite restricted. Therefore, CYP4A must have a more restricted substrate channel.

Lauric acid and its analogs have been investigated for elucidation of the CYP4A1 substrate characteristics (Alterman *et al.* 1995; Bambal and Hanzlik 1996b; Bambal and Hanzlik 1996a). Lauric acid (Figure 1-2), the substrate of CYP4A1, has an optimal chain length; shorter or longer chain length of n-alkanoic acids resulted in decreased turnover numbers with CYP4A1 (Alterman *et al.* 1995). Therefore, the substrate channel of CYP4A1 was proposed to be approximately 12-carbon chain (14Å) long (Alterman *et al.* 1995). However, CYP4A1 did not use dodecane as the substrate (Alterman *et al.* 1995).

Interestingly, CYP4A1 has also been found to hydroxylate methyl laurate and lauryl alcohol (Figure 1-2), which do not contain the carboxyl group, although the efficiencies were a lot lower than for metabolism of lauric acid (Alterman *et al.* 1995). Titration of these compounds with CYP4A1 induced a Type I difference spectra (Alterman *et al.* 1995). These results suggested that the carboxyl group may not be necessary for substrate recognition in CYP4A1, and CYP4A1 might use a polar group recognition sites to bind the substrate (Alterman *et al.* 1995). However, another analogue, lauramide, was not a substrate for CYP4A1, and did not either induce a change in difference spectrum or inhibit the activity of CYP4A1 (Alterman *et al.* 1995).

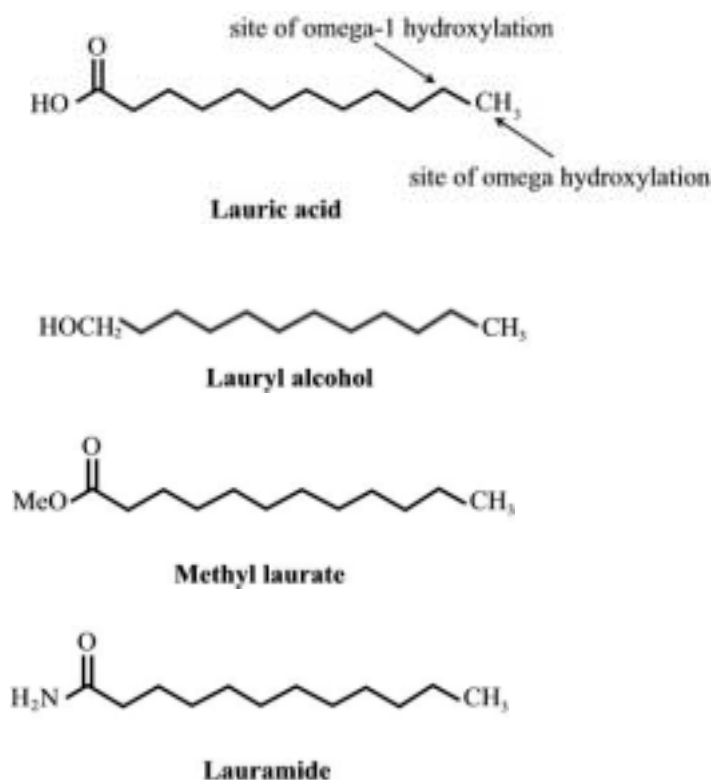


Figure 1-2. Structures of lauric acid and its analogos.

The positions of ω and ω -1 hydroxylation in lauric acid, lauryl alcohol and methyl laurate are pointed by the arrows.

CYP4A1 could use analogs of lauric acid, which have the bulky or branch group at ω -1 position, as substrates (Alterman *et al.* 1995; Bambal and Hanzlik 1996b). This suggested that the activity site of CYP4A1 is relatively open and flexible (Bambal and Hanzlik 1996b). The unsaturated analogs of lauric acid such as 11-dodecenoic acid and 11-dodecynoic acid have also been shown to be good substrates for CYP4A1 (Bambal and Hanzlik 1996b). ω -Imidazolyl-decanoic acid, a strong inhibitor of lauric acid oxidation, induced the Type II substrate binding spectrum, therefore suggesting that the imidazole nitrogen coordinates with the heme iron (Alterman *et al.* 1995; Bambal and Hanzlik 1996a).

Three groups have built CYP4A models based on alignments with CYP102: a 3-D model of CYP4A11 established by using computer technology (Chang and Loew

1999a); the homology model of CYP4A1 built by a computer program (unpublished, C. A. laughton); and structures of CYP4A1, CYP4A4 and CYP4A11 deduced by using sequence alignment between CYP102 and CYP4As (Lewis and Lake 1999). Several site-directed mutants in the 4A subfamily have also been reported. A L131F mutant of CYP4A11 has been shown to change the regioselectivity of substrate hydroxylation (Dierks *et al.* 1998b). In CYP4A1, D323E and E320A affected the hydroxylation regiospecificity (Dierks *et al.* 1998a). In CYP4A3, the insert of Ser114-Gly-Ile116 controlled the regiospecificity of ω -hydroxylation and the K92A mutant of CYP4A3 completely lost the ability to bind fatty acids (Hoch *et al.* 2000b). In CYP4A7, residues in putative substrate recognition sites (SRS) were examined (Loughran *et al.* 2000). R90W and W93S mutants decreased the activity for laurate and AA oxidation. H206Y and S255F increased the activity for the same substrates (Loughran *et al.* 2000). A H206Y mutant also showed the higher rate reaction with CPR than wild type (Loughran *et al.* 2000).

Recently, the prosthetic heme in the CYP4 family has been found to be covalently bound to the enzyme (Henne *et al.* 2001; Hoch and Ortiz De Montellano 2001), and residue E318 in CYP4A3 has been identified to form an ester bond with heme (Hoch and Ortiz De Montellano 2001).

1.4.3 Interaction between cytochromes P450 and redox partners

The interaction between P450 and redox partners has been extensively studied (Schenkman and Jansson 1999). Earlier studies of interactions between cytochrome c and cytochrome b5 revealed that these two proteins could form a tight complex by electrostatic force (Mauk *et al.* 1995). Several acidic residues in cytochrome b5 were crucial for the formation of the b5-cytochrome c complex (Wu *et al.* 2001). The

carboxyl groups in cytochrome b5 was also important to keep the interaction with rat and rabbit liver microsomal P450s (Tamburini *et al.* 1985). A computer model of cytochrome b5 and CYP101 showed possible electrostatic contacts between cytochrome b5 and basic residues in P450 (Stayton *et al.* 1989). Therefore, the positive charged surface of cytochrome P450 might be responsible for docking cytochrome b5.

Site-directed mutagenesis has been used to examine the function of basic residues on the surface of mammalian P450s. In CYP2B4, basic histidine residues were critical for electron transfer from CPR and b5 (Hlavica *et al.* 1996). A series of mutants located on the proximal and distal surface of CYP2B4 have been constructed to examine the role of b5 binding (Bridges *et al.* 1998). Seven basic residues and two hydrophobic residues at the proximal surface were identified as the crucial residues in redox partner binding (Bridges *et al.* 1998). Four other positively charged residues on the surface of CYP2B4 were also important for interaction with CPR (Lehnerer *et al.* 2000). In CYP2B1, the synthetic mimic peptide, which corresponds to residues 116-134, could inhibit the reductase derived activity and b5 binding, and two basic residues Lys-122 and Arg-125 in this region were identified as the crucial residues to keep interaction between CYP2B1 and redox partners (Omata *et al.* 1994; Omata *et al.* 2000). Two lysine residues in CYP1A1 were found to control electron transport from CPR (Cvrk and Strobel 2001). Therefore, the study of mammalian P450 by site-directed mutagenesis confirmed that the basic residues located on the surface were for binding redox partners.

1.5 Aims of the thesis

It is known that CYP4A1 is involved in various and essential physiological activities as described in section 2.1. Moreover, CYP4A1 provides an ideal model to study similar CYP forms in human, which could help us to find new medicines for some serious diseases such as hypertension. However, structure-function relationship of CYP4A1 is poorly understood.

Therefore, the aims of the first part of this project were:

- 1) To establish the bacterial expression system to express recombinant CYP4A1, and obtain enough pure and functional CYP4A1 for structure-function studies.
- 2) To provide enough functional redox partners of CYP4A1 including cytochrome P450 reductase and cytochrome b5 for reconstituting CYP4A1 activity *in vitro*.
- 3) To identify key residues in CYP4A1 which respond to substrate binding.
- 4) To elucidate the function of the conserved C-helix region in CYP4A1.

2 Materials and Methods

2.1 Materials

All chemicals were at A.R. grade purity or greater.

Ammonium acetate, bovine serum albumin, isoamylalcohol, phosphoric acid, TEMED, tetracycline, SDS, Tween 20, xylene cyanol FF, ethidium bromide, Serva blue G, dithiothreitol (DTT), dimethylsulfoxide (DMSO), β -mercaptoethanol, phenylmethylsulfonyl fluoride (PMSF), aprotinin, ampicillin (Amp), chloramphenicol (Chl), imidazole, NaCl, δ -aminolevulinic acid, cholic acid (sodium), lauric acid, dodecyltrimethylammonium bromide and $\text{FeCl}_3 \cdot 6\text{H}_2\text{O}$, $\text{ZnCl}_2 \cdot 4\text{H}_2\text{O}$, $\text{CoCl}_2 \cdot 6\text{H}_2\text{O}$, $\text{Na}_2\text{MoO}_4 \cdot 2\text{H}_2\text{O}$, $\text{CaCl}_2 \cdot 2\text{H}_2\text{O}$ and CuCl_2 were all obtained from Sigma Chemical Co. Phenol, MgCl_2 , potassium acetate was from Fisher Scientific Equipment.

K_2HPO_4 , NaCl, NaOH, NiSO_4 , boric acid, CaCl_2 , methanol, glacial acetic acid and chloroform were from Fisher Scientific UK Limited.

Tryptone and Yeast Extract were from Difco Laboratories.

Glycerol was from Courtin & Warner.

KH_2PO_4 , KCl, glycine, EDTA, glucose, bromphenol Blue, ethanol and ammonium sulphate were from BDH.

Agarose was from Boehringer Mannheim.

Sodium dithionite was purchased from Kodak.

3-[(3-cholamidopropyl) dimethylammonio]-1-propanesulfonate (Chaps) was obtained from Melford Laboratories (U.K.).

Emulgen 913 was a gift from Kao Chemicals.

Brilliant blue G was from Aldrich.

Marvel was from Premier Brand UK Ltd.

Ammonium persulphate, ampicillin, hydrochloride acid, coomassie brilliant blue R-250 were all obtained from ICN Flow.

Tris-base was from Gibco-BRL.

The Immun-Blot assay kit and goat Anti-rabbit IgG (H+L) conjugated to horseradish peroxidase were obtained from Bio-Rad.

30% acrylamide/bisacrylamide was from Severn Biotech Ltd.

X-ray film was manufactured by Fuji and obtained from Amersham. X-ray film developer and fixer were obtained from Ilford.

PVDF membrane was from Phamacia.

1Kb plus DNA ladder were obtained from Gibco-BRL.

SDS-7, 6H and 7B protein marker were form Sigma.

Human Mammary Gland Marathon Ready cDNA was from Clontech.

GeneEditor™ *in vitro* Site-Directed Mutagenesis system was from Promega

3MM paper and VectaSpin 3™ (30k MWCO) centrifuge tube filter were obtained from Whatman.

Oligonucleotides were synthesised by John Keyte of the Biopolymer Synthesis and Analysis Unit, School of Biomedical Sciences, University of Nottingham.

Ultra high purity (UHP) grade water ($> 13 \text{ Mohms/cm}^3$) was produced using a Purite Select Bio system.

PD-10 column was from Amersham pharmacia biotech

His•Bind and Ni-NTA His•Bind resin were from Novagen.

CE9500 double beam spectrophotometer was purchased from CECIL instrument Ltd.

Enzyme:

Nde I, *Xba I*, *Nhe I*, *EcoN I*, *EcoR V*, *EcoR I*, *Bgl II*, *Afl III*, *BamH I*, *Nco I*, *SgrA I* and *Sac I* were from New England Biolabs.

BstX I was purchased from Promega.

Hind III was from Boehringer Mannheim.

Shrimp alkaline phosphatase was from USB Corporation.

T4 ligase and buffer were from New England Biolabs.

Pfu was from Promega.

Extensor Hi-Fidelity PCR Master Mix and 1.1× ReddyMix PCR Master Mix (1.5mM MgCl₂) were from ABgene.

Lysozyme was from Sigma .

Strains and plasmids:

BL21(DE3)pLysS and HMS174(DE3)pLysS were from Novagen.

C41(DE3) was gift from John E. Walker (Miroux *et al.*, 1996).

SCS110, XL-1 blue and JM109 were from Stratagene.

Plasmid pRSET was from Invitrogen.

Plasmids pGEM-T, pGEMT-Easy and pGEMT-11 were from Promega.

The plasmid pGEM 11 containing CYP4A1 cDNA was a gift from Dr. David R. Bell.

The plasmid pCWori⁺ containing N-terminally modified 4A1 with six histidine tag at C-terminus was a kind gift from Prof. Paul R. Ortiz de Montellano (Dierks *et al.* 1998a).

The plasmid pRSET-b containing human cytochrome b5 sense and anti-sense cDNA was a gift from Dr. David R. Bell.

The plasmid pB55 containing human cytochrome P450 reductase cDNA was a gift for Dr Mark. J. Paine (University of Dundee).

2.2 General Methods

2.2.1 Bacterial culture

E. coli strains were streaked on LB-agar plates containing appropriate selective antibiotics then incubated overnight at 37°C. A single colony was picked from the freshly prepared plate and inoculated in 5ml of LB broth (10g Bacto-Tryptone, 5g Bacto-yeast extract and 10g NaCl in 1 litre of water) containing the appropriate selective antibiotics. The inoculum was incubated at 37°C overnight by shaking at 220 rpm. The saturated culture was used for further large-scale culture. Alternatively, the inoculum was incubated at 37°C until the OD₆₀₀ was 0.5-1.0, then 1ml of the culture was transferred into an eppendorf and mixed with 150µl of glycerol. The glycerol stock was stored at -80°C.

2.2.2 Phenol: chloroform: isoamyl alcohol (25:24:1) extraction of DNA

Phenol:chloroform:isoamyl alcohol (25:24:1) was used in order to remove protein contamination from DNA solution. Phenol:chloroform:isoamyl alcohol (25:24:1) solution was added to the same volume of nucleic acid sample and the mixture was vortexed thoroughly. The organic and aqueous phases were separated by centrifugation at 14,000g for five minutes. The aqueous phase, which contains DNA, was removed to the clean eppendorf.

2.2.3 Ethanol precipitation of nucleic acids

Ethanol precipitation was utilised to recover DNA from solution. Two volumes of 100% ethanol were added to the DNA solution containing 0.3M sodium acetate, pH 5.2 or 2.0-2.5M ammonium acetate. The solution was mixed and incubated on ice for

15-30 minutes. The sample was then centrifuged for 10 minutes at 12,000g. The DNA pellet was washed in 500µl of 70% ethanol and centrifuged at 12,000g for 5 minutes. The supernatant was discarded and the pellet was air dried for 20-30 minutes. The dried DNA pellet was dissolved in UHP water or TE buffer (10mM Tris·HCl, pH 8.0, 1mM EDTA, pH 8.0).

2.2.4 Isolation of plasmid DNA

2.2.4.1 Alkaline lysis method

1.5ml of an overnight culture was transferred into an eppendorf tube. The bacteria were harvested by centrifugation at 14,000rpm for 1 minute. The supernatant was discarded and the pellet resuspended in 150µl of solution I (50mM glucose, 25mM Tris·HCl pH 8.0, 1mM EDTA). Then 200µl of freshly prepared solution II (0.2M NaOH, 1% SDS) was added and mixed immediately by inversion of the tube several times. Finally, 150µl of solution III (5M potassium acetate, 11.5% (v/v) glacial acetic acid) was added to the mixture. The sample was again mixed immediately by inversion. The mixture was incubated on ice for 3 to 5 minutes. The cloudy precipitate was pelleted by centrifugation at 14,000rpm for 10 minutes. The supernatant was transferred into a clean tube. 500µl of phenol-chloroform (1:1) was added into the tube and mixed by vortex. The sample was centrifuged at 14,000rpm for 5 minutes. The upper aqueous phase was carefully transferred to a fresh tube. The plasmid DNA was precipitated by adding 500µl of isopropanol. The solution was mixed well and incubated at room temperature for 2 minutes. The nucleic acid was recovered by centrifugation at 14,000rpm for 10 minutes. The supernatant was

discarded and the white DNA pellet was washed with 1ml of 70% (v/v) ethanol. The sample was spun down at 14,000rpm for 5 minutes and ethanol solution was removed. The pellet was allowed to dry in air. The plasmid DNA was solubilised in UHP water containing 50µg/ml RNAase A (DNAase free).

2.2.4.2 Qiagen mini-preparation

QIAprep Spin Miniprep kit (Qiagen) was utilised to purify sequencing grade plasmid DNA. The procedure followed the manufacturer's instruction. 3ml of freshly prepared overnight culture was spun down at 14,000rpm for 1 minute. The pelleted bacteria cells were resuspended in 250µl of Buffer P1 and transferred to an eppendorf tube. 250µl of Buffer P2 was added and the tube was gently inverted 4-6 times to mix. 350µl of Buffer N3 was added into the tube and the solution was gently mixed by inversion 4-6 times. The mixture was centrifuged at 14,000rpm for 10 minutes. A compact white pellet formed in the tube. The supernatants were transferred to the QIAprep column by pipetting. The column was centrifuged at 14,000rpm for 1 minute. The flow-through was discarded. The QIAprep spin column was washed by adding 0.5ml of Buffer PB and centrifuged for 1 minute. The flow-through was discarded. Then the spin column was washed by 0.75ml of Buffer PE and spun down at 14,000rpm for 1 minute. The flow-through was decanted, the spin column was centrifuged for additional 1 minute to remove residual wash buffer. The spin column was placed in a clean 1.5ml microfuge tube and 50µl of Buffer EB (10mM Tris·HCl, pH 8.5) or UHP water was added to the centre of column. The column was allowed to stand for 1 minute at room temperature and centrifuged for 1 minute. The plasmid DNA solution was collected in the bottom of tube.

2.2.4.3 Qiagen maxi-preparation

QIAGEN-tip 500 kit (Qiagen) was used for large-scale preparation of plasmid DNA. The procedure was carried out according to the manufacturer's instruction. 1ml of overnight culture was inoculated in 500ml LB broth containing appropriate selective antibiotics. The Bacteria were grown up at 37°C overnight, shaking at 220rpm. The cells were harvested by centrifugation at 6000rpm for 15 minutes at 4°C. The bacteria pellet was resuspended in 10ml Buffer P1 (50mM Tris·HCl, pH 8.0, 10mM EDTA, 100µg/ml RNAase A). 10ml of Buffer P2 [200mM NaOH, 1% SDS (w/v)] was added to the suspension and mixed gently by inverting 4-6 times and incubated at room temperature for 5 minutes. 10ml of chilled Buffer P3 (3.0M potassium acetate, pH 5.5) was added to the sample and mixed immediately but gently by inverting 4-6 times. The mixture was incubated on ice for 20 minutes. The plasmid DNA solution was recovered by centrifugation at 12,000rpm for 30 minutes at 4°C. The supernatant containing plasmid DNA was re-centrifuged at 12,000rpm for 15 minutes at 4°C. The supernatant was applied to the QIAGEN-tip 500 column that had been equilibrated by 10ml of Buffer QBT [750mM NaCl, 50mM MOPS, pH 7.0, 15% isopropanol (v/v), 0.15% Triton X-100 (v/v)]. The sample was allowed to enter the resin by gravity flow. The QIAGEN-tip was washed by 2×30ml Buffer QC [1.0M NaCl, 50mM MOPS, pH 7.0, 15% isopropanol (v/v)]. The plasmid DNA was eluted by 15ml Buffer QF [1.25M NaCl, 50mM Tris·HCl, pH 8.5, 15% isopropanol (v/v)]. DNA was precipitated by adding 10.5ml of room temperature isopropanol to the solution. The plasmid was recovered by centrifugation at 11,000rpm for 30 minutes at 4°C. The DNA pellet was washed with 5ml of room temperature 70% ethanol and

centrifuged at 11,000rpm for 10 minutes. The supernatant was discarded without disturbing the pellet. The pellet was air-dried for 10 minutes and DNA was redissolved in 1ml TE buffer (10mM Tris·HCl, pH 8.0, 1mM EDTA) or UHP water.

2.2.4.4 Wizard maxi-preparation

Wizard Plus Maxipreps DNA purification system (Promega) was used to prepare large amount of crude plasmid DNA. 1ml of saturated inoculum was inoculated into 400ml LB broth containing appropriate selective antibiotics. The culture was incubated at 37°C overnight. The bacteria were collected by centrifugation at 6,000rpm for 15 minutes. The supernatant was poured off and the pellet was resuspended in 15ml of Cell Resuspension Solution (50mM Tris·HCl, pH 7.5, 10mM EDTA, 10µg/ml RNAase A). 15ml of Cell Lysis Solution (0.2 M NaOH, 1% SDS) was added into the sample and mixed gently but thoroughly by inverting. After the solution became clear and viscous, 15ml of Neutralization Solution (1.32M potassium acetate, pH 4.8) was immediately added and mixed by gently inverting centrifuge bottle. The cell debris was removed by centrifugation at 6,000rpm for 20 minutes. The supernatant was filtered by Whatman filter paper. The DNA was precipitated by adding 0.7 volumes of isopropanol. The DNA was recovered by centrifugation at 8,000rpm for 20 minutes. The pellet was washed using 10ml of 80% ethanol. The sample was centrifuged at 8,000rpm for 15 minutes. The DNA pellet was resuspended in 2ml of water or TE buffer (10mM Tris·HCl, pH 7.5, 1mM EDTA). 10ml of Wizard Maxipreps DNA Purification Resin were added to the DNA solution. The resin/DNA mixture was transferred into the Maxicolumn and a vacuum was applied to pull the resin/DNA into the column. 25ml of Column Wash Solution

(80mM potassium acetate, 8.3mM Tris-HCl, 40 μ M EDTA) was added to the column and drawn through by a vacuum. 5ml of 80% ethanol was used to rinse the resin and removed by a vacuum. The vacuum was allowed to draw for an additional minute. The Maxicolumn was placed in a falcon tube and spun down at 3,000rpm for 10 minutes. The resin was dried by applying a vacuum for 5 minutes. 1.5ml of water, preheated to 70°C, was added to the column and left for 2 minutes. The plasmid DNA solution was recovered by centrifugation at 3,000rpm for 5 minutes. Finally, the DNA solution was passed through a 0.2 μ m syringe filter to remove any fine resin.

2.2.5 Restriction enzyme digest of plasmid DNA

The required amount of DNA was pipetted into an eppendorf tube. The restriction enzyme and the corresponding buffer were chosen according to the manufacturer's manual and were added to the tube. Typically, the tube was incubated at 37°C for 1 hour. The reaction was stopped by adding DNA loading buffer (10 \times solution: 30% glycerol, 0.25% Bromophenol Blue and 0.25% Xylene Cyanol FF). The sample was then ready for agarose gel electrophoretic analysis.

2.2.6 Agarose gel electrophoresis

A submarine Pharmacia GNA-100 gel electrophoresis kit was used for DNA mini-agarose electrophoresis. The appropriate amount of agarose [0.6-1.5% (w/v)] was dissolved in the 60ml of 1 \times TBE (45mM Tris-HCl, 44mM Boric acid and 2mM EDTA, pH 8.0) by microwave heating. The agarose solution was cooled down to about 55°C, and then ethidium bromide (10mg/ml stock) was added into the solution to give a final concentration of 0.5 μ g/ml. The whole solution was poured into a casting mould with the gel comb. After agarose solidified, the comb was removed

and the mould with gel was placed in the electrophoresis tank. The tank was filled with 1× TBE buffer until the gel was covered. After the DNA sample was loaded, the electrophoresis was performed at 80V for 1 hour.

2.2.7 Photography methods

DNA bands in the agarose gel could be visualised by illumination with an UV trans-illuminator and photographed. Alternatively, when DNA needed to be recovered from the agarose gel, a Darker reader was used to detect the band. This is because Darker reader would not cause damage to the DNA.

2.2.8 Purification of DNA from an agarose gel

2.2.8.1 GeneClean system

GENECLEAN II kit (BIO 101 inc.) was used to purify the DNA from agarose gel. A 1× TAE (40mM Tris-HCl, 1mM EDTA and 5.71% glacial acetic acid) agarose gel was used for the gel purification of DNA. The DNA sample was separated in TAE agarose gel as described in section 2.2.6. The desired DNA band was excised from ethidium bromide stained gel under Dark Reader to prevent damage of DNA. The gel was dissolved in three volumes of 6M NaI (w/v). The eppendorf was incubated at 55°C for five minutes until the whole gel was dissolved. 5µl-20µl (for 5µg-12.5µg DNA) of glassmilk was added into the solution and gently mixed. The suspension was incubated at room temperature for 20 minutes to let DNA bind to glassmilk. The glassmilk was recovered by centrifugation at 15,000rpm for 1 minute. The supernatant was discarded. The pellet was washed with 500µl cold New Wash Buffer (50% 20mM Tris-HCl pH7.2, 0.2M NaCl, 2mM EDTA and 50% ethanol). The pellet

was recovered by centrifugation at 14,000rpm for 30 seconds. The glassmilk was washed twice more. Finally, the pellet was resuspended in 20 μ l UHP water and incubated at 55°C for three minute to elute the DNA. The DNA solution was recovered by centrifugation at 15,000rpm for three minutes. The supernatant was carefully transferred to a clean eppendorf.

2.2.8.2 QIAquick gel extraction kit

QIAquick kit provides a quicker way to purify DNA from the agarose gel. The DNA fragment was excised from the agarose gel with a scalpel. 3 volumes (v/w) of Buffer QG were added to the gel. The gel with Buffer QG was incubated at 50°C for 10 minutes until the gel slice was completely dissolved. The solution was loaded in the QIAquick spin column then centrifuged for 1 minute at 13,000rpm. The flow-through was discarded, and the column was washed by 0.75ml of Buffer PE. The column was again centrifuged at 13,000rpm for 1 minute. The flow-through was discarded. The column was centrifuged for additional 1 minute to remove the residual Buffer PE. 30 μ l of water was added to the centre of the column and left to stand for 1 minute. DNA was recovered in the flow-through by centrifugation for 1minute at 13,000rpm.

2.2.9 Phosphatase treatment of DNA

To reduce the self-recircularising background of linearised plasmids, Shrimp alkaline phosphatase (SAP) was used to remove the 5'-terminal phosphate from double-stranded DNA. 1U of SAP and 10 \times shrimp alkaline phosphatase buffer (200mM Tris·HCl, pH 8.0, 100mM MgCl₂) were added in DNA sample. Dephosphorylation of

DNA was done at 37°C for 1 hour. SAP was inactivated by heating at 65°C for 15 minutes. The final solution could then be used for further manipulations.

2.2.10 Transformation of the plasmid

2.2.10.1 Preparation of calcium chloride competent cells

A single bacteria colony was picked from a freshly prepared plate and inoculated into 50ml of LB broth. The culture was incubated at 37°C by vigorous shaking until OD₆₀₀ reached about 0.5. The cells were recovered by centrifugation at 6000rpm for 20 minutes. The supernatant was decanted and 10ml of 0.1M ice-cold CaCl₂ was added into the tube. The pellet was resuspended by vortexing. The suspension was centrifuged at 6,000 rpm for 10 minutes. After the supernatant was discarded, the pellet was resuspended in 2ml of freshly prepared 0.1M ice-cold CaCl₂. The glycerol (15%) stock was stored at -80°C. (XL-1 competent cells were cultured in medium containing 10µg/ml tetracycline. BL21(DE3)pLysS and HMS(DE3)pLysS cells were cultured in LB containing 34µg/ml chloramphenicol.)

2.2.10.2 Transformation

The 200µl aliquot of competent cells was prepared as described above. The stock cells were thawed on ice. After DNA was added to cells, the mixture was placed on ice for 30 minutes. The mixture was heat shocked at 42°C for 90 s, and then placed on ice for 2 minutes. 800µl LB broth was added and cells were incubated at 37°C for 1 hour. Finally, the cells were spread on the LB agar containing selective antibiotics.

2.3 Protein Methodologies

2.3.1 Bradford protein assay

The Bradford assay was used to determine the quantitation of protein. A standard curve was made by using bovine serum albumin (BSA) between the ranges of 0-30 μ g. The BSA was weighted and solubilised in water at 1mg/ml. 50 μ l (volume was adjusted by adding UHP water until 50 μ l) of the standard BSA sample (0, 5 μ g, 10 μ g, 15 μ g, 20 μ g, 30 μ g) was mixed with 50 μ l of 1M NaOH. 900 μ l of dye reagent (100mg Serva blue G dissolved in 100ml of 85% phosphoric acid and 50ml of 95% ethanol, bring the volume to 1 litre) was added into the sample and incubated for 5 minutes. The absorbance at 590nm was measured in polystyrene cuvettes. UHP water with 1M NaOH and dye reagent was used as a reference. All assay were carried out in triplicate and the resultant means determined. R^2 was required to be better than 0.95. The protein sample was measured in the same way as the BSA standard. The concentration of protein was determined using the standard curve, with BSA as a standard.

2.3.2 SDS-polyacrylamide gel electrophoresis (SDS-PAGE)

The protein could be separated by SDS-PAGE. Bio-Rad Mini-PROTEAIN II electrophoresis kit was used for SDS-PAGE. The 0.75mm spacer and comb were used. After the kit was set up, the separating gel (7.5%-12% as showing below) was poured. The top of gel was about 2cm from the top of the glass. The surface of the gel was covered with 0.1% SDS.

Table 2-1. The component of separating gel (50ml)

	7.5%	10%	12%
30% acrylamide/bisacrylamide	12.5ml	16.7ml	20.0ml
H ₂ O	24.0ml	19.8ml	16.5ml
1.5 M Tris·HCl (pH 8.8)	12.5ml	12.5ml	12.5ml
10% SDS	0.5ml	0.5ml	0.5ml
10% Ammonium persulphate (APS)	0.5ml	0.5ml	0.5ml
TEMED	0.02ml	0.02ml	0.02ml

After the gel polymerised, the stacking gel [10ml stacking gel: 1.7ml acrylamide/bisacrylamide (30%), 6.8ml H₂O, 1.25ml 1M Tris-HCl (pH 6.8), 0.1ml 10% SDS, 0.01ml TEMED and 0.1ml 10% APS] was poured into the gel kit, and the comb was inserted into the 5% stacking gel. After the stacking gel was polymerised, the comb was carefully removed, and the gel was ready to be used. The protein samples were diluted by the same volume of 2× Sample buffer (100mM DTT, 2% SDS, 80mM Tris-HCl, pH 6.8, 15% glycerol, 0.006% bromophenol blue) and boiled at 100°C for 3 minutes. The prepared samples were stored on ice until needed. After the samples were loaded in the gel, the gel was run at 120V (15V/cm) for about 1hour. The protein could be stained in Coomassie staining solution [0.25g coomassie, 90ml methanol: H₂O (1:1, v/v), 10ml glacial acetic acid] for more than 4 hours by gentle agitation. The gel then was destained using destaining solution (30% methanol, 10% glacial acetic acid) until the protein band became clear. During destaining, the solution should be changed 3-4 times. The destained gels were placed on Whatman paper and covered by film, then dried at 80°C for 60 minutes using Bio-Rad 583 gel dryer.

2.3.3 Western blotting

After protein samples were separated by SDS-PAGE, immunodetection could be used with an ECL Western Blotting Detection Kit (Amersham Life Science). The stacking gel was cut away from the separating gel. The separating gel was then placed onto two pieces of 3MM Whatman paper pre-soaked with 1×transfer buffer [25mM Tris·HCl, 192mM glycine, 20% methanol (v/v) and 0.1% SDS (w/v)]. A piece of PVDF membrane (just larger than the gel) was put in 100% methanol then in 1× transfer buffer. The pre-wet membrane was placed onto the gel and all bubbles removed. Two pieces of 3MM pre-soaked Whatman paper then covered the membrane. The electroblotting sandwich was placed into the electroblotting cassette. The cassette was transferred into the tank filled with 1×transfer buffer. The transfer of protein was carried out at 90V for 1hour. The membrane was taken out and blocked in 100ml of 1×TBS [20mM Tris-HCl (pH 7.5), 500mM NaCl] containing 10% Marvel for at least 1hour. The membrane was washed with TTBS (1×TBS+ 0.1% Tween 20,v/v) for 10 minutes. The washing was repeated an additional 4 times. The membrane was then incubated at room temperature in 1× TTBS containing 10% Marvel and the appropriate primary antibody for 1hour. Excess primary antibody was washed out by 1×TTBS 5 times. The membrane was then incubated in 1×TTBS+10% Marvel containing the secondary antibody for 1 hour. The membrane was washed using 1×TTBS a total of 5 times (5-10 minutes each time). The membrane was incubated in the mixture of detection solution 1 and detection solution 2 (1:1 v/v) for 1 minute at room temperature without agitation. Excess detection reagent was drained off. The membrane was wrapped in cling film. The

blot, protein side up, was placed in the film cassette. A sheet of Hyperfilm (Amersham Life Science) was placed on top of the membranes in the dark room. The film was exposed for different lengths of time (15, 30, 60 seconds) then developed and fixed.

2.3.4 Nickel affinity chromatography

2.3.4.1 His•Bind resins

The purification of protein was carried out according to the manufacturer's description. 10ml of His•Binding resin (Novagen) was loaded into 20ml syringe and washed with 30ml distilled water to remove ethanol in the resin. The resin was charged with 50ml 1×Charge Buffer (50mM NiSO₄). The column was washed with 30ml of deionised water to remove the excessive Ni²⁺. The resin was equilibrated in 30ml 1×Binding buffer. The sample was loaded in the column at the rate of 0.25ml/min. The resin was washed with 50ml 1×Binding Buffer to remove unbound protein and followed by 50ml 1×Washing Buffer to remove weakly binding protein. The desirable protein was eluted using 30ml 1×Eluting Buffer.

2.3.4.2 Ni-NTA His•Bind Resins

Four volumes of Ni-NTA Bind Buffer were added to a pre-charged 50% Ni-NTA His•Bind slurry (Novagen). The resin was gently mixed with Bind Buffer and allowed to settle by gravity. The supernatant was then removed using a pipette. The protein sample was mixed with pre-equilibrated resin by stirring on ice for 1 hour. The protein- Ni-NTA resin mixture was loaded on to the column. The column was

washed with 10× bed volume of Wash Buffer. The desirable protein was then eluted using 2-3× bed volume of Elute Buffer.

2.3.5 Protein Desalting by size exclusive PD-10 columns

PD-10 desalting columns (Amersham Pharmacia Biotech) contain prepacked Sephadex G-25 Medium for desalting and buffer change. The columns were used to separate proteins ($M_r > 5000$) from low molecular weight substances ($M_r < 1000$) according to the manufacturer's instructions. The procedure of desalting and buffer change was according to the manufacturer's instruction. Firstly, the column was equilibrated with approximately 25ml buffer and then 2.5ml of sample was loaded on the column. After the sample ran into the column, the protein was eluted using 3.5ml buffer. The protein eluent was collected and analysed.

2.4 Expression of cytochrome b5

2.4.1 Spectrophotometric measurement

The content of cytochrome b5 was measured by spectrophotometry. The sample was diluted 10-50 fold with 0.1M potassium phosphate (pH 7.5). A 2ml aliquot of the diluted sample was split and added to the sample cuvette and reference cuvette (1ml in each cuvette). The baseline was recorded by scanning samples from 500nm to 400nm. Then, a few milligrams of sodium dithionite were added to the sample cuvette. After the sodium dithionite had dissolved, the samples were scanned again and the change of absorbance recorded. Cytochrome b5 produces a peak at around 424nm. The millimolar extinction coefficient of $118\text{mM}^{-1}\cdot\text{cm}^{-1}$ (Holmans *et al*, 1994) was used to calculate the concentration of b5.

2.4.2 Expression of cytochrome b5

2.4.2.1 Transformation and preparation of plasmids

Plasmid pRSET containing b5 in the sense and anti-sense orientations were transferred into JM109 by the standard method as described in section 2.2.10. 1µl of plasmid was added to 200µl of calcium chloride competent cells. The cells were incubated on ice for 30 minutes, and then were heat shocked at 42°C for 90 seconds. Bacteria were spread on the LB agar plate containing 50µg/ml Amp and 34µg/ml Chl. The cells containing the plasmid were selected by ampicillin resistance.

The plasmids were purified by the wizard resin (Promega Maxi Preps) as described in section 2.2.4.4. The plasmids were digested with *Bst*X I and *Nco* I in order to verify the insert orientation of b5 fragment. The plasmid containing pRSET-b5 sense was transferred into BL21(DE3)pLysS, HMS174(DE3)pLysS and C41(DE3) to express cytochrome b5.

2.4.2.2 Optimising expression of cytochrome b5

A single colony was picked from the freshly prepared Amp/Chl plate and inoculated into 5ml LB broth containing Amp (100µg/ml) and Chl (34µg/ml). The inoculum was incubated at 37°C overnight by standing until the culture became lightly turbid. Then, 1%(v/v) overnight cultures were inoculated into 50ml of LB or Terrific broth (12g Bacto-Tryptone, 24g Bacto-yeast extract, 4ml glycerol in 900ml of water, 2.31g KH₂PO₄ and 12.54g K₂HPO₄ in 100ml of water, mix before use) containing 0.3%(v/v) rare salt (27g FeCl₃·6H₂O, 2g ZnCl₂·4H₂O, 2g CoCl₂·6H₂O, 2g Na₂MoO₄·2H₂O, 1g CaCl₂·2H₂O, 1g CuCl₂, 0.5g H₃BO₃, 100ml HCl conc. in 1litre of water). The cells were incubated at 37°C with a shaking rate of 240rpm until the

cultures were reached an OD₆₀₀ of 0.5-1.5. The cultures were cooled down to induction temperature and IPTG was added to induce the expression of b5. The rate of shaking was kept at 125rpm.

The cells were harvested by centrifuging at 6000rpm for 15 minutes. The pellets were weighed, then resuspended in 5 volumes (v/w) of PBS (8g NaCl, 0.2g KCl, 1.44g Na₂HPO₄, 0.24g KH₂PO₄ in 1 litre of water, pH 7.4). After centrifugation at 6000rpm for 10 minutes, the cells were resuspended in 2 volumes (v/w) buffer A (75mM Tris·HCl pH 8.0, 0.1mM EDTA, 10µg/ml of aprotinin and 1mM PMSF). The suspension was used to measure the content of b5 in intact cells.

The host strain (BL21(DE3)pLysS and HMS174(DE3)pLysS), media (LB and TB), induction time (0-41 hours), induction temperature (24°C, 27°C and 28°C) and the concentration of IPTG (0.1mM, 0.5mM and 1mM) were optimised.

2.4.2.3 The preparation of cytochrome b5 by large-scale culture

Cytochrome b5 was expressed under the optimal condition based on the previous experiment. A single colony (HMS174 (DE3) pLysS + pRSET b5 sense) was picked from Chl/Amp plate and inoculated into 20ml LB broth containing 100µg/ml Amp and 34µg/ml Chl. The inoculums were incubated overnight at 37°C but no shaking was used. The overnight cultures were inoculated into 2 litres TB broth containing 100µg/ml Amp and 34µg/ml Chl with 0.3% (v/v) rare salt. The inoculums were incubated at 37°C with vigorous shaking (220rpm) until OD₆₀₀ reached 0.5-1.0. Cultures were cooled down to 27°C and 0.1mM IPTG was added to induce expression of b5. The shaking speed was kept at 125rpm. After 24 hours, the cells were harvested by centrifugation at 6,000rpm for 20 minutes. The supernatant was

decanted and the pellet was washed with 5 volumes of PBS (w/v). The suspension was again centrifuged at 6,000rpm for 20 minutes. The cells were resuspended in 50ml of buffer A and stored at -80°C for future use.

The cells were thawed at room temperature then frozen and thawed again. Bacteria were broken by sonication for 9×30 seconds and then the suspension was centrifuged at 12,000g for 20 minutes. The pellet was resuspended in 10ml buffer A and again sonicated for 9×30 seconds. The supernatants were combined and centrifuged for 1 hour at 100,000g. The pellets were collected and washed with 10 ml buffer B (20mM Tris·HCl pH 8.0, 1.9µg/ml Aprotinin and 20% glycerol). The membrane-binding b5 fractions were suspended in 10 ml buffer B. Membrane-binding b5 was solubilised in 1% Chaps (w/v). The sample was stirred in the ice bath for 1 hour and then the solubilised b5 was recovered by centrifugation at 100,000g for 1hour again. The supernatant was collected.

The His-binding resin (Novagen) was used to purify b5 as described in section 2.3.4.1 because the recombinant b5 contains (His)₆ tag. The components of buffer are listed below.

Table 2-2. The components of buffer for purifying cytochrome b5

	Components*
Bind Buffer	5mM imidazole, 500ml NaCl, 20mM Tris·HCl pH 8.0
Wash Buffer	100mM imidazole, 500ml NaCl, 20mM Tris·HCl pH 8.0
Elute Buffer	250mM imidazole, 500ml NaCl, 20mM Tris·HCl pH 8.0

*All buffers contained 20% glycerol (v/v), 0.05% Chaps and 1.9µg/ml Aprotinin.

The purified b5 was checked by 12% SDS-PAGE. The fraction containing b5 was combined and dialysed for 24 hours in the buffer C (10mM potassium phosphate buffer, pH7.5, 20% glycerol, 0.5mM EDTA, 0.1mM DTT and 0.05% Chaps) to remove the imidazole. The purified b5 was stored at -80°C.

2.5 Expression of human cytochrome P450 Reductase (CPR)

2.5.1 Expression of recombinant CPR

The plasmid pB55 containing human CPR cDNA was transferred in JM109 as described in section 2.2.10. A single colony was picked from the plate and inoculated in 5ml of LB containing 100µg/ml Amp. The inoculum was cultured at 37°C overnight. The overnight culture was diluted 500 fold in TB media. The bacteria grew up until the OD₆₀₀ reached about 0.6. Expression of CPR was induced by adding 0.25mM IPTG, and then culture was left at 28°C overnight. The shaking speed was kept at 120rpm.

The bacteria were harvested by centrifugation at 4,000g for 20 minutes. The pellets were suspended in 100mM Tris-acetate, pH 7.6, 500 mM sucrose and 0.5 mM EDTA. The suspensions were kept on ice for 20 minutes, and then diluted with an equal volume of water containing 0.1 mg/ml lysozyme. After bacteria were incubated on ice for 30 minutes, the protoplast was recovered by centrifugation at 4,000g for 10 minutes. Pellets were resuspended in 20mM Tris-HCl, pH 8.0, 10% glycerol (v/v), 150 mM NaCl, 1mM DTT, 0.1 mM PMSF and 1µg/ml of aprotinin, leupeptin and pepstain. This suspension was sonicated (40% power, 8×25 seconds), and then centrifuged at 12,000g for 20 minutes. The supernatant was collected, and then centrifuged at 100,000g for 1 hour. The pellets were resuspended in 100mM potassium phosphate buffer buffer, pH 7.4 with 20% glycerol. The samples were diluted to 2 mg protein/ml by the same buffer. CPR was solubilised in 0.2% (v/v) Triton X-100 by stirring on ice for one hour. The insoluble part was removed by

centrifuge at 100,000g for 1 hour. The solubilised CPR was stored at -80°C until purification.

2.5.2 Affinity purification of CPR

The recombinant human CPR was purified by 2', 5'-ADP agarose. The solubilised CPR was loaded on 2', 5'-ADP agarose column, which was previously equilibrated in 50 mM Tris-HCl, pH 7.4, 20% glycerol, 0.1 mM DTT, 0.1% (v/v) Triton X-100. The affinity column was washed with 10× bed volume of the same buffer. CPR was eluted by 5 mM 2'-AMP, 50 mM Tris-HCl, pH 7.4, 20% glycerol, 0.1 mM DTT, 0.1% (v/v) Triton X-100. The purified CPR protein was loaded on the PD-10 column and eluted by 20mM potassium phosphate buffer, pH 7.4, 20% glycerol as described in section 2.3.5. The purified CPR was then stored at -80°C.

2.5.3 Assay method (reduction of cytochrome c)

Cytochrome P450 reductase can reduce cytochrome c in the presence of NADPH. Therefore, the activity of CPR is determined by measuring reduction of cytochrome c (Strobel and Gignam, 1978). The solution containing 300mM of potassium phosphate buffer, pH 7.7, 40µM of cytochrome c and the CPR sample was made according to the reference (Strobel and Dignam 1978). The reaction was started by adding NADPH to the final concentration of 0.1mM. The absorbance at 550nm was recorded. The extinction coefficient of $21\text{cm}^{-1}\text{ mM}^{-1}$ (Williams and Kamin, 1962) at 550nm was used to calculate the rate of reduction of cytochrome c.

2.6 Expression of CYP4A1

2.6.1 Spectrophotometer measurement

2.6.1.1 The P450 assay

The content of P450 was determined by using Omura and Sato's method. (Omura and Sata, 1964) The sample was diluted to 2ml with 20mM potassium phosphate buffer (pH 7.5), 20% glycerol. A few milligrams of sodium dithionite were added to the solution to reduce the iron in P450. The sample was incubated at room temperature for 1 minute to permit the reaction to finish. Then the solution was divided into equal amounts, the sample and reference. The baseline was recorded by scanning samples from 400nm to 500nm. The sample cuvette was taken out and the sample solution was gently aerated with carbon monoxide (CO) for one minute. The P450-CO compound was scanned again from 400nm to 500nm. The concentration of P450 was calculated by using extinction coefficient of $91\text{mM}^{-1}\cdot\text{cm}^{-1}$ (Omura et al., 1964)

2.6.1.2 The absolute spectrum and substrate binding difference spectrum

The absolute spectrum was obtained by scanning P450 from 350nm to 600nm. 20mM potassium phosphate buffer (pH 7.5) with 20% glycerol was used as the reference.

The difference spectra between P450 with and without substrate was recorded according to the reference (Jefcoate 1978). Lauric acid and dodecyltrimethyl-ammonium bromide were used as the substrates. The structures of substrates are shown in Figure 2-1.

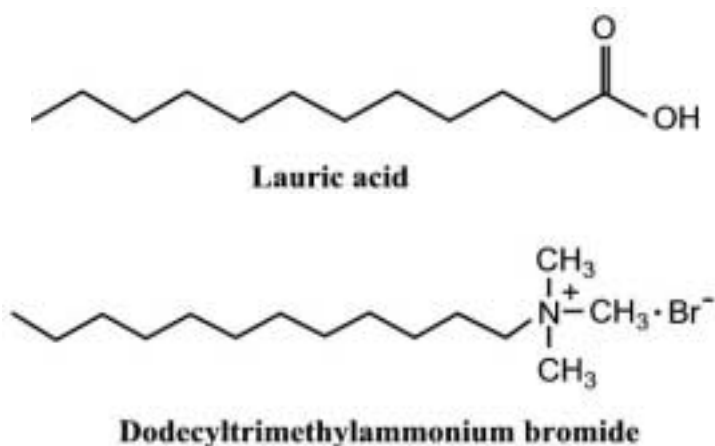


Figure 2-1. Structures of lauric acid and dodecyltrimethylammonium bromide.

Lauric acid carries the carboxyl group and dodecyltrimethylammonium bromide carries the positively charged amine group. Both substrates contain a twelve-carbon chain.

Substrates used in this experiment were dissolved in solvent shown in Table 2-3.

Table 2-3. Substrates dissolved in solvents

Substrates	Solvent
Lauric acid	Dimethylsulfoxide (DMSO)
Dodecyltrimethylammonium bromide	UHP water

Both the P450 solution and phosphate buffer (20mM potassium phosphate buffer, pH 7.5, 20% glycerol) were divided into two cuvettes. The substrate, lauric acid, was titrated into the P450 solution in the sample cell and phosphate buffer in the reference cell (see Figure 2-2). The total volume change was kept at less than 1%. The spectrum was then recorded by scanning from 350nm to 500nm. The procedure was then repeated using dodecyltrimethylammonium bromide as the substrate.

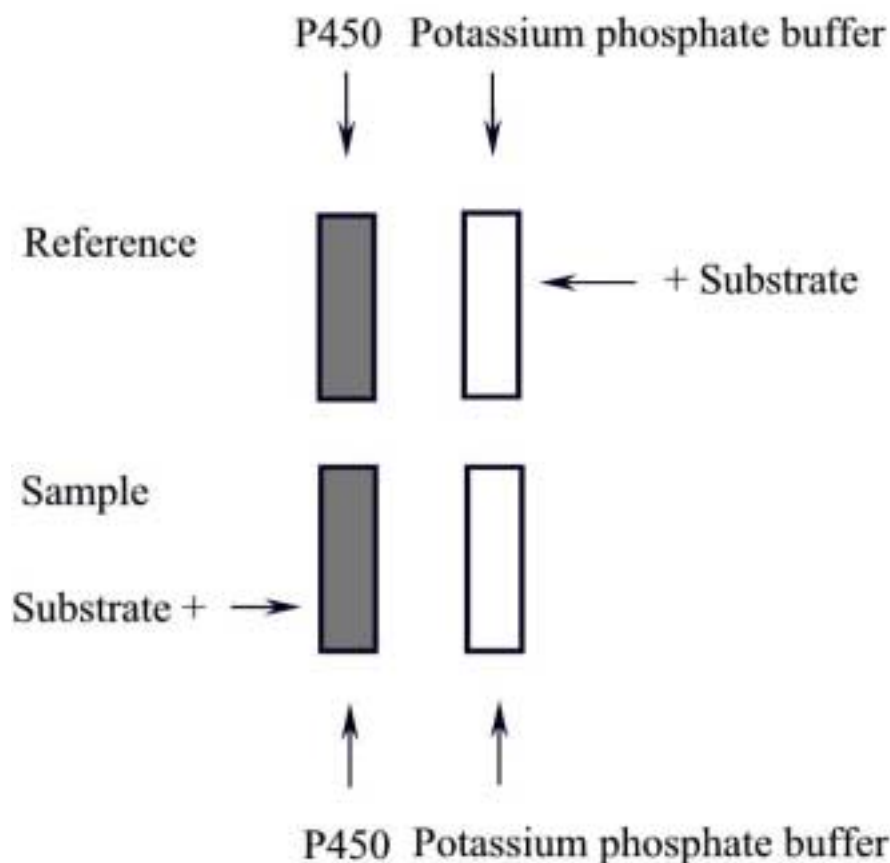


Figure 2-2. Measurement of difference spectra of substrate binding.

The cuvettes containing P450 are grey; cuvettes containing potassium phosphate buffer with 20% glycerol are white. The substrates are added in sample and reference as shown by arrows.

The K_s (spectral dissociation coefficient) values of substrates binding to P450s were calculated from the different absorbance between the trough (around 390nm) and the peak (around 420nm).

K_s was defined as below (Alterman *et al.* 1995; Chaurasia *et al.* 1995).

$$K_s = \frac{[E][S]}{[ES]}$$

[E]: the concentration of the free enzyme,

[S]: the concentration of the free substrate,

[ES]: the concentration of enzyme and substrate complex

K_s values were determined by fitting the equation, $Y=a*X/(K_s+X)$, with the assumption that total substrate concentration is much higher than P450 concentration. (Alterman *et al.* 1995; Chaurasia *et al.* 1995)

Y: $A_{390}-A_{420}$

X: the concentration of substrate

2.6.2 Expression of CYP4A1

Owing to the difficulty of expressing CYP in a bacterial system, the N-terminal sequence of CYP was often modified. The new strategy to express P450 in *E.coli* was developed by using fusion protein of OmpA with CYP (Pritchard *et al.* 1997). This strategy could minimise the change of sequence. It was supposed to give the high level expression because 1) OmpA was one of abundant protein in *E.coli*, which was easy to be expressed, 2) OmpA also was the signal protein that could lead the target protein to the periplasm to avoid proteolysis (Pritchard *et al.* 1997). In order to obtain enough CYP4A1, the OmpA-CYP4A1 fusion system was constructed to express recombinant CYP4A1 in *E.coli*.

2.6.2.1 Construction of the plasmid pGEM-T.OmpA.4A1.HT

OmpA fragment was obtained from JM109 chromosome by PCR. The primers are shown below. The *Nde I* site in the left primer and *Sac I* site in the right primer are underlined.

OmpA-Left (Forward): GGAATTCCATATGAAAAAGACAGCTATCGCG
OmpA-Right (Reverse): GAGCTCGCGCCTGCGCTACGGTAGCGA

The PCR was performed in presence of *pfu*. The cycles were as follows: 94°C for 1 minute, 50°C for 1 minute and 72°C for 1 minute for 25 cycles. The approximate 70bp PCR product was cloned in pGEM-T plasmid.

CYP4A1 DNA fragment was amplified from CYP4A1 cDNA by PCR. The primers are shown below. The *Sac I* site in the forward primer and *Nde I* site in the reverse primer are underlined.

5'CYP4A1(Forward): ATGAGCGTCTCTGCACTGAGCTCCACCCGC
3'CYP4A1(Reverse): ATTTCTGGAGCTCCACATCCATATGGTGGAGCTTCTT
GA

The PCR product of approximately 1500bp was cloned in pGEM-T easy plasmid.

The plasmid pGEM-T Easy containing CYP4A1 cDNA was digested by *Nde I*, which produced the AT and TA hangs. The synthetic oligos containing (His)₆ tag and *Xba I* site (see below) were inserted into the *Nde I* site. Six-histidine tag is shown in bold and *Xba I* site is underlined.

TATTCACCATCACCATCACCATTGATCTAGA
AAGTGGTAGTGGTAGTAGTAACTAGATCTAT

The fragment of *CYP4A1* with (His)₆ tag DNA (*CYP4A1.HT*) was lifted from plasmid pGEM-T Easy/*CYP4A1.HT* by *Sac I* digest. This approximately 1500bp *CYP4A1.HT* fragment was gel-purified as described in section 2.2.8, and inserted in the *Sac I* site of pGEM-T/*OmpA* plasmid. The strategy of constructing pGEM-T/*OmpA.4A1.HT* plasmid is shown in Figure 2-3.

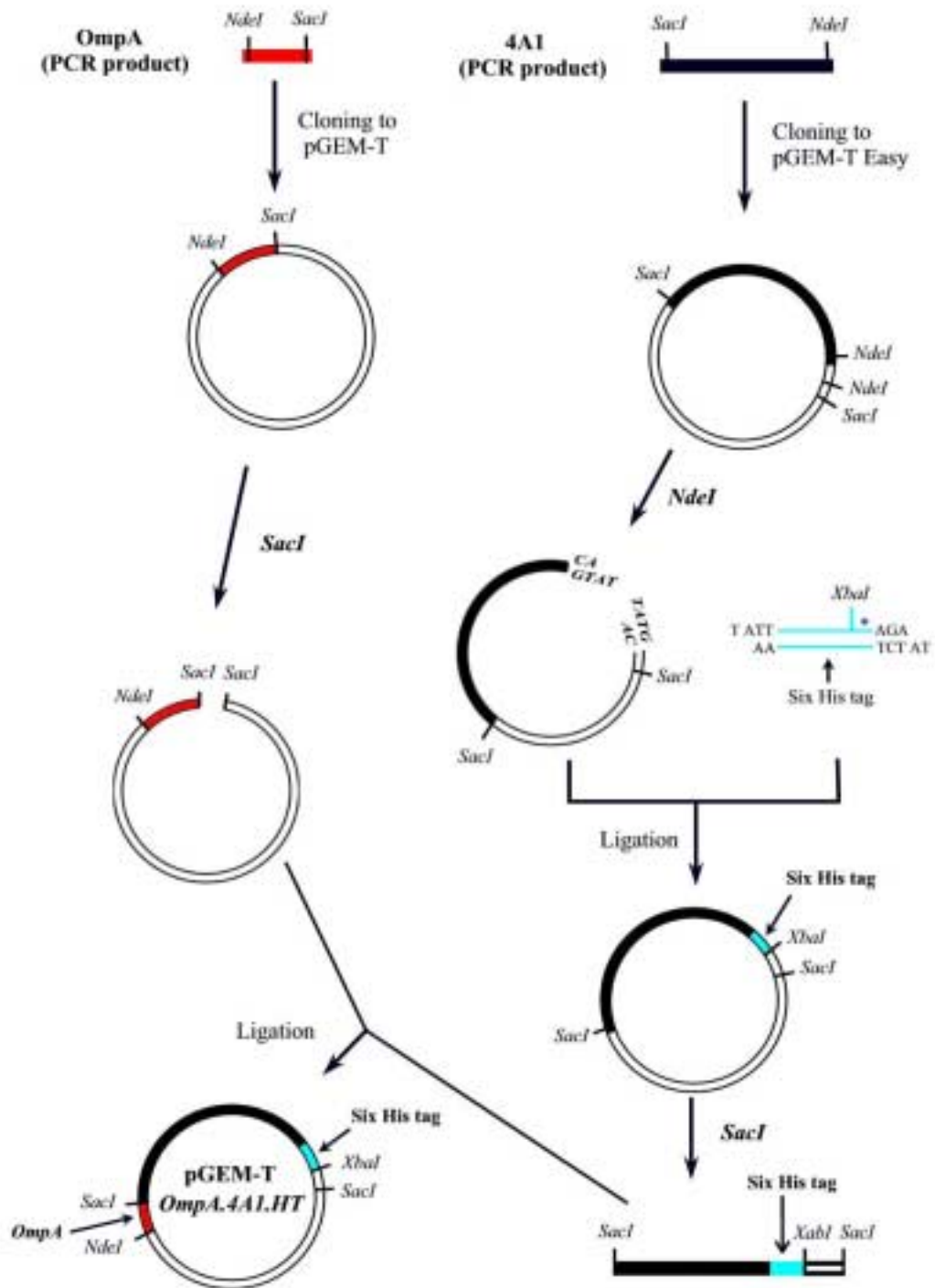


Figure 2-3. Construction of plasmid pGEM-T.OmpA.4A1.HT.

The *OmpA* sequence is determined by the red filling. Six Histidine tag is determined by the blue filling. *CYP4A1* cDNA is determined by the black filling. *Nde I*, *Sac I* and *Xba I* sites are labelled. The stop code in six-histidine tag oligo is shown as the star.

2.6.2.2 Subcloning: Construction of pCWori⁺/OmpA.4A1.HT plasmid

The plasmid pGEM-T containing *OmpA.4A1.HT* (CYP4A1 cDNA with the *OmpA* leader sequence and a C-terminal six histidine tag) and the plasmid pCWori⁺ containing the N-terminally modified CYP4A1 were digested with *Nde I* and *Xba I*. The reaction products were separated by electrophoresis on a 1% TAE agarose gel. Gel containing the approximate 6000bp DNA fragment from pCWori⁺ and the approximate 1600bp fragment from pGEM-T were excised and placed in clean eppendorf tubes.

DNA fragments were purified by GENECLLEAN II kit (BIO 101 inc.) as described in section 2.2.8.1. The DNA fragments were ligated using T4 ligase. The ligation mixture was incubated at 4°C for 21 hours. The mixture was directly transferred into SCS110 competent cells.

The desired plasmid was identified by *Sac I* digest (Figure 2-4). The *OmpA* sequence was confirmed by DNA sequencing.

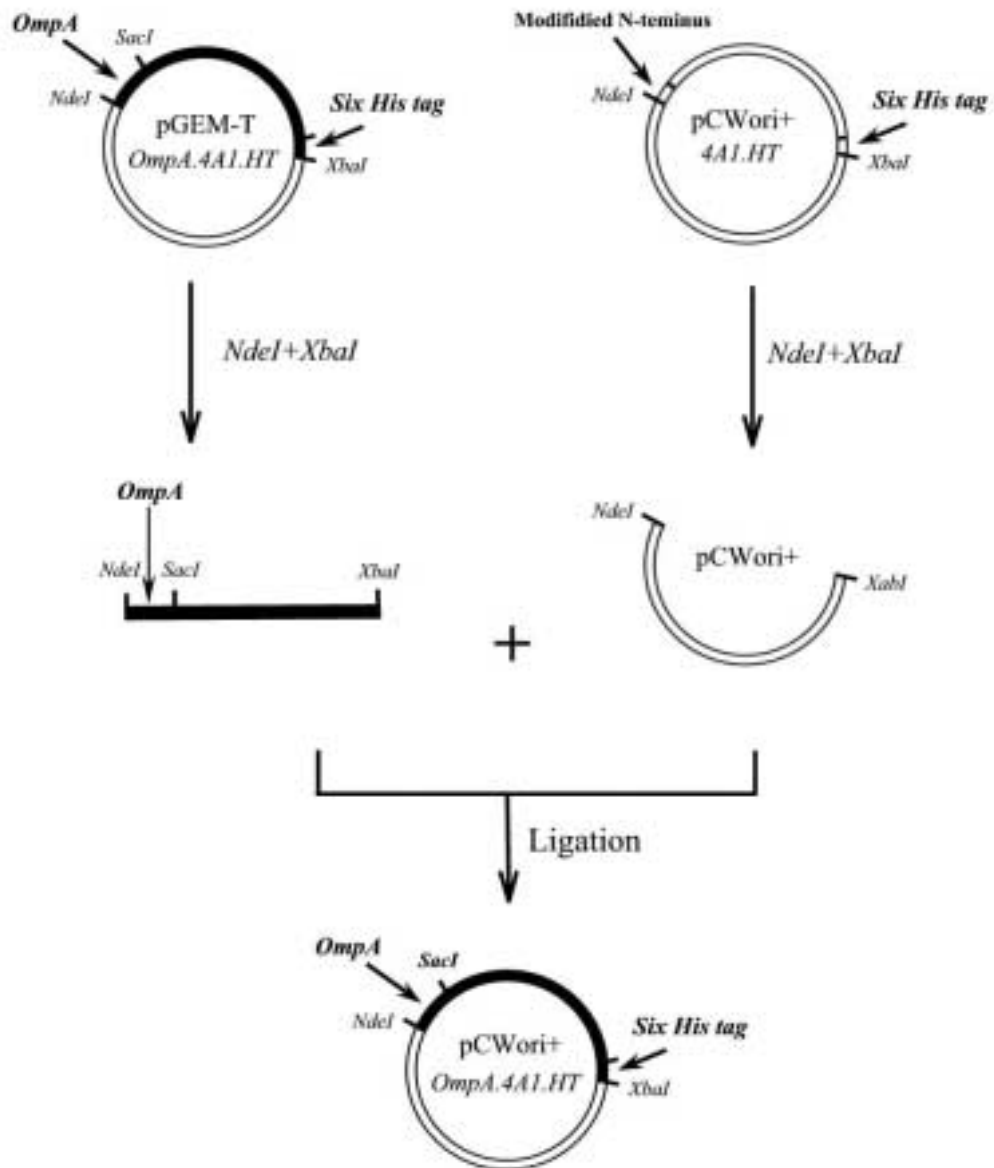


Figure 2-4. Construction of pCWori⁺.OmpA.4A1.HT plasmid.

The *OmpA.4A1.HT* sequence is determined by the black filling. The *OmpA.4A1.HT* fragment was obtained by *Nde I* and *Xba I* double digest, and then subcloned into the plasmid pCWori⁺. The new plasmid (pCWori⁺.*OmpA.4A1.HT*) contains the new *Sac I* site from the *OmpA.4A1.HT* sequence.

2.6.2.3 Expression and purification of OmpA.CYP4A1.HT

The plasmid pCWori+/OmpA.CYP4A1.HT was prepared by QIAGEN-tip 500 kit as described in section 2.2.4.3. The plasmid was transformed into *E.coli*. A fresh transformed colony was picked and inoculated into 5mls of LB containing 100µg/ml Amp. The saturated overnight culture (0.05%, v/v) was inoculated into TB or LB broth and grown at 37°C until the OD₆₀₀ reached 0.1. At this point, δ-ALA was added into the culture. When the OD₆₀₀ was 0.3 to 0.6, IPTG was added to induce expression. The cells were incubated at 28°C by shaking at 120rpm until harvested. The choice of host cells (XL-1 and JM-109), induction time (17, 24, 41 and 48 hours), the concentration of IPTG (0.1mM and 1mM) and δ-ALA (0, 80, 160 and 300µg/ml) were optimised.

Bacteria were harvested by centrifugation at 6,000rpm for 20 minutes, and the pellet was suspended in 40ml buffer A (100mM Tris·HCl pH 7.8, 0.5mM EDTA pH 8.0, 20% glycerol, 1mM PMSF, 1µg/ml aprotinin and 1mM DTT). Lysozyme (10mg/ml) was added to the suspension to final concentration 0.5mg/ml. The solution was gently stirred on ice for 1 hour, and then centrifuged at 6000rpm for 30 minutes. The pellet was resuspended in 30ml sonication buffer (10mM Tris·HCl pH 7.4, 0.1mM EDTA, 1mM PMSF, 1µg/ml aprotinin and 10% glycerol), and sonicated for 8×30 seconds. The cell debris and unbroken cells were removed by centrifugation at 12,000rpm for 20 minutes.

The pellet was resuspended in sonication buffer and sonicated again. The combined 12,000g supernatant were centrifuged at 100,000g for 1 hour. The membrane pellet was suspended in 0.1M potassium phosphate buffer (pH 7.4) buffer with 20%

glycerol. The P450 was solubilised in detergent by gently stirring for 1 hour. The use of detergent was optimised. The debris was removed by centrifugation at 100,000g for 1hour. The supernatant containing P450 was stored at -80°C until purified.

The solubilised P450 was purified by nickel affinity resin as described in section 2.3.4. The buffers, which were used in purification of CYP4A1, were shown in Table 2-4 and Table 2-5.

Table 2-4. The components of buffer of purification by His•Bind resin

	Components*
Bind Buffer	5mM imidazole, 500mM NaCl, 20mM Tris-HCl pH 8.0
Wash Buffer	75mM imidazole, 500mM NaCl, 20mM Tris-HCl pH 8.0
Elute Buffer	750mM imidazole, 500mM NaCl, 20mM Tris-HCl pH 8.0

*All buffers contained 20% glycerol (v/v) and 0.1% (v/v) Emulgen 913

Table 2-5. The components of buffer of purification by Ni-NTA His•Bind resin

	Components*
Bind Buffer	10mM imidazole, 300mM NaCl, 50mM NaH ₂ PO ₄ , pH 8.0
Wash Buffer	20mM imidazole, 300mM NaCl, 50mM NaH ₂ PO ₄ , pH 8.0
Elute Buffer	250mM imidazole, 300mM NaCl, 50mM NaH ₂ PO ₄ , pH 8.0

*All buffers contained 20% glycerol (v/v) and 0.1% (v/v) Emulgen 913

The fractions were checked by 10% SDS-PAGE. The fractions containing pure CYP4A1 were combined. The salt and imidazole were removed by PD-10 column (Pharmacia). The purified P450 was stored in 20mM potassium phosphate buffer (pH 7.4) with 20% glycerol at -80°C for future analysis.

2.7 Construction of mutants of CYP4A1

2.7.1 Site-directed mutagenesis

The GeneEditor™ *in vitro* Site-Directed Mutagenesis system (Promega) was used to generate mutations. This system provided selection oligonucleotides that modify the ampicillin resistance gene and result in the resistance to GeneEditor™ Antibiotic

Selection Mix. The Selection Oligonucleotide is annealed to the plasmid template at the same time as a mutagenic oligonucleotide. Therefore, a high frequency of mutants is obtained by selection of Antibiotic Mix resistance.

The procedure of mutagenesis was performed according to the manufacturer's instruction. The DNA template was prepared by QIAprep Miniprep system (Qiagen) as described in section 2.2.4.2. The plasmid template was chosen as in Table 2-6.

Table 2-6. Templates for mutants

Mutants	Templates
K93E	pGEM-11/4A1
F149Y	pGEM-T Easy/4A1
F149I	pGEM-11/4A1
R87E	pCWori+/OmpA.4A1.HT
R87E/K93E	pCWori+/OmpA.K93E.HT
R87W/K93E	pCWori+/OmpA.K93E.HT
N116E	pCWori+/OmpA.4A1.HT
N116E/K93E	pCWori+/OmpA.K93E.HT
H141R	pCWori+/OmpA.4A1.HT
H141F	pCWori+/OmpA.4A1.HT
H141L	pCWori+/OmpA.4A1.HT
R142A	pCWori+/OmpA.4A1.HT
R143A	pCWori+/OmpA.4A1.HT

The double stranded plasmid DNA was denatured by alkaline treatment. The reaction was set up in the eppendorf as shown in Table 2-7.

Table 2-7. Denaturation of the plasmids

dsDNA template	10 μ l (0.5pmol)
2M NaOH, 2mM EDTA	2 μ l
Sterile, deionised water	8 μ l

The mixture was incubated at room temperature for 5-10 minutes. 2 μ l of 2M ammonium acetate (pH 4.6) was added to the eppendorf then 75 μ l of 100% ethanol was added to precipitate DNA. The eppendorf was incubated at -80°C for 30

minutes. The denatured DNA was recovered by centrifugation at 14,000rpm for 15 minutes at 4°C. The supernatant was removed and the pellet was washed using 200µl of 70% ethanol. The eppendorf was again centrifuged at 14,000rpm for 15 minutes again. The ethanol was drained and the pellet was air-dried. The DNA was resuspended in 100µl of TE buffer (pH 8.0) and stored at -20°C. The denatured DNA could be analysed on an agarose gel because the denatured, single-stranded DNA will run faster than non-denatured, double-stranded DNA, and denatured DNA appears more smeared.

The hybridisation reaction was set up as described in Table 2-8. The mutagenic oligo-nucleotides were designed to hybridise to either coding or non-coding strand of denatured plasmids were listed in Table 2-9.

Table 2-8. The hybridisation reaction

Template DNA	5µl
Selection Oligonucleotide, 5'-phosphorylated	1µl
Mutagenic oligonucleotide, 5'-phosphorylated	Various
10× Annealing buffer*	2µl
Sterile, deionised water	To a final volume of 20µl

*10× Annealing Buffer: 200mM Tris·HCl (pH 7.5), 100mM MgCl₂, 500mM NaCl

Table 2-9. The oligonucleotides for mutagenesis

	Mutagenic oligonucleotides*
R87E (non-coding) ¹	CAATTAAGTA AaGCTTT GCTTCCCCAGAACCA Attc AGGAAAGG
R87E/K93E (non-coding) ²	CAATTAAGTA AaGCTTcGGAT CCCCAGAACCA Attc AGGAAAGG
R87W/K93E (coding) ²	CCAAGTGCCTTTCTC ttg TGGTTCTGGGG AtcCgaaGct TACTTA ATTGTCTATG
H141R (coding) ³	CCGTGGTTCCAG cg tCGGCCGAATGCTAACC
H141L (coding) ³	CCGTGGTTCCAG ctg CGGCCGAATGCTAACC
H141F (non-coding) ⁴	GGTTAGCATTCGCC Gaaa CTGGAAC CgTG GTTCTCC
R142A (non-coding) ⁴	GGTTAGCATAC Gagc GTGCTGGAAC CaTG GTTGTCC
R143A (non-coding) ⁴	GGTTAGCAT agc CCGGTGTGGAAC CaTG GTTGTCC
N116E/K93E (non-coding) ⁴	CCATATCCGAT CCaTG GAGCTAGCAATCTGTAGACGCC ttc GG CCTTTGG
N116E (non-coding) ⁵	GCAATCTGTAGACGCC ttc GGCCTTT GGATC cgATCGCCCCG
K93E (non-coding) ⁵	CAATTAAGTAGGCT TTcGGAT CCCCAGAACC
F149Y (non-coding) ⁶	GGTTTCAG gATaTC ATAGTGG At GGCTGGGGTTAGC
F149I (non-coding) ⁶	GGTTTCAG gATaTC ATAGTGG ta GGCTGGGGTTAGC

* The nucleotides that are different from wild type are showed by small letters. The mutations are underlined.

¹ The novel restriction enzyme (*Hind III*: AAGCTT) sites introduced by silent mutation is in bold.

² The novel restriction enzyme (*Hind III*: AAGCTT, *BamH I*: GGATCC) sites are in bold.

³ The *SgrA I* site (CPuCCGGPyG) in wild type was eliminated in mutants.

⁴ The novel *Nco I* site (CCATGG) introduced by silent mutation is in bold.

⁵ The novel *BamH I* site (GGATCC) is in bold.

⁶ The novel *EcoR V* site (GATATC) is in bold.

Typically, three reactions were carried out at the same time. Each reaction contained a different amount of mutagenic oligonucleotide (eg. 2µl, 4µl, 6µl). 2 litres of water were heated in a microwave oven to around 90°C. The reaction mixtures were incubated in the hot water and then these were allowed to cool down to 37°C at room temperature. Once the temperature cooled to 37°C, then the following components were added in the order listed in Table 2-10.

Table 2-10. The synthesis reaction of mutants

Sterile, deionised water	5µl
10× Synthesis Buffer*	1µl
T4 DNA Polymerase	1µl (5-10u)
T4 DNA ligase	1µl (1-3u)
Final volume	30µl

*10× Synthesis Buffer: 100mM Tris-HCl (pH 7.5), 5mM dNTPs, 10mM ATP, 20mM DTT

The eppendorfs were incubated at 37°C for 90 minutes, and then kept on ice until transformation. BMH 71-18 mutS competent cells were used for an initial transformation to enhance the efficiency of mutagenesis because the mutS strain could reduce the chance of repairing mismatch in bacteria. The competent cells were thawed on ice and transferred into a pre-chilled eppendorf. Typically, 5µl of mutagenesis reaction was added into 50µl BMH 71-18 mutS competent cells. The transformation was described in section 2.2.10. 950µl of LB was added into the cells and incubated at 37°C for 1 hour. 1ml of mixture was transferred into the tube, and 4ml of LB containing 50µl GeneEditor™ Antibiotic Selection Mix was added. The culture was incubated at 37°C with shaking (220rpm) for 16-18 hours.

The DNA plasmid from overnight culture was purified by QIAprep Miniprep (Qiagen). 5-10ng of plasmid DNA was transferred into 50µl of JM109 competent cells. 100-200µl of cells were spread on two LB plates containing 190µl GeneEditor™ Antibiotic Selection Mix and 50µl of 100mg/ml ampicillin in 50ml LB agar. The plates were incubated at 37°C overnight. Colonies were picked from the plates and inoculated in 5ml of LB. The plasmid was purified by alkaline lysis method. The mutant was screened by the novel incorporated or deleted restriction site. All mutants sequences were confirmed by DNA sequencing.

2.7.2 Subcloning K93E mutant

In order to express the K93E mutant, the fragment containing the K93E mutant needed to be subcloned into plasmid pCWori⁺ with OmpA sequence. The plasmid pGEM-T containing the OmpA leader sequence clone was digested with *Nde I* and *Afl III*, and the 277bp band was gel-purified as described in section 2.2.8. Plasmid

pGEM-11 containing the K93E mutant was digested with *Afl III* and *Nhe I*, and the 137bp band was gel-purified as described in section 2.2.8. Plasmid pCWori⁺ containing ambiguous 4A1 was digested with *Nde I* and *Nhe I*, and the approximate 6500bp band was gel-purified as described in section 2.2.8. All of gel-purified fragments were ligated using T4 DNA ligase at 4°C for 20 hours. The ligation mixture was transferred into XL-1 competent cells.

The recombinant construct was identified by the *Sac I* and *BamH I* sites (Figure 2-5). *OmpA* and K93E sequences were confirmed by DNA sequencing.

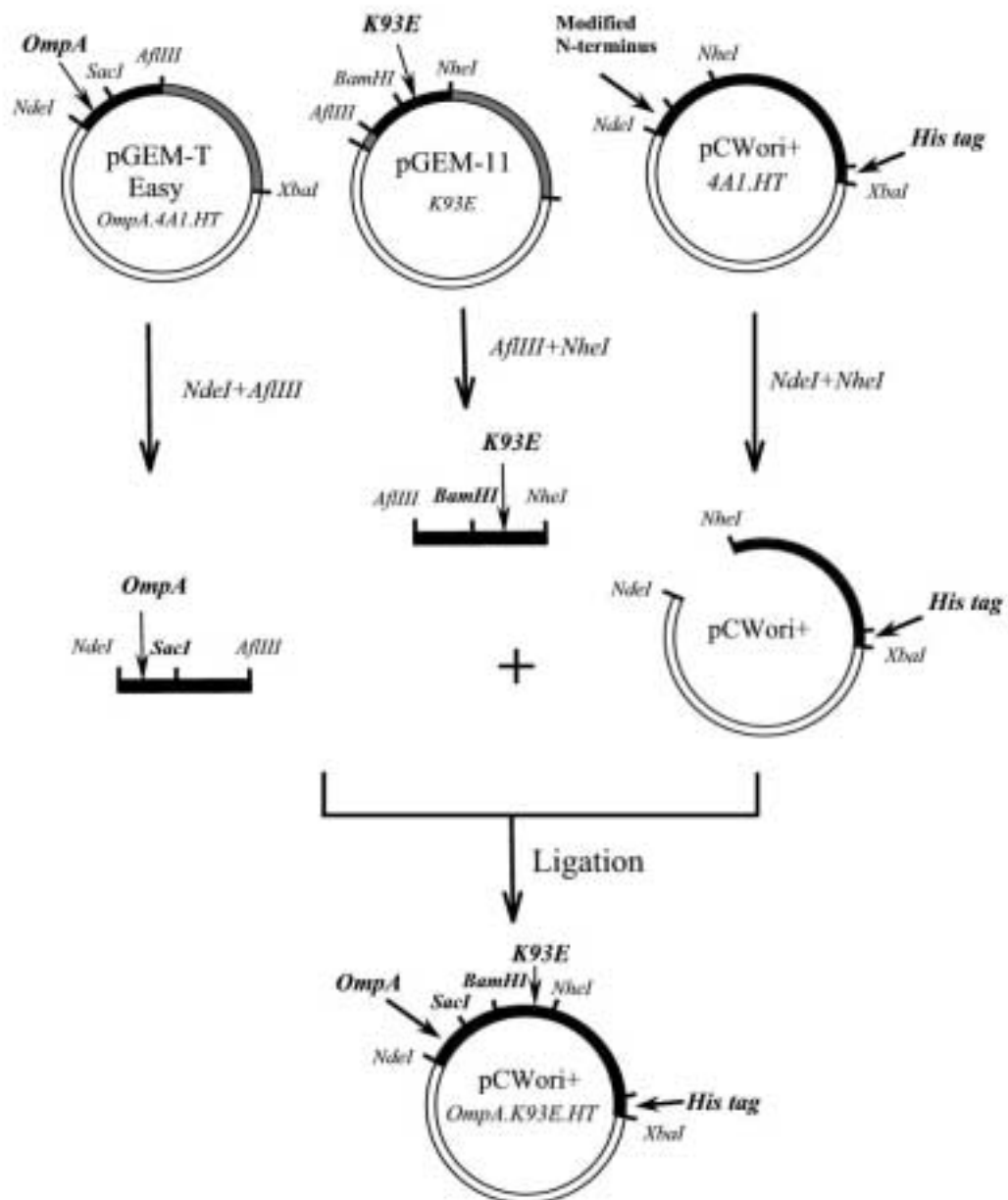


Figure 2-5. Construction of K93E mutant expression plasmid.

The DNA fragment containing *OmpA* sequence (the black filling) was obtained by *Nde I* and *Afl III* double digest. The fragment containing K93E mutant (the black filling) was obtained by *Afl III* and *Nhe I* double digest. These fragments were ligated with the plasmid pCWori⁺.4A1.HT that has been digested with *Nde I* and *Afl III*. The black filled part is the sequence of modified 4A1 with His tag. The new plasmid contained the new *Sac I* site from the *OmpA* sequence and *BamH I* site from the K93E fragment.

2.7.3 Subcloning F149Y and F149I mutants

The F149Y and F149I fragments were subcloned into pCWori⁺ to express these mutants in *E.coli*. Plasmids containing F149Y and F149I mutants were digested with *Nhe I* and *EcoN I*, and the resulting 791bp fragments were gel-purified as described in section 2.2.8. Plasmid pCWori⁺.OmpA.4A1.HT was digested with *Nhe I* and *EcoN I*, and the approximate 6200bp fragment was gel-purified as described in section 2.2.8. The ligation was transformed into XL-1 Blue competent cells. The desired plasmid was identified by *EcoR V* digest (Figure 2-6 and 2-7). All constructs including *OmpA* and mutants, were confirmed by DNA sequencing.

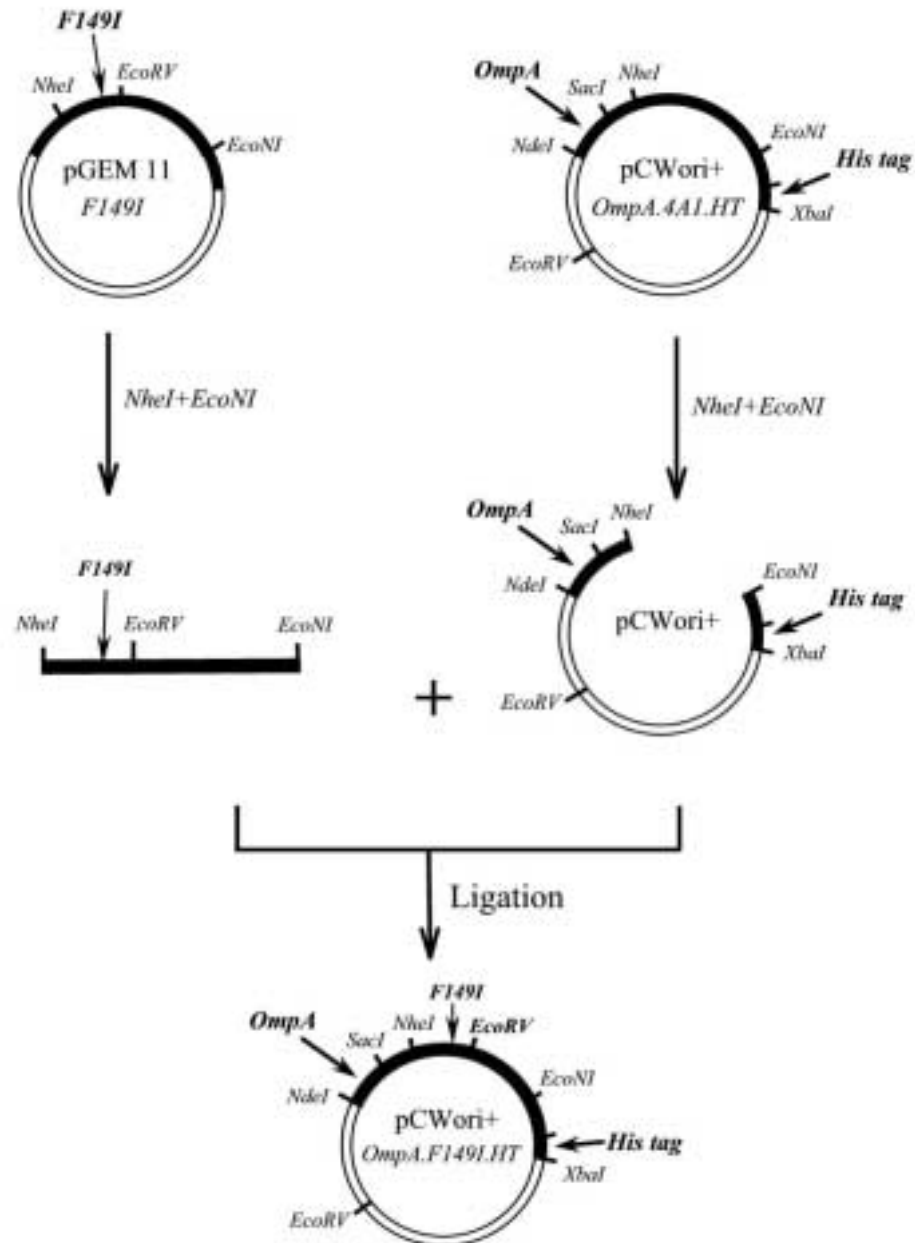


Figure 2-6. Construction of F149I mutant expression plasmid.

The F149I fragment (the black filled part) was obtained by *Nhe I* and *EcoN I* digest, and then subcloned into the plasmid pCWori+ (the black filled part is the *OmpA.4A1.HT* sequence). The new plasmid contains the second new *EcoR V* site from the F149I fragment.

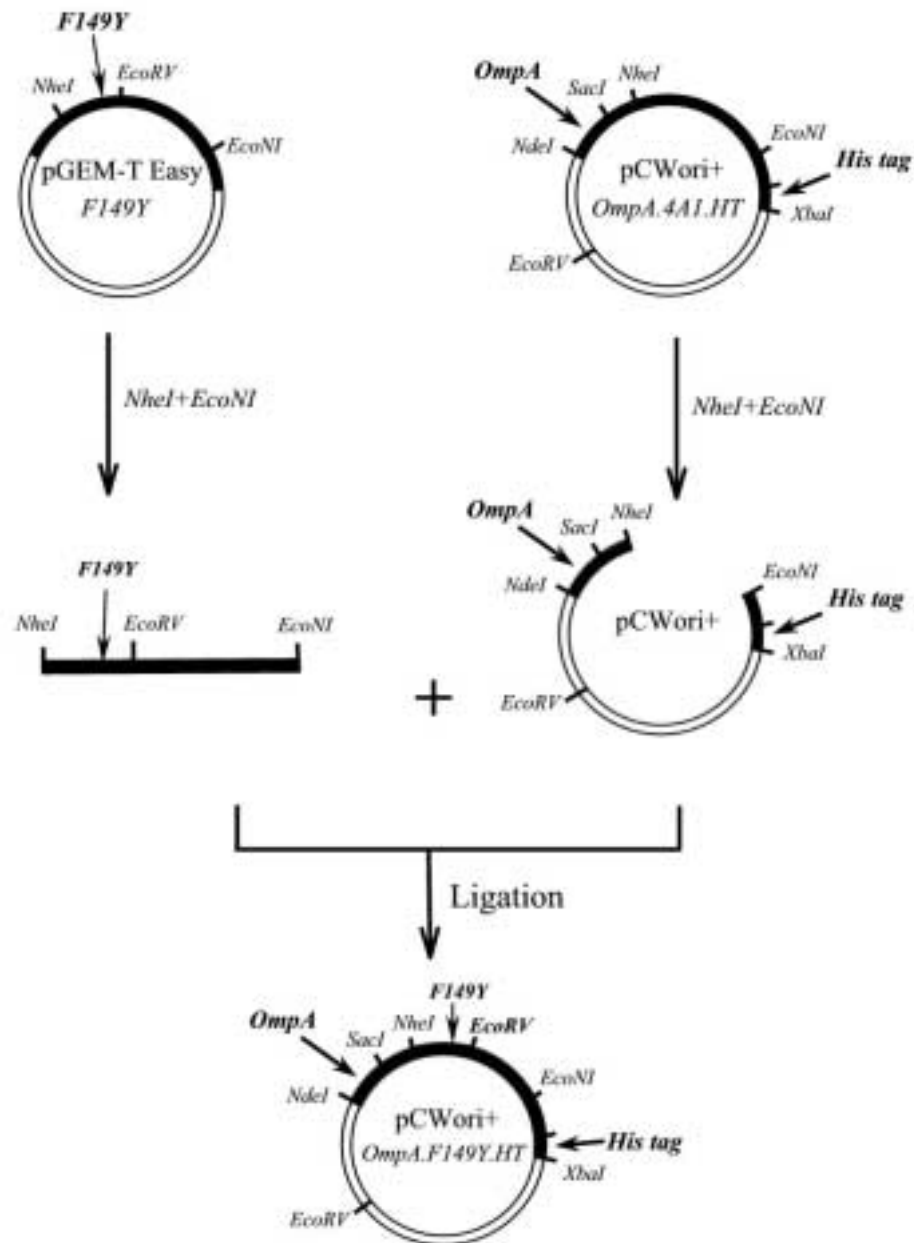


Figure 2-7. Construction of F149Y mutant expression plasmid.

The F149Y fragment (the black filled part) was obtained by *Nhe I* and *EcoN I* digest, and then subcloned into the plasmid pCWori+ (the black filled part is the *OmpA.4A1.HT* sequence). The new plasmid contains the second new *EcoR V* site from the F149Y fragment.

All mutants were expressed in *E.coli* and purified by nickel affinity chromatography as described in section 2.6.2.3 for expression and purification of OmpA.4A1.HT.

3 Results

3.1 Expression of cytochrome b5

3.1.1 Restriction enzyme analysis of pRSET cytochrome b5 sense and anti-sense plasmids

Human cytochrome b5 cDNA (a gift from Dr. W.L. Miller, California, USA) (Yoo and Steggles 1988) was previously cloned in the *EcoR I* site of plasmid pRSET-b in our laboratory. Human cytochrome b5 cDNA encodes 134 amino acids. The N-terminal fusion peptide from pRSET-b contained 44 amino acids including a six-histidine tag. Therefore, the whole cytochrome b5 fusion protein contained 178 amino acids as shown in Figure 3-1, which has the molecular mass of 20,196 Da.

```

ATGCGGGGTTCTCATCATCATCATCATCATGGTATGGCTAGCATGACTGGTGGACAGCAA
M R G S H H H H H H G M A S M T G G Q Q

ATGGGTCGGGATCTGTACGACGATGACGATAAGGATCCGAGCTCGAGATCTGCAGCTGGT
M G R D L Y D D D D K D P S S R S A A G

      EcoRI
      |
NcoI | |
      | |
ACCATGGAATTCATGGCAGAGCAGTCGGACGAGGCCGTGAAGTACTACACCCTAGAGGAG
T M E F M A E Q S D E A V K Y Y T L E E

ATTCAGAAGCACAACCACAGCAAGAGCACCTGGCTGATCCTGCACCACAAGGTGTACGAT
I Q K H N H S K S T W L I L H H K V Y D

      BstXI
      |
TTGACCAAATTTCTGGAAGAGCATCCTGGTGGGGAAGAAGTTTTAAGGGAACAAGCTGGA
L T K F L E E H P G G E E V L R E Q A G

GGTGACGCTACTGAGAACTTTGAGGATGTCTGGGCACTCTACAGATGCCAGGGAAATGTCC
G D A T E N F E D V G H S T D A R E M S

AAAACATTCATCATTGGGGAGCTCCATCCAGATGACAGACCAAAGTTAAACAAGCCTCCG
K T F I I G E L H P D D R P K L N K P P

```

```

GAAACTCTTATCACTACTATTGATTCTAGTTCCAGTTGGTGGACCAACTGGGTGATCCCT
E T L I T T I D S S S S W W T N W V I P
                                     EcoRI
                                     |
GCCATCTCTGCAGTGGCCGTCGCCTTGATGTATCGCCTATAACATGGCAGAGGACTGAGAA
A I S A V A V A L M Y R L Y M A E D *

TTCGAAGCTTCA

```

Figure 3-1. Sequence of cytochrome b5 fusion.

The nucleotide and amino acids sequences of cytochrome b5 are shown in bold. The stop code is shown as a star. The six histidine tag in the N-terminal fusion peptide is underlined. The *EcoR I*, *Nco I* and *BstX I* sites are shown in the nucleotide sequence.

The orientation of cytochrome b5 cDNA insertion was identified by double digestion with *BstX I* and *Nco I* (Figure 3-2).

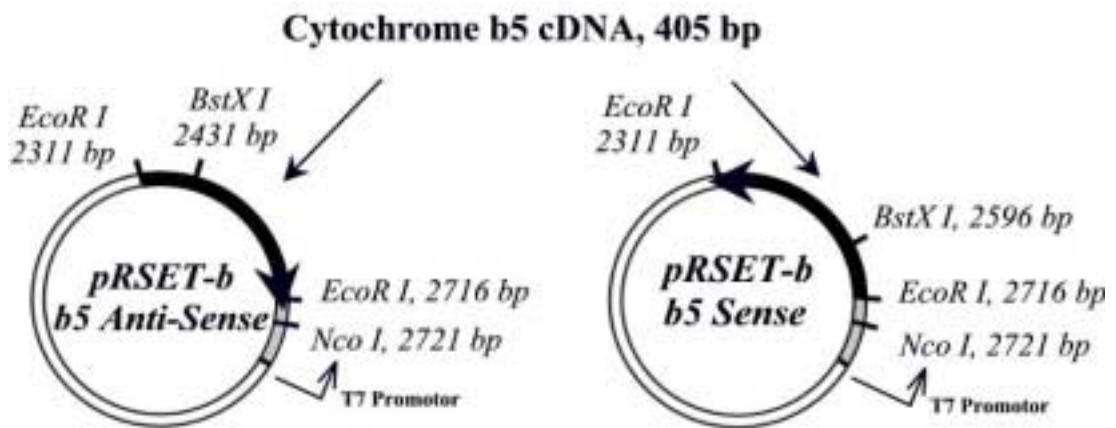


Figure 3-2. Maps of plasmids pRSET-b b5 Sense and Anti-Sense.

Cytochrome b5 cDNA (black filled part) was inserted in the *EcoR I* site of pRSET-b plasmid. The arrows show the orientation of cytochrome b5. The N-terminal fusion peptide including a six histidine tag in plasmid pRSET-b (grey filled part) is positioned upstream of cytochrome b5. The positions of *BstX I* site in cytochrome b5 and *Nco I* site in pRSET-b are labelled. The fragments of double digestion with *BstX I* and *Nco I* in pRSET-b b5 sense and anti-sense are 125bp and 290bp, respectively.

According to the nucleotide sequences of cytochrome b5 and pRSET-b, double digestion with *Nco I* and *BstX I* would give a 125bp fragment from the plasmid pRSET-b5 sense and a 290bp fragment from the plasmid pRSET-b5 anti-sense. An agarose gel of the digest with *Nco I* and *BstX I* showed that an approximately 100bp DNA fragment from pRSET-b5 sense and 300bp from pRSET-b5 anti-sense were

detected on the gel (Figure 3-3), which corresponded to the prediction. Therefore, the orientation of cytochrome b5 insertion was determined.

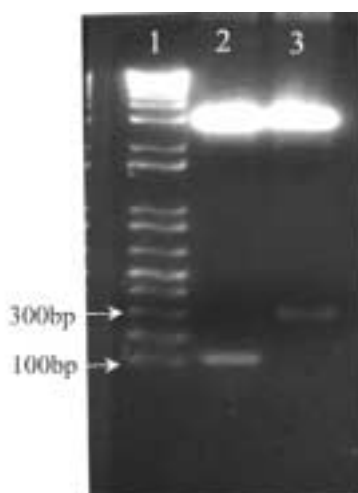


Figure 3-3. Restriction enzyme analysis of plasmid pRSET-b5 sense and anti sense.

The plasmids were digested with *Nco I* and *BstX I* at 37°C for 1 hour. DNA was separated on 1% agarose gel and stained by ethidium bromide. *Lane 1*, 1Kb plus DNA ladder, the positions of 100bp and 300bp DNA are labelled; *lane 2*, pRSET-b5 sense digested by *BstX I* and *Nco I*; and *lane 3*, pRSET-b5 anti-sense digested by *BstX I* and *Nco I*

3.1.2 Optimising expression of cytochrome b5

In order to maximally express recombinant cytochrome b5, a series of conditions, including host strain, media, induction time, induction temperature and the concentration of IPTG were optimised.

3.1.2.1 Host strain and media

BL21(DE3)pLysS and HMS174(DE3)pLysS were used to express cytochrome b5 in LB or TB. Expression was induced by 1mM IPTG at 24°C for overnight. The level of expression in HMS174(DE3)pLysS was similar to BL21(DE3)pLysS in LB but higher in TB (Figure 3-4). The highest level of expression was obtained in HMS174(DE3)pLysS cultured in TB .

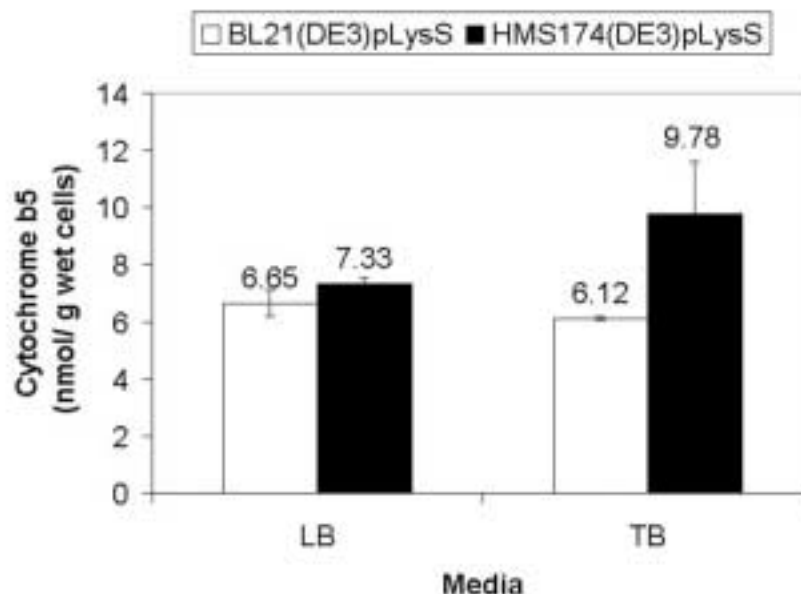


Figure 3-4. Effect of strains and media on expression of cytochrome b5.

BL21(DE3)pLysS and HMS174(DE3)pLysS containing plasmid pRSET-b5 Sense were grown in LB or TB. Expression was induced by 1mM IPTG at 24°C overnight. The values are the average of three separate experiments and standard deviation was used to represent variation. The content of cytochrome b5 in per gram wet cells was measured by difference spectrum (reduced minus oxidised) as described in Materials and Methods section 2.4.1.

3.1.2.2 Induction time and concentration of IPTG

The concentrations of IPTG and induction time were also optimised. HMS174(DE3)LysS containing plasmid pRSET-b5 sense was chosen to express cytochrome b5. The bacteria were cultured in 50ml TB. The different concentration of IPTG: 1mM, 0.5mM and 0.1mM were used to induce the expression of b5 at 24°C. At the 0, 2, 17, 24, 41, 48 hours, the samples were taken out and the content of b5 was measured.

The concentration of IPTG (from 1mM to 0.1mM) did not critically effect expression of b5 but the level of expression depended on the induction time (Figure 3-5). The level of expression increased as time passed. Induction should not last more than 24 hours, since there is increased background in the negative control (pRSET-b5 anti-

sense) after 24 hours, which probably was caused by the accumulation of bacterial heme proteins after long culture time.

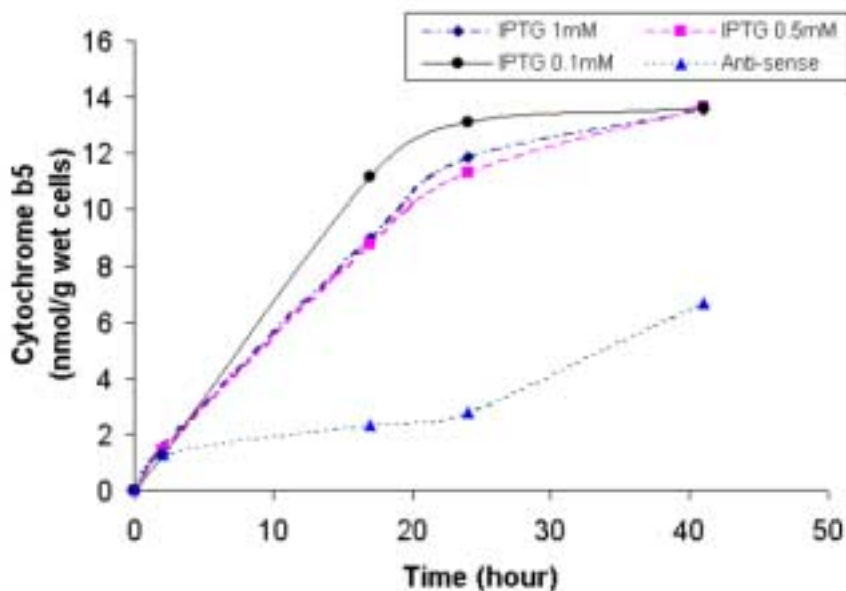


Figure 3-5. Effect of time and IPTG on expression of cytochrome b5.

Cytochrome b5 was expressed in HMS174(DE3)pLysS. The bacteria were cultured in 50ml TB. Plasmid pRSET containing anti-sense b5 was used as negative control. Induction lasted up to 41 hours at 24°C. The content of cytochrome b5 in intact cell was determined by difference spectrum (reduced minus oxidised) as described in Materials and Materials and Methods section 2.4.1.

3.1.2.3 Induction temperature

HMS174(DE3)pLysS containing plasmid pRSET b5 sense was cultured in 50ml TB. Cytochrome b5 was expressed at 24°C, 27°C and 28°C, respectively. The content of b5, expressed at different temperatures in the intact cell, was measured.

It seems that the expression of b5 was sensitive to the induction temperature, when the temperature was higher than 27°C, the expression level of b5 decreased. The highest expression level of b5 was at 27°C (Figure 3-6).

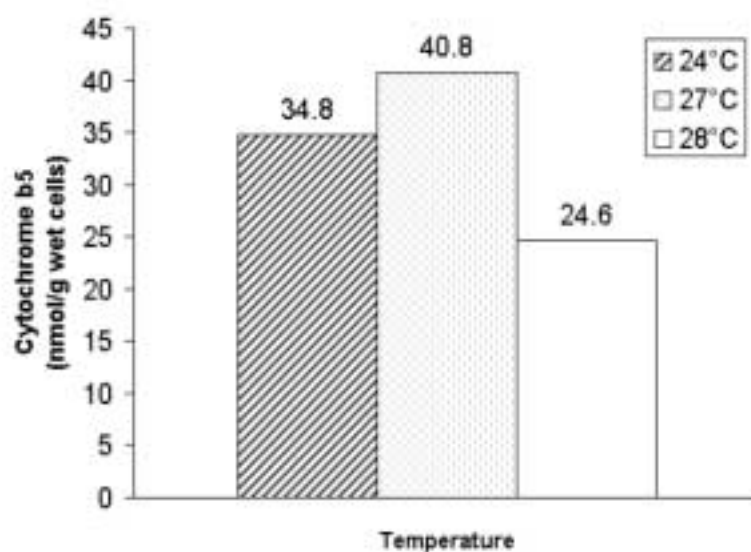


Figure 3-6. Effect of temperature on expression of cytochrome b5.

Cytochrome b5 was expressed in HMS174(DE3)pLysS. Bacteria were cultured in 50ml TB. Expression was induced by 0.1mM IPTG for 24 hours at 24°C, 27°C or 28°C. The content of cytochrome b5 in intact cells was determined by difference spectrum (reduced minus oxidised) as described in Materials and Methods section 2.4.1.

In summary, the optimum conditions for expressing recombinant cytochrome b5 are listed below:

The host strain: HMS174(DE3)pLysS

The growth media: Terrific broth

The concentration of IPTG: 0.1mM

The induction time: 24 hours

The induction temperature: 27°C

3.1.2.4 Recovery of cytochrome b5

Recovery of cytochrome b5 is critical since cytochrome b5 can lose the membrane-binding region during recovery (Holmans, Shet *et al.* 1994). Therefore, the method of recovering membrane-binding cytochrome b5 was optimised. Cytochrome b5 was expressed in 100ml media under optimal conditions. The harvested cells were diluted

to 25ml in buffer A (75mM Tris·HCl, pH 8.0, 0.1mM EDTA, 10µg/ml aprotinin and 1mM PMSF). Three types of process were used. 5ml of samples were used in each process.

- 1) The cells suspended in buffer A were frozen at -80°C then thawed in the water bath at room temperature. This process was repeated twice.
- 2) After the cells were frozen and thawed once, lysozyme (67µg/ml) was added. After the cells were incubated on ice for 30 minutes, the suspension was sonicated for 20 seconds.
- 3) The suspension was sonicated directly at different times (4×30 second, 6×30 second, 8×30 second).

Fraction	Freeze/ Thaw Twice	Lysozyme+ Sonication (20 seconds)	Sonication 4×30s	Sonication 6×30s	Sonication 8×30s
Intact cells	100%	100%	100%	100%	100%
12,000g Supernatant	14%	34%	54%	64%	75%
100,000g Pellet	7.2%	9.5%	11%	11%	13%

Table 3-1. Recovering membrane-bound cytochrome b5 from cells

Cytochrome b5 was recovered from intact cells in 12,000g supernatant. The membrane-bound b5 was recovered in the pellet after 100,000g centrifugation. Cytochrome b5 in each step was measured by the spectrometer to evaluate the recovery of b5. Cytochrome b5 content was arbitrarily set as 100% in the intact cells, and recovery in the 12,000g supernatant and 100,000g pellet was determined.

Table 3-1 demonstrates different methods that were used to recover cytochrome b5. Cytochrome b5 was recovered from the cell in the supernatant after 12,000g centrifugation and was then separated into the membrane-bound b5 in the pellet after 100,000g centrifugation. Without sonication, the recovery of cytochrome b5 (12,000g, supernatant) was very low although approximate 50% (7.2% vs. 14%) of b5 was membrane-bound (100,000g, pellet). Sonication could improve recovery of cytochrome b5. As the time of sonication was increased, recovery of b5 was higher.

However, sonication also made b5 lose the membrane-binding region. As a consequence, up to 13% membrane-binding b5 could be recovered in the 100,000g pellet by sonication 8 times. Lysozyme was supposed to reduce sonication time because it could destroy the cell wall. However, recovery of b5 in 12,000g supernatant was still low when shorter time sonication was used. Therefore, lysozyme was not used in further experiments.

The freeze/thaw cycle and sonication were combined to recover cytochrome b5 (Table 3-2). The time of sonication was optimised.

Fraction	6×30s	9×30s	12×30s	15×30s
Intact cells	100%	100%	100%	100%
12,000g Supernatant	55%	63%	65%	73%
100,000g Pellet	23%	31%	30%	23%

Table 3-2. Recovering membrane-bound cytochrome b5 from cells.

Cytochrome b5 was expressed in 100ml TB under optimal conditions. The bacterial pellet was resuspended in 25ml buffer A. 5 ml of samples were used for the recovery experiment. After the cells were frozen and thawed twice, the suspension was sonicated at different times (6×, 9×, 12×, 15×30 seconds). The membrane-binding b5 was recovered by differential centrifugation. The amount of b5 was determined by spectrophotometer. Cytochrome b5 content was arbitrarily set as 100% in the intact cells.

Table 2 shows that, after cells were subjected to a freeze/thaw cycle twice then sonicated for 9×30 seconds, the highest recovery of whole b5 (31%) was obtained.

This process was chosen to recover cytochrome b5 from bacteria.

3.1.3 Preparation of cytochrome b5 by large-scale culture

The process of preparing b5 was shown on the Table 3-3.

Fraction	Cytochrome b5 (nmol)	Percentage of recovery
Intact cells	530	100
12,000g Supernatant	456	86
100,000g Pellet	173	33
Solubilised in Chaps	167	32
Purification	15.3	3

Table 3-3. The isolation and purification of cytochrome b5.

HMS174(DE3)pLysS containing plasmid pRSET-b5 sense was cultured in 2 liters of TB medium. Expression of cytochrome b5 was induced by 0.1mM IPTG, induction was lasted to 24 hours at 27°C. The shaking speed was 120rpm. The content of cytochrome b5 in different stage was determined by different spectrum. 2% (w/v) Chaps was used to solubilised membrane-bound b5.

The level of expression of b5 was 42.4nmol/g wet cells (265nmol/l). Compared with the previous experiment, more b5 (86%) was found in the supernatant after 12,000g centrifugation, which was possibly due to the higher concentration of cells during sonication. However, recovery of whole membrane-bound b5 was similar to the previous experiment. After solubilisation, almost all b5 was recovered.

It was not expected that recovery of b5 would be so low after nickel-chelate chromatography. There might be several causes. Firstly, the His tag of some cytochrome b5 might be lost during solubilisation. As a result, cytochrome b5 could not bind to resin. Secondly, the solubilised cytochrome b5 solution may contain histidine or other salts, which also prevent protein binding to resin.

When less detergent (1%, w/v) was used, higher recovery of purification was obtained though less cytochrome b5 was solubilised (Table 3-4).

Fraction	Percentage of recovery
Intact cells	100
100,000g Pellet	73
Solubilisation	48
Purification	14

Table 3-4. Improvement of recovery of cytochrome b5 purification.

Cytochrome b5 in the microsomes was solubilised in 1% Chaps (w/v). After purification, 14% of cytochrome b5 was recovered.

Figure 3-7 shows the process of purification of b5. After purification, an approximate 21 kDa single band, which corresponded to the previous calculation (20,196Da) based on the amino acids sequences, was detected on SDS-PAGE. The difference spectrum of b5 (Figure 3-8) showed an absorption peak at 420nm, which is characteristic of cytochrome b5. Therefore, the purified recombinant cytochrome b5 was homogeneous and spectrally functional.

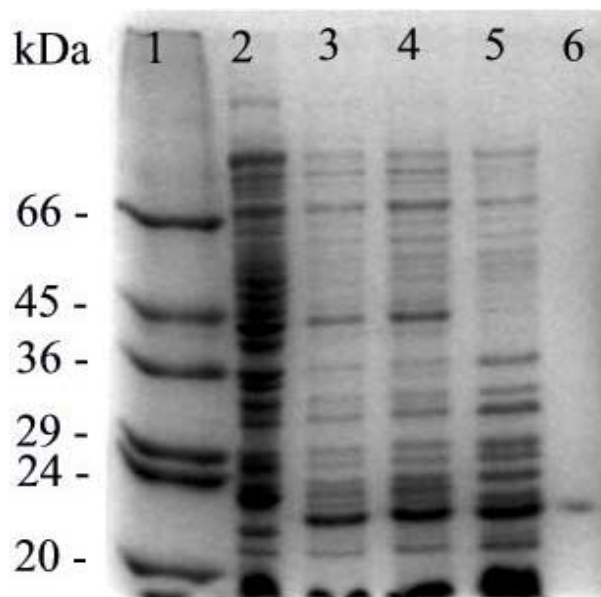


Figure 3-7. SDS-PAGE evaluation of the process of cytochrome b5 purification.

Samples were separated on 12% polyacrylamide gel. The Gel was stained by coomassie blue. *Lane 1*, protein Marker (unit=kDa); *lane 2*, induced cells transformed with plasmid pRSET-b5 Sense (20µg); *lane 3*, *E.coli*-expressed cytochrome b5 in induced cells (10µg); *lane 4*, *E.coli*-expressed cytochrome b5 released from cells in the supernatant after centrifugation at 12,000g for 20 minutes (15µg); *lane 5*, membrane-fraction of *E.coli*-expressed cytochrome b5 (15µg); and *lane 6*, purified cytochrome b5 (3µg).

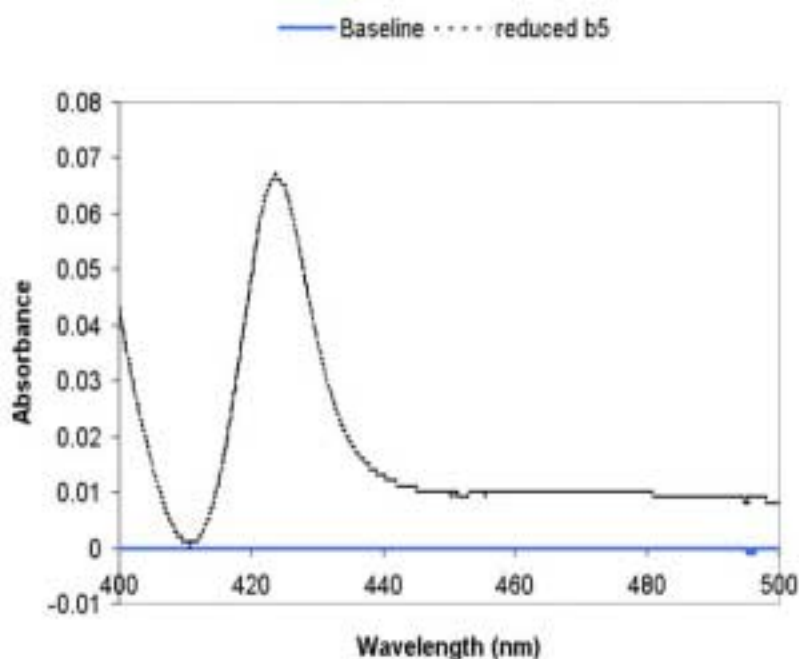


Figure 3-8. Difference spectrum of cytochrome b5.

Cytochrome b5 was in 0.1M potassium phosphate buffer (pH 7.4). 1ml of sample was reduced by sodium dithionite. The different spectrum (dash line) was recorded by comparing reduced sample with oxidised sample.

3.2 Expression of recombinant human cytochrome P450 reductase (CPR)

The recombinant CPR was expressed in JM109 and purified by 2', 5'-ADP agarose as described in Materials and Methods section 2.5.2. The process of purification is shown in Table 3-5.

Fraction	Protein (mg)	Activity ($\mu\text{mol}/\text{min}$)	Specific Activity ($\mu\text{mol}/\text{min}/\text{mg}$)	Yield (%)
Bacteria	360	74	0.21	100
12,000g, Supernatant	377	131	0.35	177
100,000g, Pellet	103	37	0.36	50
Solubilised CPR	87	62	0.71	84
Purified CPR	3.5	37	11	50

Table 3-5. Purification of cytochrome P450 reductase.

Protein content was determined by Bradford assay as described in Materials and Methods section 2.3.1. Activity of CPR was determined by reduction of cytochrome c as described in Materials and Methods section 2.5.3.

Table 3-5 shows the activity of CPR in the 12,000g supernatant was almost twice than that in bacteria. This could be caused by the fact that CPR was released from

intact cells after sonication and centrifugation, as a result, the released CPR could make contact with cytochrome c better.

Solubilised CPR microsomes showed higher activity than pelleted microsomes, which were also found during purification of CPR from rat liver (Shephard *et al.*, 1983). This could be due to solubilised CPR being easier than membrane-bound CPR to reduce cytochrome c.

Porter *et al.* (1987) previously expressed CPR in *E.coli*, but the level was low due to protein degradation. Shen *et al.* (1989) used the secretion vector to express CPR, in which CPR cDNA was fused with OmpA signal peptide to avoid proteolysis. We used the vector pB55, which contained *pelB* leader sequence fusing at 5' terminal of CPR, to express CPR in *E.coli*.

The recombinant CPR showed activity to reduce cytochrome c. Therefore, CPR expressed in *E.coli* was functional. After CPR was purified by 2', 5'- ADP agarose, most of the impure proteins were removed, but two bands were identified on SDS-polyacrylamide gel (Figure 3-9). The high molecular weight band was approximately 79kDa, which is consistent with the size of intact CPR; the low molecular weight band was approximate 66kDa, which is similar to the degraded CPR form reported in previous study (Potter *et al.*, 1987). The purified CPR had strong cytochrome c reduction activity, and this was then used for reconstitution CYP4A1 activity *in vitro*.

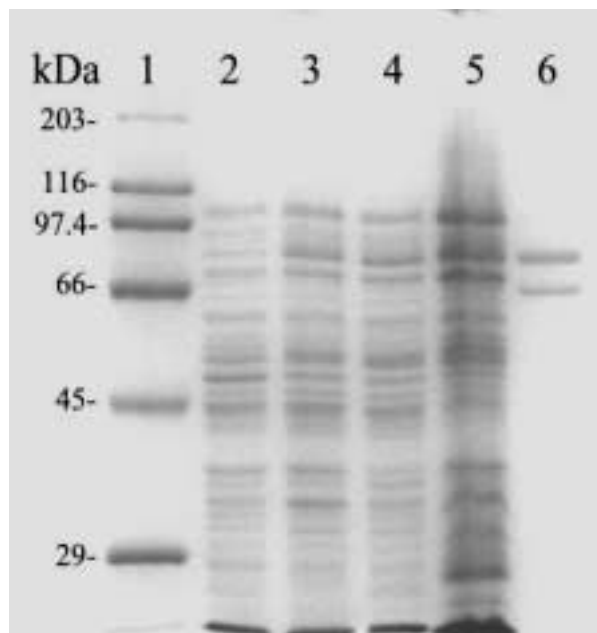


Figure 3-9. SDS-PAGE evaluation of CPR purification process.

Proteins were separated by 10% SDS-PAGE and detected by coomassie blue. *Lane 1*, molecular weight marker (unit=kDa); *lane 2*, uninduced cells transformed with plasmid pB55/CPR (12 μ g); *lane 3*, *E.coli* expressed CPR in induced cells (12 μ g); *lane 4*, CPR released from cells in the supernatant after centrifuge at 12,000g (12 μ g); *lane 5*, membrane-fraction of *E.coli*-expressed CPR (20 μ g); and *lane 6*, purified CPR (5 μ g).

3.3 Expression of CYP4A1 (OmpA.4A1.HT)

Functional mammalian cytochrome P450 is difficult to express in bacteria because firstly it is bound in the membrane, and this could disturb the normal environment in the host cell, and secondly heterologous P450 requires the extra heme as the prosthetic group (Barnes 1996). The problem was originally circumvented by modifying the N-terminal cDNA sequence of mammalian P450s (Barnes *et al.* 1991). Fusing cytochrome P450 with bacterial signal sequences provides another way to express functional P450 in bacteria (Pritchard, Ossetian *et al.* 1997). This strategy can minimise the change in the CYP cDNA sequence. CYP3A4, 2A6 and 2E1 were successfully expressed in *E.coli* with the OmpA leader sequence, and the expression level of CYP3A4 and 2A6 was higher than the modified N-terminus version

(Pritchard, Ossetian *et al.* 1997). Therefore, the fusion of signal peptides with CYP might also lead to high level expression.

In order to study the structure-function relationship of CYP4A1, it is important to obtain a large quantity of CYP4A1. In the present study, we expressed CYP4A1 with the OmpA leader sequence of *E.coli*, and optimised the expressing conditions.

OmpA DNA fragment was amplified from *E.coli* DNA as described in Materials and Methods section 2.6.2.1, and then cloned into plasmid pGEM-T. The CYP4A1 cDNA was cloned in the plasmid pGEM-T Easy as described in Materials and Methods section 2.6.2.1. The synthesised oligonucleotide containing a six-histidine tag was inserted at the 3'-terminus of CYP4A1 cDNA in plasmid pGEM-T Easy. The fragment of CYP4A1 cDNA with a histidine tag was released from the plasmid by restriction enzyme digestion, and then fused downstream of OmpA sequence in the plasmid pGEM-T. The whole CYP4A1 with OmpA and histidine tag fusion DNA (*OmpA.CYP4A1.HT*) was subcloned in pCWori⁺ plasmid as described in Materials and Methods section 2.6.2.2.

The nucleotide sequence of *OmpA.CYP4A1.HT* (1611bp) is shown in Figure 3-10. The *OmpA.CYP4A1.HT* DNA encodes for 534 amino acids, including 23 amino acids from OmpA signal peptide, six-histidine tag at C-terminus, and two extra amino acids (HL) connecting CYP4A1 and the histidine tag. The first six amino acids (MSVSAL) at the N-terminus of CYP4A1 were deleted during construction of the expression plasmid pCWori⁺.OmpA.4A1.HT.

NdeI

|
CATATGAAAAAGACAGCTATCGCGATTGCAGTGGCACTGGCTGGTTTCGCTACCGTAGCG
 M K K T A I A I A V A L A G F A T V A

SacI

|
CAGGCCGAGCTCCACCCGCTTACGGGCAGCATCTCTGGCTTCTCCAAGTGGCCTCC
 Q A A S S T R F T G S I S G F L Q V A S

GTGCTTGGTCTGCTTCTGCTGCTGGTCAAAGCAGTCCAGTTCTACCTGCAAAGGCAATGG
 V L G L L L L L V K A V Q F Y L Q R Q W

CTACTCAAGGCTTTCCAGCAGTTCCCATCACCTCCCTTCCACTGGTTCTTTGGGCACAAG
 L L K A F Q Q F P S P P F H W F F G H K

CAGTTTCAAGGTGACAAAGAACTACAGCAAATTATGACATGTGTGGAGAATTTCCCAAGT
 Q F Q G D K E L Q Q I M T C V E N F P S

GCCTTCTCGATGGTTCTGGGGAAGCAAAGCCTACTTAATTGTCTATGACCCTGACTAC
 A F P R W F W G S K A Y L I V Y D P D Y

ATGAAGGTGATTCTCGGGCGATCAGATCCAAAGGCCAATGGCGTCTACAGATTGCTAGCT
 M K V I L G R S D P K A N G V Y R L L A

CCTTGGATCGGATATGGTTTCTGCTTGAATGGACAACCGTGGTTCCAGCACC GGCGA
 P W I G Y G L L L N G Q P W F Q H R R

ATGCTAACCCAGCCTTCCACTATGACATTCTGAAACCCTATGTAAAAACATGGCTGAC
 M L T P A F H Y D I L K P Y V K N M A D

TCCATTGACTGATGCTAGACAAATGGGAACAGCTGGCAGGTCAAGACTCCTCTATAGAA
 S I R L M L D K W E Q L A G Q D S S I E

ATCTTTCAACATATCTCCTTAATGACCCTAGACACTGTCATGAAGTGTGCCTTCCAGCCAC
 I F Q H I S L M T L D T V M K C A F S H

AATGGCAGTGTTCAGGTGGATGGAAATTACAAGAGCTATATCCAGGCCATTGGGAACTTG
 N G S V Q V D G N Y K S Y I Q A I G N L

AATGACCTCTTTCACTCCCGTGTGAGGAACATCTTTCATCAGAATGATACCATCTATAAT
 N D L F H S R V R N I F H Q N D T I Y N

TTTTCTTCCAATGGCCACTTGTTCACCCGTGCTTGTCAACTTGCCCATGATCACACAGAT
 F S S N G H L F N R A C Q L A H D H T D

GGTGTGATCAAGCTAAGGAAGGATCAGCTGCAGAATGCGGGAGAGCTGGAAAAGGTCAAG
 G V I K L R K D Q L Q N A G E L E K V K

AAGAAAAGACGTTTGGATTTTCTGGACATCCTCTTACTTGCCAGAATGGAGAATGGGGAC
 K K R R L D F L D I L L L A R M E N G D

AGCTTGTCTGACAAGGACCTACGTGCTGAGGTGGACACATTTATGTTTCGAGGGTCATGAC
 S L S D K D L R A E V D T F M F E G H D

ACCACAGCCAGTGGAGTCTCCTGGATCTTCTATGCTCTGGCCACACACCCTAAGCACCAA
 T T A S G V S W I F Y A L A T H P K H Q

CAAAGATGCAGAGAGGAAGTTCAGAGTGTCTGCGGGGATGGGTCCTCCATTACCTGGGAT
 Q R C R E E V Q S V L G D G S S I T W D

```

CACCTGGACCAGATTCCCTACACCACCATGTGTATCAAGGAGGCCCTGAGGCTTTACCCA
H L D Q I P Y T T M C I K E A L R L Y P

CCTGTTCCAGGCATTGTCAGAGAACTCAGCACATCTGTCACCTTCCCTGATGGGCGCTCT
P V P G I V R E L S T S V T F P D G R S

TTACCCAAGGGTATCCAAGTCACACTCTCCATTTATGGTCTCCACCACAACCCGAAGGTG
L P K G I Q V T L S I Y G L H H N P K V

TGGCCAAACCCAGAGGTGTTTGACCCTTCCAGGTTTGACCAGACTCTCCCCGACACAGC
W P N P E V F D P S R F A P D S P R H S

CACTCATTCCTGCCCTTCTCAGGAGGAGCGAGGAACTGCATTGGGAAAACAATTTGCTATG
H S F L P F S G G A R N C I G K Q F A M

AGTGAGATGAAGGTGATTGTGGCCCTGACCCTGCTCCGCTTTGAGCTACTGCCAGATCCC
S E M K V I V A L T L L R F E L L P D P

ACCAAGGTCCCCATCCCCTTACCACGACTTGTGCTGAAGTCCAAAAATGGGATCTACCTG
T K V P I P L P R L V L K S K N G I Y L

                                     XbaI
                                     |
TATCTCAAGAAGCTCCACCATATTCACCATCACCATCACCATTGATCTAGA
Y L K K L H H I H H H H H H *

```

Figure 3-10. Nucleotide sequences for *OmpA.4A1.HT*.

The 5'-terminal *OmpA* leader sequence and 3'-terminal six histidine tag are shown in bold. The extra two amino acids (H and I) between (His)₆ tag and CYP4A1 are underlined. The *Nde I* site containing start code ATG and *Xba I* site containing stop code TGA are labelled. The *Sac I* site connect *OmpA* sequence and *CYP4A1* cDNA is also shown in the sequence.

The structure of the *OmpA.CYP4A1.HT* fusion protein was compared with the N-terminally modified CYP4A1 protein, constructed in a previously study (Dierks *et al.* 1998a). The first six amino acids (MSVSAL) at the N-terminus were absent in *OmpA.4A1.HT*, but 26 amino acids (MSVSALSSTRFTGSISGFLQVASVLG) were deleted at the N-terminus in the modified CYP4A1 (Dierks *et al.* 1998a). Therefore, *OmpA.CYP4A1.HT* contained more N-terminal amino acids of the original CYP4A1. *OmpA.4A1.HT* can better represent the original CYP4A1 than N-terminally modified CYP4A1.

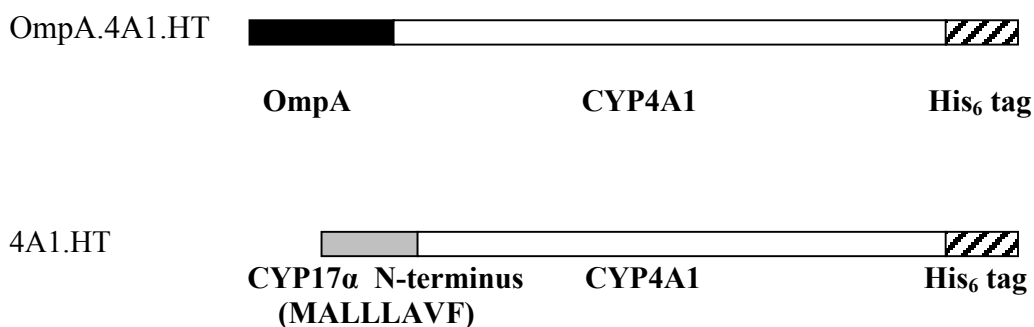


Figure 3-11. Comparison of construction of OmpA.4A1.HT and N-terminally modified CYP4A1. The OmpA sequence in OmpA.4A1.HT is shown as the black filling. The (His)₆ tag was shown as the slanting bar. N-terminally modified CYP4A1 was reported by Dierks *et al* (1998). The N-terminus from CYP17α is shown as the grey filling and the amino acids are included.

The expression level of OmpA.4A1.HT was compared with that of N-terminally modified CYP4A1 in present study, in order to examine whether the OmpA peptide could improve the expression level of P450.

3.3.1 Optimising expression of OmpA.4A1.HT

3.3.1.1 Different host strains on expression of cytochrome P450

Two strains, JM109 and XL-1 blue, which are commonly used in expression of P450s (Barnes 1996), were investigated in our experiment. Our results showed that the choice of host strain affected the expression level of OmpA.4A1.HT. The highest level of OmpA.4A1.HT was obtained in JM109, which was almost double that in XL-1 (Figure 3-12).

The expression level of OmpA.4A1.HT depended on the induction time. The expression level peaked at 24 hours both in JM109 and XL-1, before the content of OmpA.4A1.HT gradually fell down. Therefore, JM109 was chosen as the host strain and induction lasted for 24 hours.

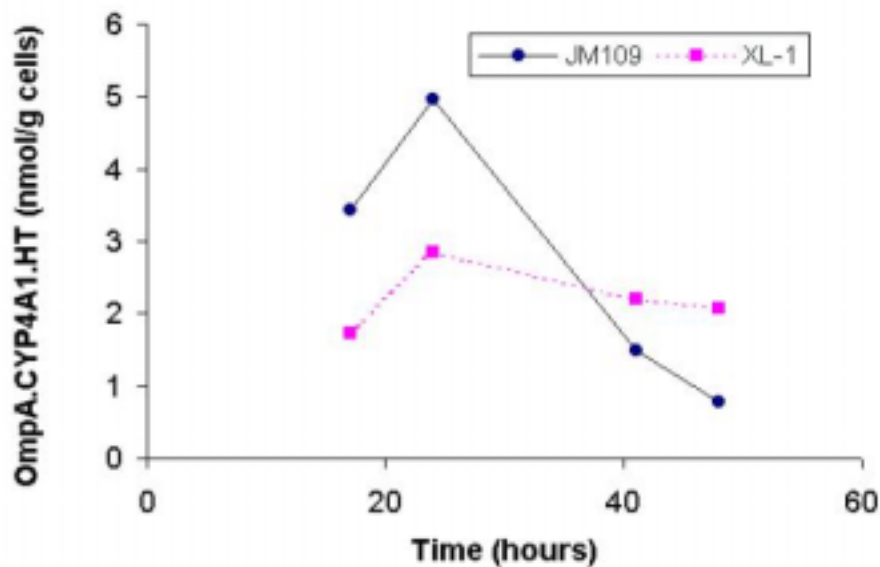


Figure 3-12. Different host strains on expression of P450.

OmpA.4A1.HT was expressed in JM109 and XL-1. The bacteria were cultured in 50ml of TB at 37°C. Expression was induced by 1mM IPTG at 28°C. At 17, 24, 41 and 48 hrs, the bacteria were collected by centrifugation at 6,000g for 20 min. The content of P450 in intact cells was determined by Fe^{2+} : Fe^{2+} -CO difference spectrum as described in Materials and Methods section 2.6.1.1.

3.3.1.2 Effect of temperature and concentration of IPTG

The temperature and concentration of IPTG could also possibly affect expression of cytochrome P450 (Barnes 1996). In the present study, 0.1mM and 1mM IPTG were used to induce expression of CYP4A1 at different temperatures (26.5°C, 28°C and 30°C). When expression was induced by 1mM IPTG, the expression level did not significantly change at different induction temperatures. However, when expression was induced by 0.1mM IPTG, various expression levels were observed at different induction temperature. The expression level was lower (3.3 and 2.8nmol/g cells) at 28°C and 30°C than that (5.1nmol/g cells) at 26°C. The highest level of expression was obtained by induction using 1mM IPTG at 28°C. Therefore, this condition was chosen for expression of P450.

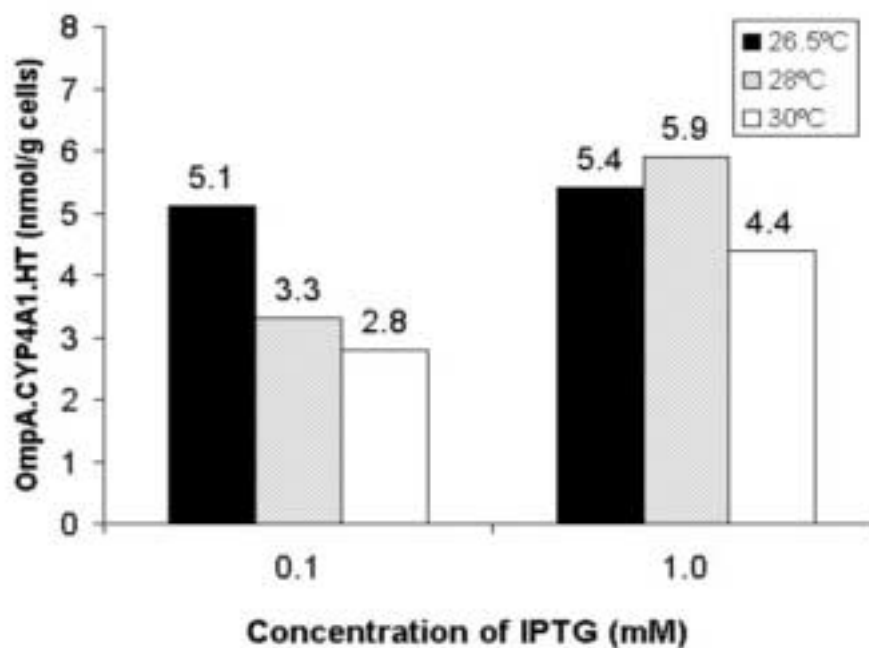


Figure 3-13. Effect of temperature and IPTG on expression of P450.

Bacteria were cultured in 50ml TB at 37°C until OD_{600} reach 0.3-0.6. OmpA.4A1.HT was expressed in JM109 at 26.5°C, 28°C and 30°C, respectively. Expression was induced by 0.1mM IPTG or 1mM IPTG. Induction lasted 24 hours. The content of P450 in intact cells was determined by Fe^{2+} : Fe^{2+} -CO difference spectrum.

3.3.1.3 Effect of δ -ALA

δ -ALA is the precursor of heme, therefore, it is widely used in expression of recombinant P450s, but the effect of addition of δ -ALA is variable (Barnes 1996). In this experiment, additional δ -ALA clearly increased expression of OmpA.4A1.HT (Figure 3-14). However, too much δ -ALA decreased the level of expression. The optimal amount of δ -ALA was 160 μ g/ml.

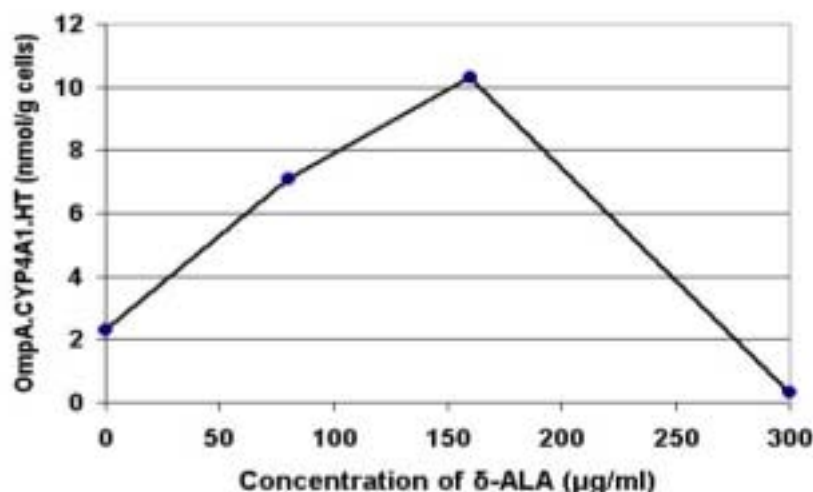


Figure 3-14. Effect of δ -ALA on expression of cytochrome P450.

JM109 cells were cultured in 50ml of TB at 37°C. Different amounts of δ -ALA (0, 80, 160, 300 $\mu\text{g/ml}$) were added to the media when OD_{600} reached 0.1. The expression was induced by 1mM IPTG at 28°C for 24 hours. The content of P450 in intact cells was determined by Fe^{2+} : Fe^{2+} -CO difference spectrum as described in methods.

3.3.1.4 Optimal conditions of expressing OmpA.4A1.HT

In summary, the optimal conditions of expressing OmpA.4A1.HT were determined as:

The host strain: JM109

Induction time: 24 hours

The concentration of IPTG: 1mM

Induction temperature: 28°C

δ -ALA: 160 $\mu\text{g/ml}$

3.3.1.5 Solubilisation of membrane-bound OmpA.4A1.HT

The amount of detergent critically affected the solubilisation of CYP4A1 (Table 3-6).

Too much detergent would denature the enzyme and too little detergent would result in poor recovery. The combination of 0.75% (v/v) Emulgen 913 with 0.6% cholic acid led to the highest recovery after solubilisation.

Detergent	Recovery of OmpA.4A1.HT (nmol/ml microsomes)
0.35% Emulgen 913	0.22
0.75% Emulgen 913	0.56
1.15% Emulgen 913	0.56
0.75% Emulgen 913 + 0.6% cholic acid (sodium)	1.32

Table 3-6. Effect of detergent on recovery of membrane-bound OmpA.4A1.HT.

Different amounts of detergent were added to 5ml membrane protein suspension. The suspension was stirred for 1 hour on ice. The solubilised fraction was recovered by centrifugation at 100,000g for 1 hour, then P450 was measured by spectrometer as described in Materials and Methods section 2.6.1.1.

3.3.2 Comparison of the expression level of OmpA.4A1.HT and N-terminally modified CYP4A1

In order to investigate whether the OmpA leader sequence can improve the expression level of CYP4A1, the expression level of CYP4A1 fusion with OmpA was compared with that of the N-terminally modified CYP4A1. The modified CYP4A1 was expressed in *E.coli* under the optimal conditions described by Dierks *et al.* (1998). Briefly, *E.coli* transformed with plasmid pCWori⁺/CYP4A1 was cultured in TB medium. Expression was induced by 1mM IPTG at 28°C overnight, and 80µg/ml δ-ALA was supplied in the TB medium before induction. OmpA.4A1.HT was expressed under the optimal conditions determined above. We found that the level of expression was similar between OmpA.4A1.HT and modified 4A1 (Figure 3-15). Therefore, fusion of CYP4A1 with OmpA signal peptide did not enhance the expression level when compared with the expression level of N-terminally modified CYP4A1.

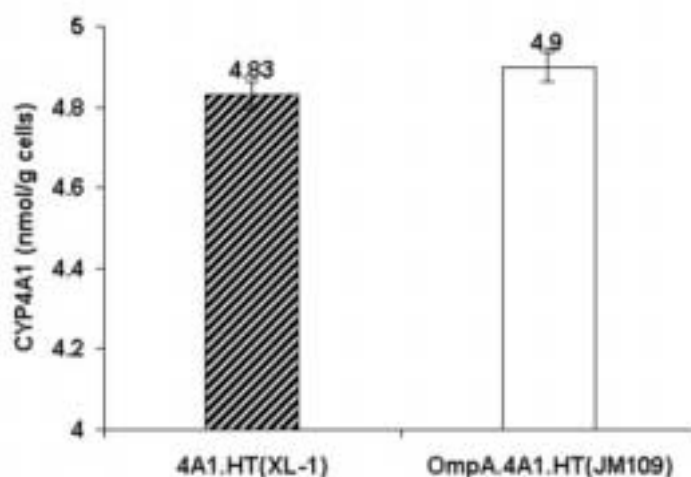


Figure 3-15. Expression level of OmpA.4A1.HT and modified CYP4A1 (n=3).

OmpA.4A1.HT was expressed under optimal conditions as described in section 3.3.1.4. Expression of modified 4A1 was induced by 1mM IPTG at 28°C overnight and 80µg/ml δ-ALA was supplied in the medium according the previous report (Dierks *et al.* 1998a). Data represent the average of three separate experiments and standard deviation was used to show the variation.

3.3.3 Expression and purification of CYP4A1 by large-scale culture

CYP4A1 was usually expressed at 60-100nmol/l of bacterial culture under optimal conditions. A typical purification procedure is shown in Table 3-7.

	P450 (nmol)	Protein (mg)	Specific content (nmol/ mg protein)	Recovery (%)
Intact cells	77	1080	0.071	100
12,000g supernatant	62	407	0.15	81
100,000g pellet	50	57	0.88	65
100,000g pellet (solubilised)	35	33	1.06	48
Purified by His-bind resin	8.2	6.0	1.37	11
Buffer change by PD-10	8.6	3.9	2.2	11

Table 3-7. Extraction and Purification of OmpA.4A1.HT.

OmpA.4A1.HT was expressed in 1 liter TB medium. Induction by 1mM IPTG for 24 hours at 28°C. The content of protein was measured by Bradford assay and content of P450 was determined by different spectrum.

Table 3-7 shows that purification by nickel column seriously affected the recovery of P450. More than 70% of the P450 activity was lost during this step. The specific content of P450 was not greatly increased after this stage. The specific content of purified CYP4A1 was only 2.2 nmol P450/mg protein, which is lower than the

theoretical value (16.4 nmol/mg protein, based on a molecular weight of OmpA.4A1.HT of 60.8 kDa). However, the purified OmpA.4A1.HT showed a single band on SDS-PAGE (Figure 3-16A), indicating the protein was homogenous. This data suggests there is a considerable amount of protein without spectral activity. However, little P420 was observed in the difference spectrum of purified CYP4A1 (Figure 3-16B). Therefore, some protein must have lost the ability to bind carbon monoxide, suggesting the protein lost the heme or iron in heme.

After purified CYP4A1 was desalted on a PD-10 column, the amount of total protein decreased by 30% but the content of P450 did not. This was probably because some non-functional P450 protein was not recovered after the sample passed the PD-10 column.

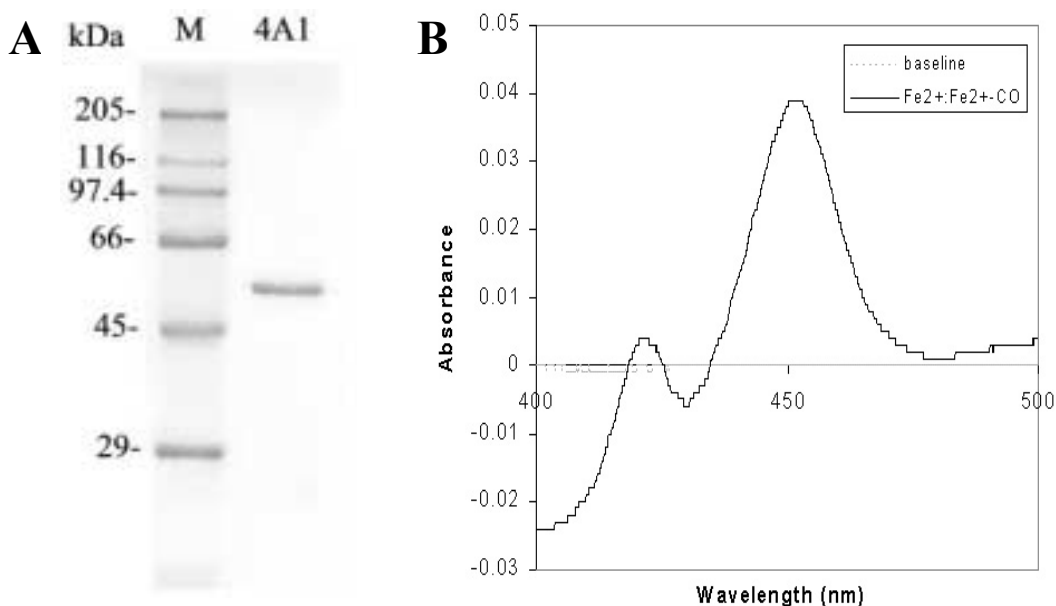


Figure 3-16. Purification of OmpA.4A1.HT.

(A) SDS-PAGE of purified OmpA.4A1.HT. 8 pmol of P450 was loaded on the 10% polyacrylamide gel and stained by coomassie blue. The protein marker is indicated (M=Marker, the mass unit is kDa).

(B) The difference spectrum of purified OmpA.4A1.HT. The sample was diluted four fold to 2ml in 20mM potassium phosphate buffer, 20% glycerol, pH 7.4. A few grains of sodium dithionite were added into the solution. The solution was equally divided as the reference and the sample. After the baseline was recorded by scanning from 400nm to 500nm, the sample was gently bubbled with carbon monoxide and scanned again.

Figure 3-17 exemplifies the process of preparing the pure CYP4A1. The purified protein was checked by SDS-PAGE, and a single band was observed in the gel. The pure recombinant CYP4A1 was obtained.

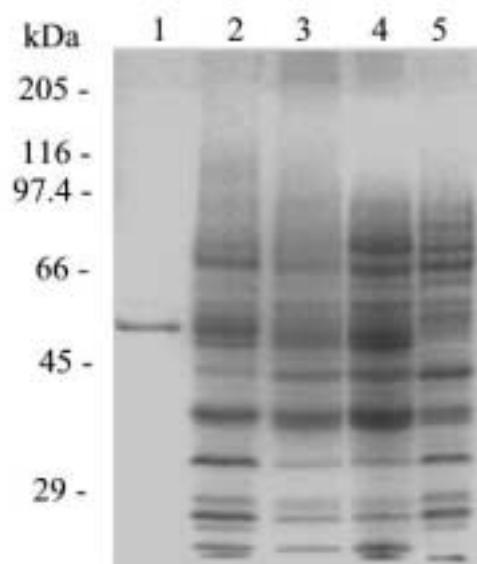


Figure 3-17. PAGE of OmpA.4A1.HT during purification.

Samples were analysed by 10% polyacrylamide gel and stained by coomassie blue. The positions of molecular-weight marker (kDa) are indicated. *Lane 1*, purified OmpA.4A1.HT (8 pmol); *lane 2*, membrane-fraction of *E.coli*-expressed OmpA.4A1.HT in pellets after centrifugation at 100,000g (15 μ g); *lane 3*, *E.coli*-expressed OmpA.4A1.HT released from cells in the supernatant after centrifugation at 12,000g (15 μ g); *lane 4*, *E.coli*-expressed OmpA.4A1.HT in induced cells (20 μ g); and *lane 5*, uninduced cells transformed with plasmid pCWori⁺/OmpA.4A1.HT (20 μ g).

The recombinant CYP4A1 was also analysed by western blotting. The CYP4A1 antibody from rabbits was prepared as in the previous report (Heng, Kuo *et al*, 1997). The strong single band was detected in both bacteria expressed OmpA.4A1.HT and with purified protein; no band was found in induced JM109 (Figure 3-18). Thus, the identification of recombinant CYP4A1 was also supported by western blotting.

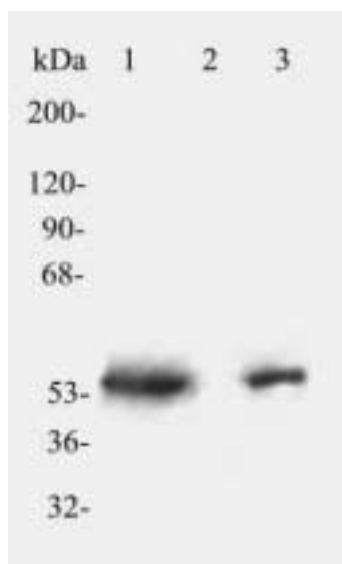


Figure 3-18. Western analysis of recombinant CYP4A1.

Samples were separated by 10% SDS-PAGE and blotting with the primary antibody against CYP4A1 and detected using enhanced chemiluminescence. The position of molecular-weight marker (kDa) is indicated. *Lane 1* purified OmpA.4A1.HT; *lane 2*, induced JM109 cell without plasmid; and *lane 3* induced JM109 cells containing pCWori⁺.CYP4A1 plasmid.

3.3.4 Spectral characteristics of recombinant OmpA.CYP4A1.HT

The recombinant CYP4A1 showed the typical P450 spectrum (Figure 3-19). In the absolute spectrum of recombinant CYP4A1, there is a clear absorption peak around 420nm, which is caused by the heme in P450. In the Fe²⁺: Fe²⁺-carbon monoxide spectrum, the recombinant CYP4A1 gave the characteristic absorbance at 450nm.

Therefore, the bacterial system produced pure and spectrally functional CYP4A1.

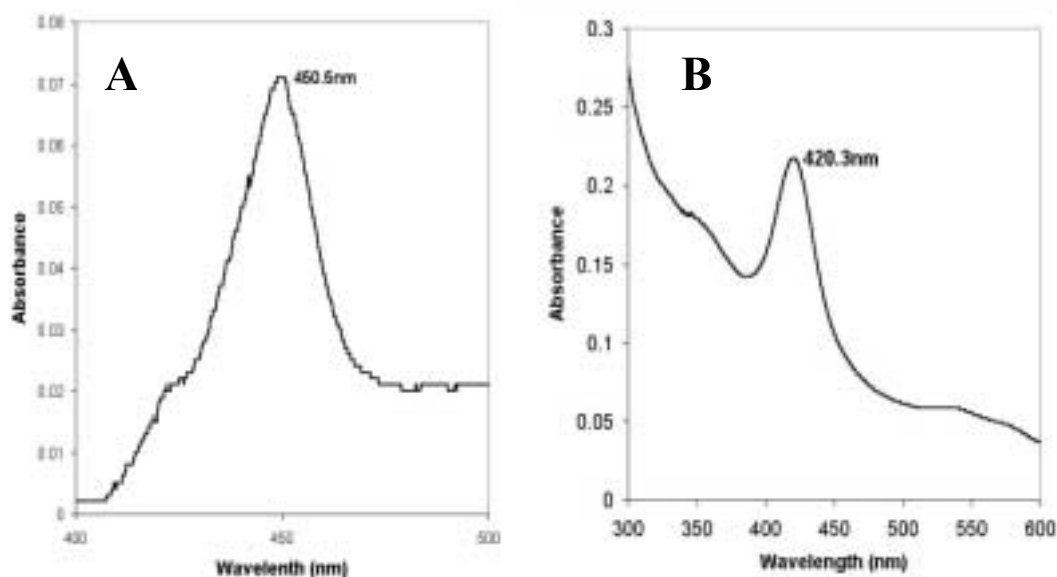


Figure 3-19. The spectrum of OmpA.4A1.HT.

(A) The difference spectrum of OmpA.4A1.HT ($\text{Fe}^{2+} : \text{Fe}^{2+}\text{-CO}$). OmpA.4A1.HT ($0.56\mu\text{M}$) was in 20mM potassium phosphate buffer (pH 7.4) with 20% glycerol. A few crystals of sodium dithionite were added in 2ml of OmpA.4A1.HT solution. The solution was divided the equal part. 1ml of solution was used as the reference. Another aliquot of sample was taken out and gently bubbled by carbon monoxide. The spectrum was recorded by scanning sample from 400nm to 500nm as described in Materials and Methods section 2.6.1.1. **(B) The absolute spectrum of OmpA.4A1.HT.** 1ml of 20mM potassium phosphate buffer (pH 7.4) with 20% glycerol was used as the reference. 1ml of OmpA.4A1.HT ($0.57\mu\text{M}$) was scanned from 400nm to 500nm, and the spectrum was recorded as described in Materials and Methods section 2.6.1.2.

3.4 Study in structure-function relationships of CYP4A1

3.4.1 Substrate binding residues

3.4.1.1 K93

3.4.1.1.1 Prediction

The residues in CYP4A1, which could be involved in substrate binding, were studied.

The first residue that we focus on is K93.

The alignment of CYP4A proteins (Figure 3-20) shows that the position corresponding to the residue K93 in CYP4A1 is well conserved. There are the same

residue lysine in CYP4A3, CYP4A4, CYP4A5 and CYP4A11, and similar basic residue arginine in 4A6. Therefore, the positively charged residues often appear in this position among CYP4As. CYP4A2, CYP4A7 and CYP4A8 differ: CYP4A2 and CYP4A8 have polar residues, threonine and asparagine, while CYP4A7 has negative charged glutamic acid in the corresponding position. Thus, these positively charged residues including K93 in CYP4A1 may have a similar function, which is important for keeping P450 catalytic activity.

Moreover, the alignment (Figure 3-20) shows the position of K93 in CYP4A1 to be similar to that of R47 in BM3. According to the crystal structure of CYPBM3 in the presence of palmitoleic acid, R47 and Y51 residues are substrate contact residues (Li and Poulos 1997). Site-directed mutagenesis of BM3 also supports the hypothesis that R47 and Y51 are important for substrate binding (Graham-Lorence *et al.* 1997; Oliver *et al.* 1997; Noble *et al.* 1999; Cowart *et al.* 2001). Both K93 and R47 residues carry positive charges; therefore, these two residues may share similar functions. Thus, the alignment of CYP4As and CYPBM3 also suggest the residue K93 is a potential substrate-binding residue.

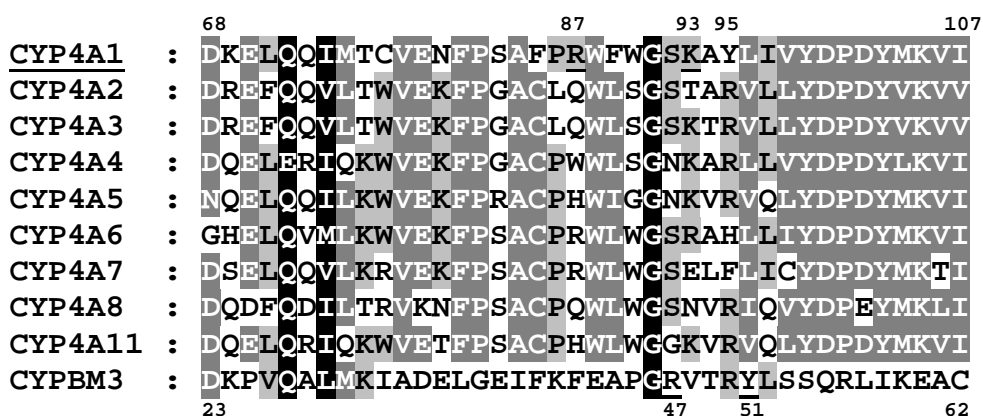


Figure 3-20. Alignment of CYP4As and CYPBM3.

Alignment was created up by pileup program and displayed by GeneDoc program. Different shading shows the conserved region. The black shade is 100% identity, the deep gray shade is 80% identity and the light gray shade is 60% identity. The similar residues are considered to be identity. K93 and R87 in CYP4A1 are underlined. R47 and Y51 in CYPBM3 are also underlined.

The model of CYP4A1, based on the crystal structure of CYPBM3 (CYP102) (Ravichandran *et al*, 1993), was built to predict the function of residues in CYP4A1 (unpublished, C. A. Laughton, School of Pharmaceutical Sciences, University of Nottingham). It has been proposed that the positively charged residue, K93, located at the entrance of the substrate channel according to our CYP4A1 model (Figure 3-21), plays an important role in substrate binding because it could form an ion-pair with fatty acids, the substrate of CYP4A1. The distance between K93 and the heme in CYP4A1 (21.2 Å) as shown in Figure 3-21 is sufficient to fit lauric acid (ca. 14 Å). As a result, the residue K93 was chosen for these substrate-binding studies.

We proposed that K93 could bind to lauric acid by electrostatic attraction. In order to test this, site-directed mutagenesis was used in this experiment. However, many reasons can cause a mutant to lose affinity for a substrate, such as altered enzyme tertiary structure. Therefore, we designed the mutant, K93E, which was supposed to change the substrate specificity from fatty acid to fatty amine, due to the ion-pair formation between negatively charged residue E and positively charged fatty amine. This mutant should not only diminish the affinity for fatty acid, but should also confer a new fatty amine-binding ability. Therefore, the role of K93 in substrate binding can be clearly demonstrated.

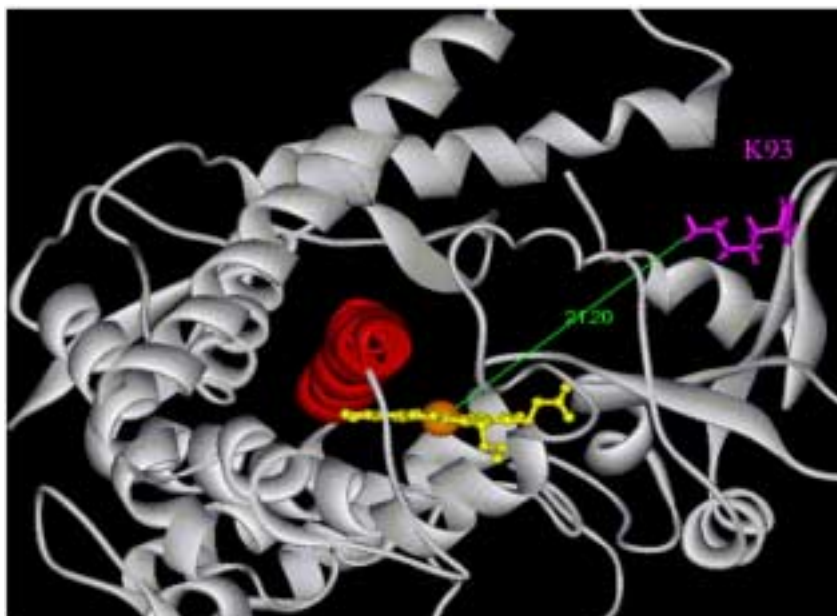


Figure 3-21. Homologous model of CYP4A1.

The computing model of CYP4A1 was created by C. A. Laughton (School of Pharmaceutical Sciences, University of Nottingham) based on the crystal structure of CYPBM3. The pink residue is K93, which is located at the mouth of the substrate channel. The heme group in CYP4A1 is yellow, and the iron in the heme is orange. The distance between K93 and heme-iron is 21.20Å in the model of CYP4A1. The I-helix above the heme is red.

3.4.1.1.2 Expression and purification of the K93E mutant

The K93E mutant was constructed by site-directed mutagenesis using the GeneEditor Kit as described in Materials and Methods section 2.7.1. The DNA sequence of K93E was confirmed by double-strand sequencing as shown below.

K93E:

```
GCCTTTCCTCGATGGTTCTGGGGATCCGAAGCCTACTTAATT
A F P R W F W G S E A Y L I
```

Figure 3-22. DNA Sequence of K93E mutant and deduced amino acids.

The mutation is shown in bold and the novel *Bam*HI is underlined.

The K93E mutant was expressed in *E.coli* as described in Materials and Methods section 2.6.2.3 for wild type CYP4A1. The level of expression was 60-90nmol/l, which is similar to wild type CYP4A1. After purification by His•Binding resin, a single band was detected on SDS-PAGE (Figure 3-23A). The Fe²⁺: Fe²⁺-CO difference spectrum of K93E showed that the main peak was at 450nm, though a

small amount of P420 still existed (Figure 3-23B). Therefore, the pure and spectrally functional K93E was obtained and used for substrate binding and activity assays.

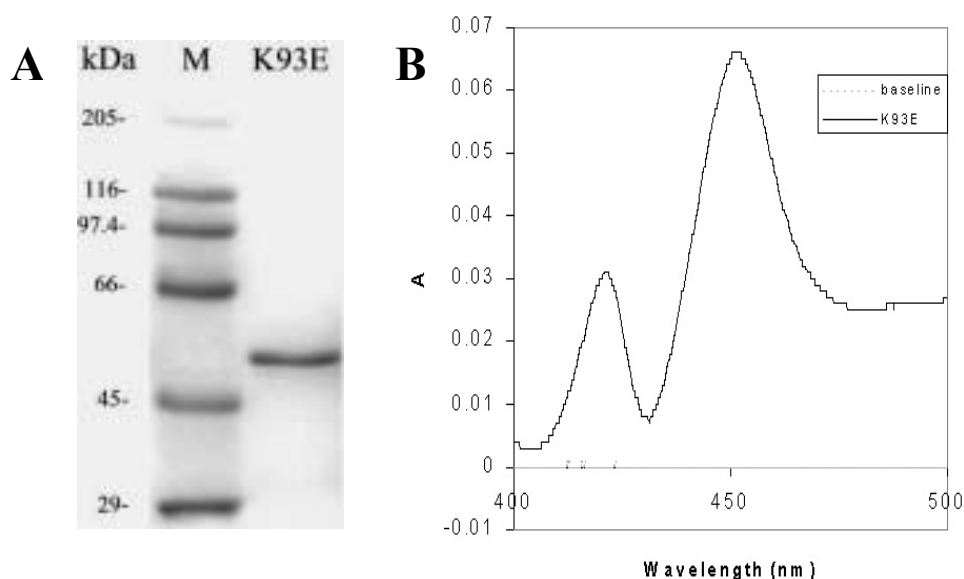


Figure 3-23. The purified K93E mutant protein.

(A) Purified K93E mutant on SDS-PAGE. 8pmol of K93E was loaded in 10% polyacrylamide gel and detected by coomassie blue. The position of protein marker (kDa) was indicated (M= Marker). **(B) $\text{Fe}^{2+} : \text{Fe}^{2+}\text{-CO}$ difference spectrum of K93E mutant.** The concentration of enzyme was $0.44\mu\text{M}$. The difference spectrum was recorded as described in Materials and Methods section 2.6.1.1.

3.4.1.1.3 Substrate binding assay of K93E

The substrate binding difference spectra was used to evaluate the ability of the enzyme to bind substrate. The K_s values (Spectral dissociation constant) were obtained from difference spectra. K_s was defined as below (Alterman *et al.* 1995; Chaurasia *et al.* 1995).

$$K_s = \frac{[E][S]}{[ES]}$$

[E]: the concentration of the free enzyme,

[S]: the concentration of the free substrate,

[ES]: the concentration of enzyme and substrate complex.

K_s values were determined using the equation, $\Delta A = \frac{[S][E_0]}{K_s + [S]}$ ($\Delta A = A_{390} - A_{420}$,

[S]: the concentration of substrate, $[E_0]=k \Delta A_{\max}$), with the assumption that total substrate concentration is much higher than P450 concentration (Alterman *et al.* 1995; Chaurasia *et al.* 1995).

Lauric acid and dodecyltrimethylammonium bromide, which carry negative and positive charge respectively, were chosen as the substrates to examine the effect of electrostatic interaction between CYP4A1 or K93E mutant and substrates.

The difference spectra of CYP4A1 binding to lauric acid are shown in Figure 3-24. K_s value is shown in Table 3-8. CYP4A1 binding to lauric acid resulted in the typical Type I difference spectrum, which showed a maximum at approximately 390nm and a minimum at approximately 420nm (Jefcoate 1978; Ortiz de Montellano 1997). As expected, wild type CYP4A1 bound well with lauric acid, shown by the low K_s value (9.7 μ M). The binding of lauric acid to K93E also showed a Type I difference spectrum (Figure 3-25). The K_s value (32 μ M) of the K93E mutant binding to lauric acid was lower than expected for the electrostatic repulsion between two carboxyl groups in lauric acid and E93, only approximately three times higher than that of CYP4A1 binding to lauric acid. This K_s data demonstrated that lauric acid was still a good substrate for the K93E mutant. This substrate binding assay result was further supported by the activity assay, the activity assay showed no large difference between CYP4A1 and K93E for metabolising lauric acid (CYP4A1: $K_m=6.25\mu$ M, $V_{\max}=32.5$ nmoles/min/nmol P450, K93E: $K_m=10.5\mu$ M, $V_{\max}=26.2$ nmoles/min/nmol P450. Data was provided by V. E. Holmes, School of Pharmaceutical Sciences, University of Nottingham).

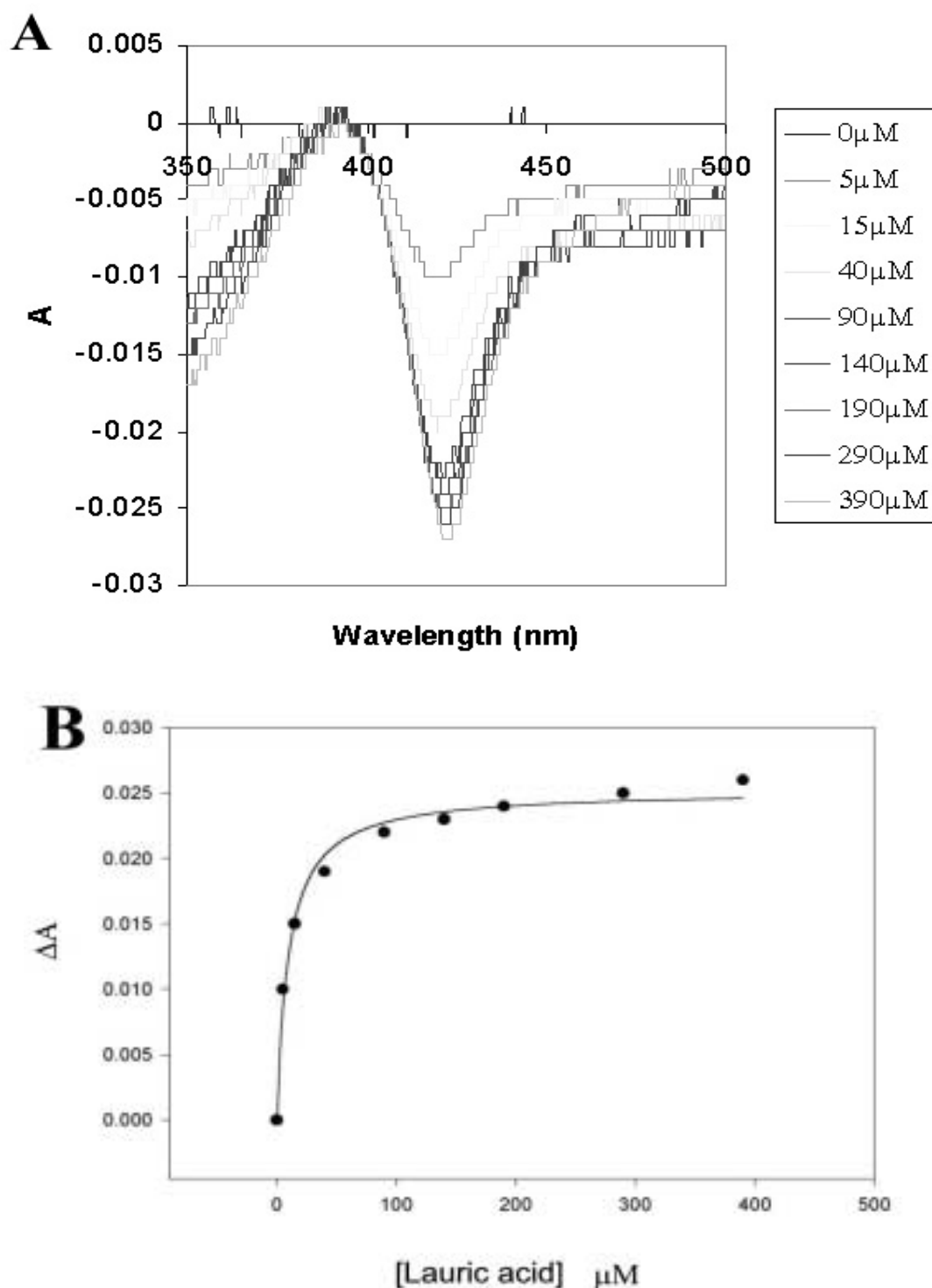


Figure 3-24. Interaction of lauric acid and CYP4A1.

(A) The difference spectrum of substrate binding. The difference spectrum was recorded as described in Materials and Methods section 2.6.1.2. The concentration of CYP4A1 was 0.44 μ M. **(B) Regression plot of lauric acid concentration versus ΔA .** Data was analysed by SigmaPlot. The K_s value was determined by fitting the equation $\Delta A = [S][E_0]/(K_s + [S])$ ($n=1$).

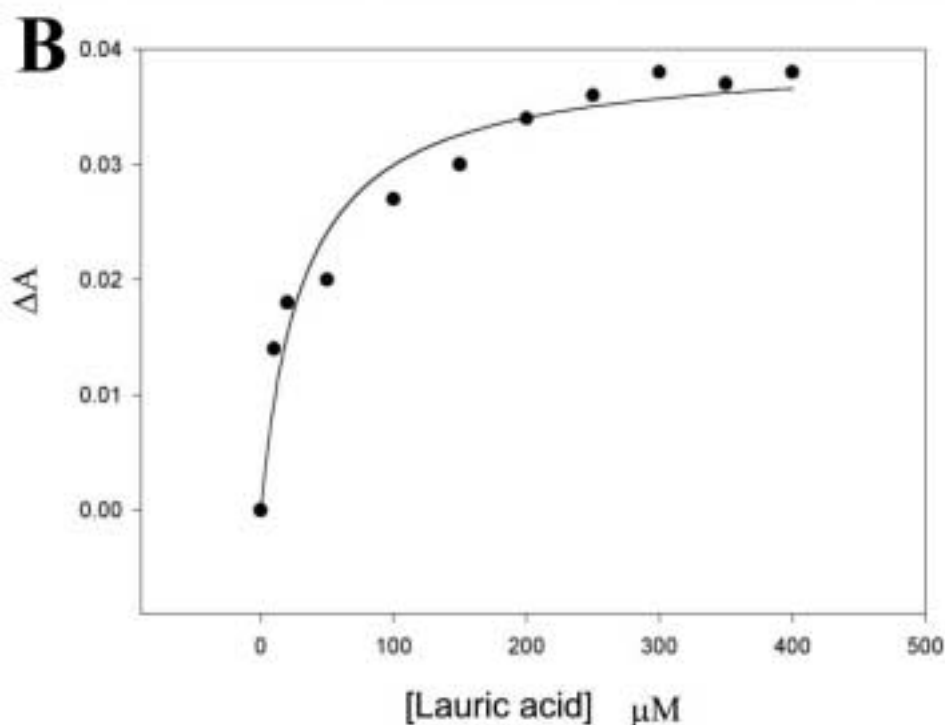
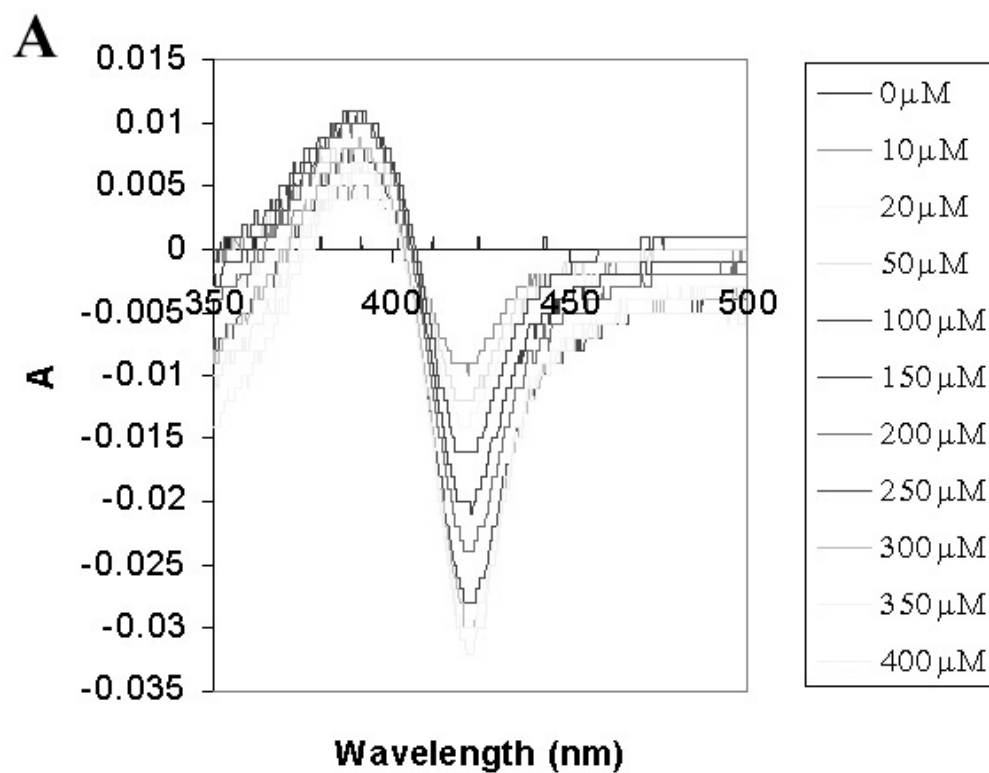


Figure 3-25. Interaction of lauric acid and K93E.

(A) The difference spectrum of substrate binding. The difference spectrum was recorded as described in Materials and Methods section 2.6.1.2. The concentration of enzyme was $0.44\mu\text{M}$. **(B)** Regression plot of lauric acid concentration versus ΔA . Data was analysed by SigmaPlot. The K_s value was determined by fitting the equation $\Delta A = [S][E_0]/(K_s + [S])$ ($n=1$).

CYP4A1 failed to bind to dodecyltrimethylammonium bromide; no absorbance difference was observed (Figure 3-26). For the K93E mutant, there was a trough at 420nm in the difference spectrum but no peak at 390nm (Figure 3-27) after titration of dodecyltrimethylammonium bromide. Concentrations of dodecyltrimethylammonium bromide up to 400 μ M were assayed but no higher because higher concentrations of detergent were likely to damage the P450 tertiary structure. This difference spectrum has not been previously reported (Jefcoate 1978; Ortiz de Montellano 1997). The regression of ΔA against concentration of dodecyltrimethylammonium bromide showed an almost linear relationship and as a result, the K_s value of K93E binding to dodecyltrimethylammonium bromide could not be determined.

The slope of the line was $7.91 \times 10^{-5} \mu\text{M}^{-1} \cdot \mu\text{M}^{-1}$ P450. The maximum absorption change caused by dodecyltrimethylammonium bromide (0.014) was approximately half of that caused by lauric acid (0.038). It is apparent that the change in difference spectrum, produced by the interaction of lauric acid with CYP4A1, resulted in the K_s regression curve at low concentrations of the substrate, which is difficult to distinguish from linearity. Therefore, the interaction of dodecyltrimethylammonium with K93E reflects a low affinity substrate binding.

The activity assay showed that both CYP4A1 and K93E could not metabolise dodecyltrimethylammonium bromide (unpublished, V. E. Holmes, School of Pharmaceutical Sciences, University of Nottingham).

In summary, CYP4A1 and K93E bound well to lauric acid. The K_s value of wild type CYP4A1 binding to lauric acid was approximately three times lower than that of K93E binding to lauric acid. The difference in K_s values between CYP4A1 and

K93E was smaller than expected for the effect of electrostatic interaction between K93 and the substrate. CYP4A1 does not bind to amine compound; K93E weakly binds to amine compound.

Therefore, no major difference of substrate specificity was found between K93E mutant and CYP4A1. The K93 residue in CYP4A1 is probably not critical for the substrate contacting. It is possible that there are other residues in CYP4A1, which are involved in substrate binding.

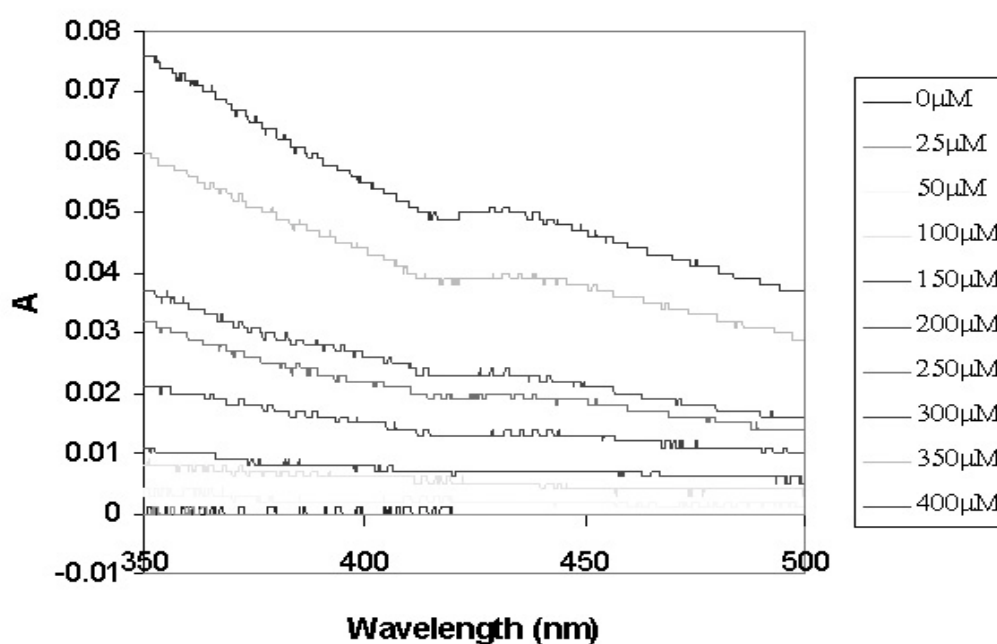


Figure 3-26. Interaction of dodecyltrimethylammonium bromide and CYP4A1.

Up to 400 μM dodecyltrimethylammonium bromide was added to CYP4A1. The difference spectrum was recorded as described in Materials and Methods section 2.6.1.2.

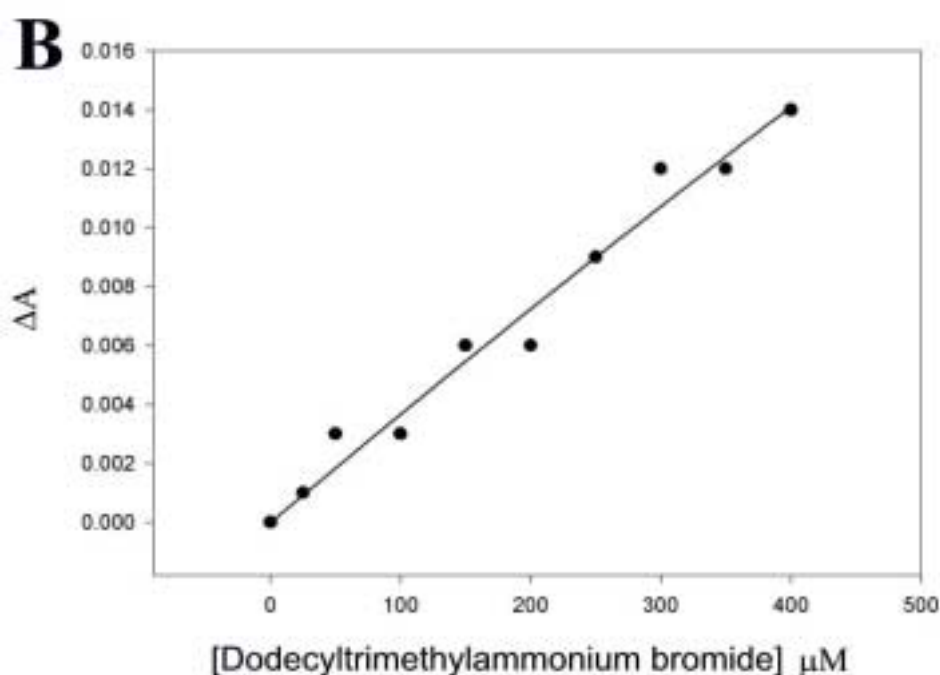
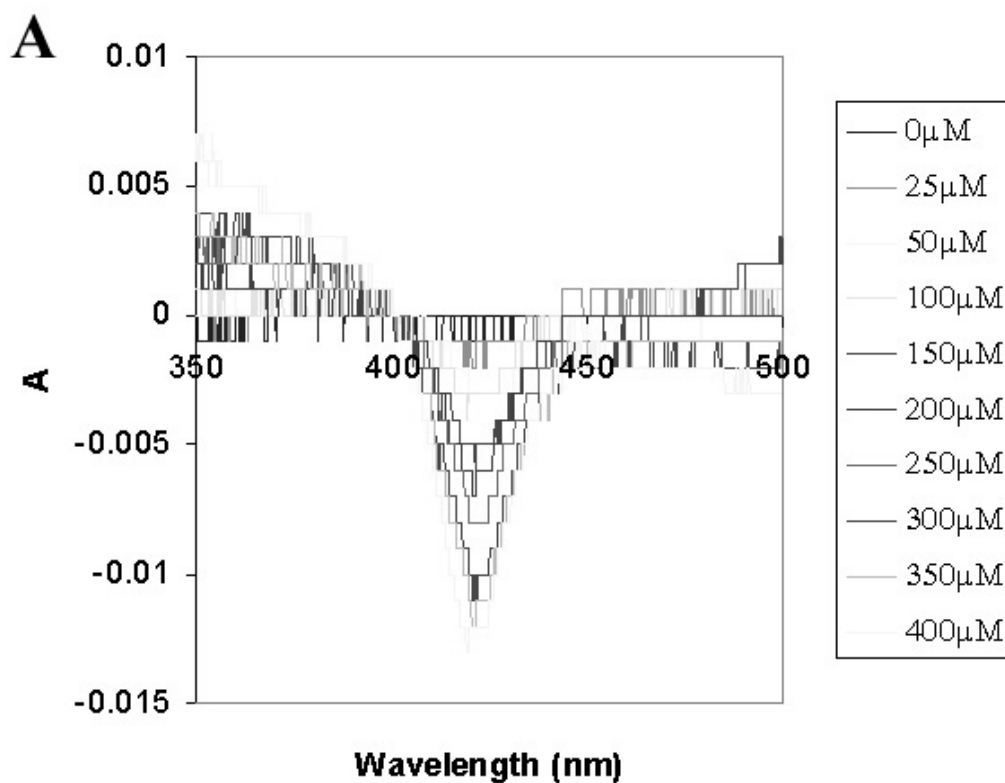


Figure 3-27. Interaction of dodecyltrimethylammonium bromide and K93E.

(A) The difference spectrum of substrate binding. The concentration of K93E mutant was 0.44 μM. The difference spectrum was recorded as described in Materials and Methods section 2.6.1.2. **(B) Regression plot of dodecyltrimethylammonium bromide concentration versus ΔA .** Data was analysed by SigmaPlot (n=1).

	4A1	K93E
Lauric acid	9.7 μ M	32 μ M
Dodecyltrimethylammonium bromide	Not binding ^a	Linear (No saturated) ^b

a. The absorbance did not change up to 400 μ M dodecyltrimethylammonium bromide.

b. ΔA continually changed up to 410 μ M dodecyltrimethylammonium bromide. The resulting regression curve was close to straight line.

Table 3-8. Binding of substrate to CYP4A1 and K93E.

The concentration of CYP4A1 and K93E are 0.44 μ M. The difference spectra were recorded as described in Materials and Methods section 2.6.1.2. The K_s values (μ M) were obtained by nonlinear regression as described in Materials and Methods section 2.6.1.2.

3.4.1.2 R87

Owing to the negative results obtained from the K93E substrate-binding assay, we presumed that other residues could respond to substrate binding. We examined the computing model of CYP4A1 again and found that residue R87 also carried the positive charge, and was located at the other side of the substrate channel (Figure 3-28). Therefore, it was proposed that R87 could be another potential candidate for substrate binding.

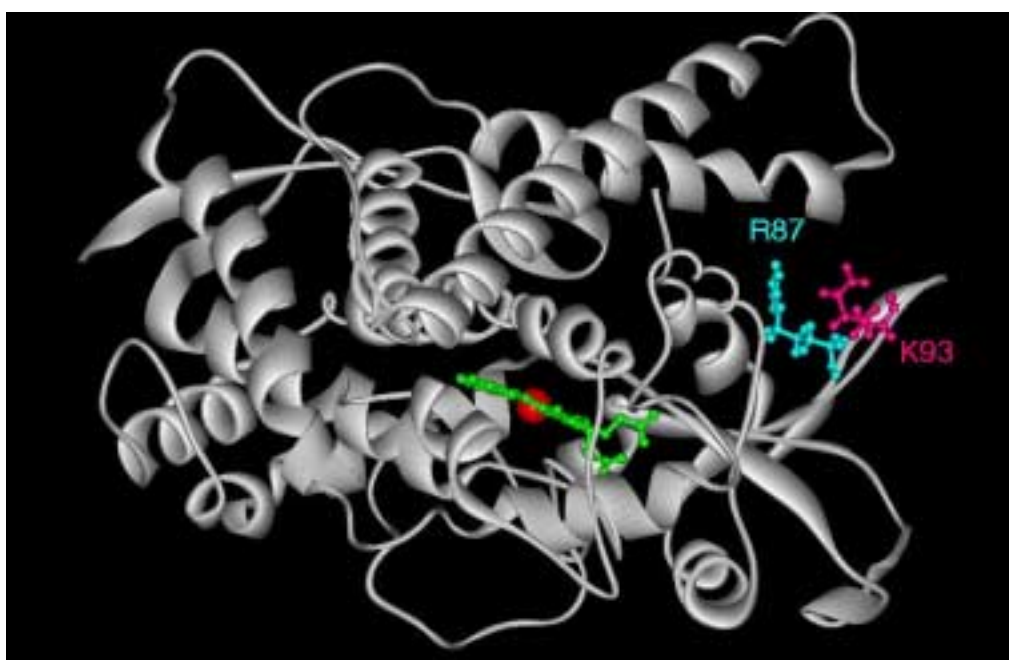


Figure 3-28. R87 and K93 in CYP4A1 model.

The R87 residue is light blue and the K93 residue is pink. Both of them are close to substrate channel. The heme is green. The iron in the heme is red.

3.4.1.2.1 R87E and R87E/K93E mutants

We designed two mutants: R87E and R87E/K93E to study structure-function relationship of R87 residue in CYP4A1. In these mutants, the positively charged residue R87 was replaced by negatively charged E. The substrate specificity of these mutants was investigated.

The mutants were constructed by the GeneEditor Kit as described in Materials and Methods section 2.7.1, and expressed in JM109 as described in Materials and Methods section 2.6.2.3 for CYP4A1. The DNA sequences of mutants were confirmed by double-strand sequencing as showed below.

R87E/K93E:

GCCTTTCCT**GAA**TGGTTCTGGGGATCC**GAA**GCTTACTTAATT
 A F P **R** W F W G S **E** A Y L I

R87E:

GCCTTTCCT**GAA**TGGTTCTGGGGAAGCAAAGCTTACTTAATT
 A F P **R** W F W G S K A Y L I

Figure 3-29. DNA sequences of R87E/K93E and R87E mutants and deduced amino acids.

The mutations are shown in bold; the novel *Hind III* (AAGCTT) and *BamH I* (GGATCC) sites are underlined.

The expression level of mutants was low. R87E and R87E/K93E were expressed in 26nmol/l and 33nmol/l, respectively. After purification on a nickel column, R87E and R87E/K93E showed single protein bands on SDS-PAGE (Figure 3-30). The difference spectrum of these mutants showed the typical P450 spectrum, but there was small amount of P420 in the purified proteins (Figure 3-31). The purified protein was stored at -80°C and used for substrate binding assay and activity assay.

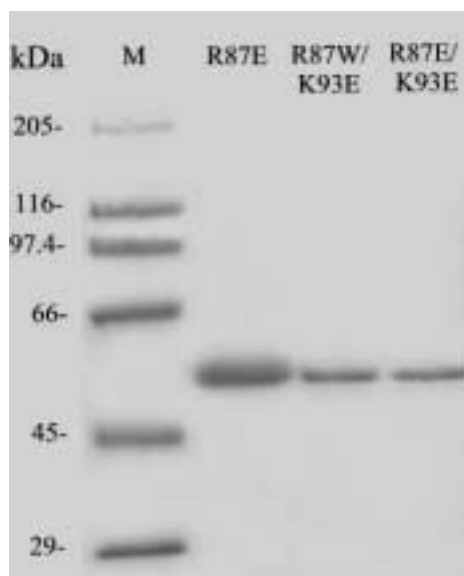


Figure 3-30. Purified R87E, R87E/K93E and R87W/K93E mutants protein.

14pmol of R87E, 5pmol of R87W/K93E and 5pmol of R87E/K93E were loaded on gel. Proteins were separated by 10% SDS-PAGE and detected by coomassie blue. The protein marker was indicated (M=Marker, the unit is KDa).

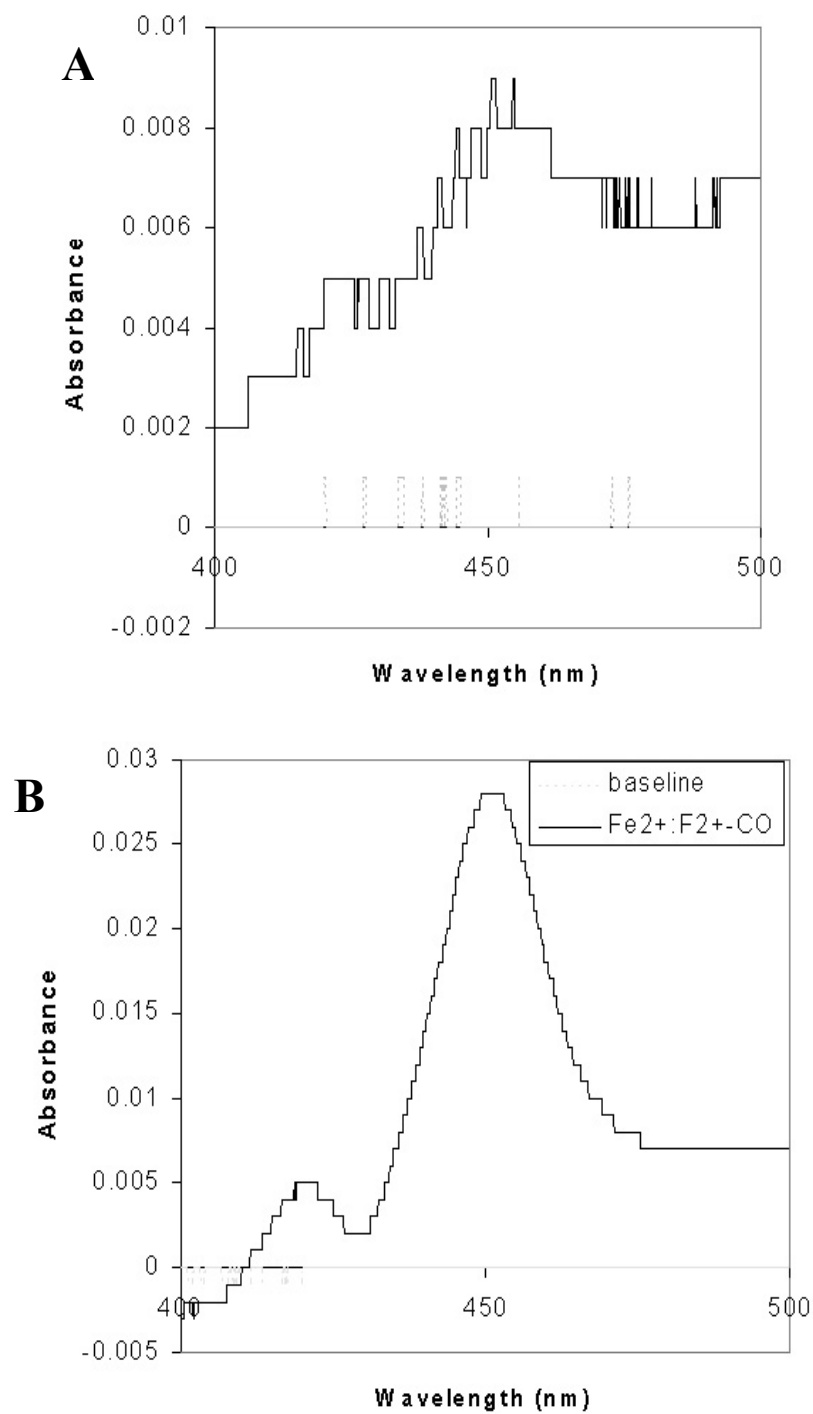


Figure 3-31. The difference spectra of (A) R87E and (B) R87E/K93E mutants.

The concentration of R87E and R87E/K93E were $0.03\mu\text{M}$ and $0.23\mu\text{M}$. The CO-binding difference spectra were recorded as described in Materials and Methods section 2.6.1.1.

The binding of lauric acid to R87E or R87E/K93E mutants resulted in a Type I difference spectrum, which showed a peak at around 390nm and a trough at around 420nm (Figure 3-32,33). The substrate-binding assay showed both R87E and R87E/K93E mutants had very high values of K_s for binding to lauric acid (544 μ M and 370 μ M, respectively). These K_s values were not accurate because the maximal value for ΔA at steady state was not obtained in the range of 0-410 μ M lauric acid. Concentrations higher than 410 μ M of lauric acid were not used because it could lead to protein denaturing. Compared with the K_s value of CYP4A1 binding to lauric acid (9.7 μ M), R87E and R87E/K93E mutants weakly bind to lauric acid.

Moreover, the activity assay showed that R87E and R87E/K93E did not metabolise lauric acid (unpublished, V. E. Holmes, School of Pharmaceutical Sciences, University of Nottingham). This result demonstrates that P450 is unable to metabolise substrate when it only binds to substrate weakly. This was also observed in the interaction of K93E and amine compound.

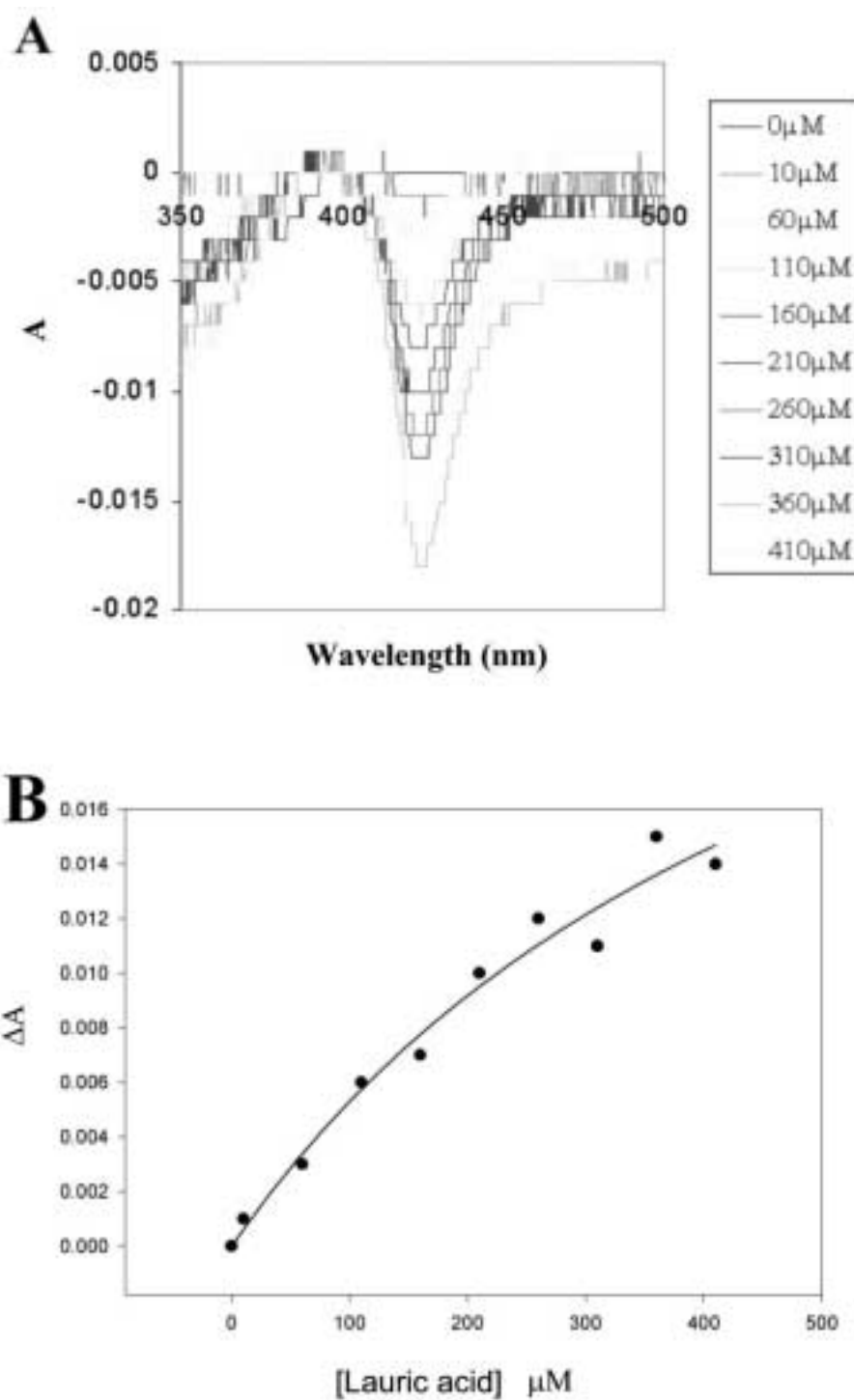


Figure 3-32. Interaction of lauric acid and R87E.

(A) The difference spectrum of substrate binding. The concentration of R87E mutant was 0.33 μM. The difference spectrum was recorded as described in Materials and Methods section 2.6.1.2. (B) Regression plot of lauric acid concentration versus ΔA . Data was analysed by SigmaPlot. K_s value was determined by fitting the equation $\Delta A = [S][E_0]/(K_s + [S])$ ($n=1$).

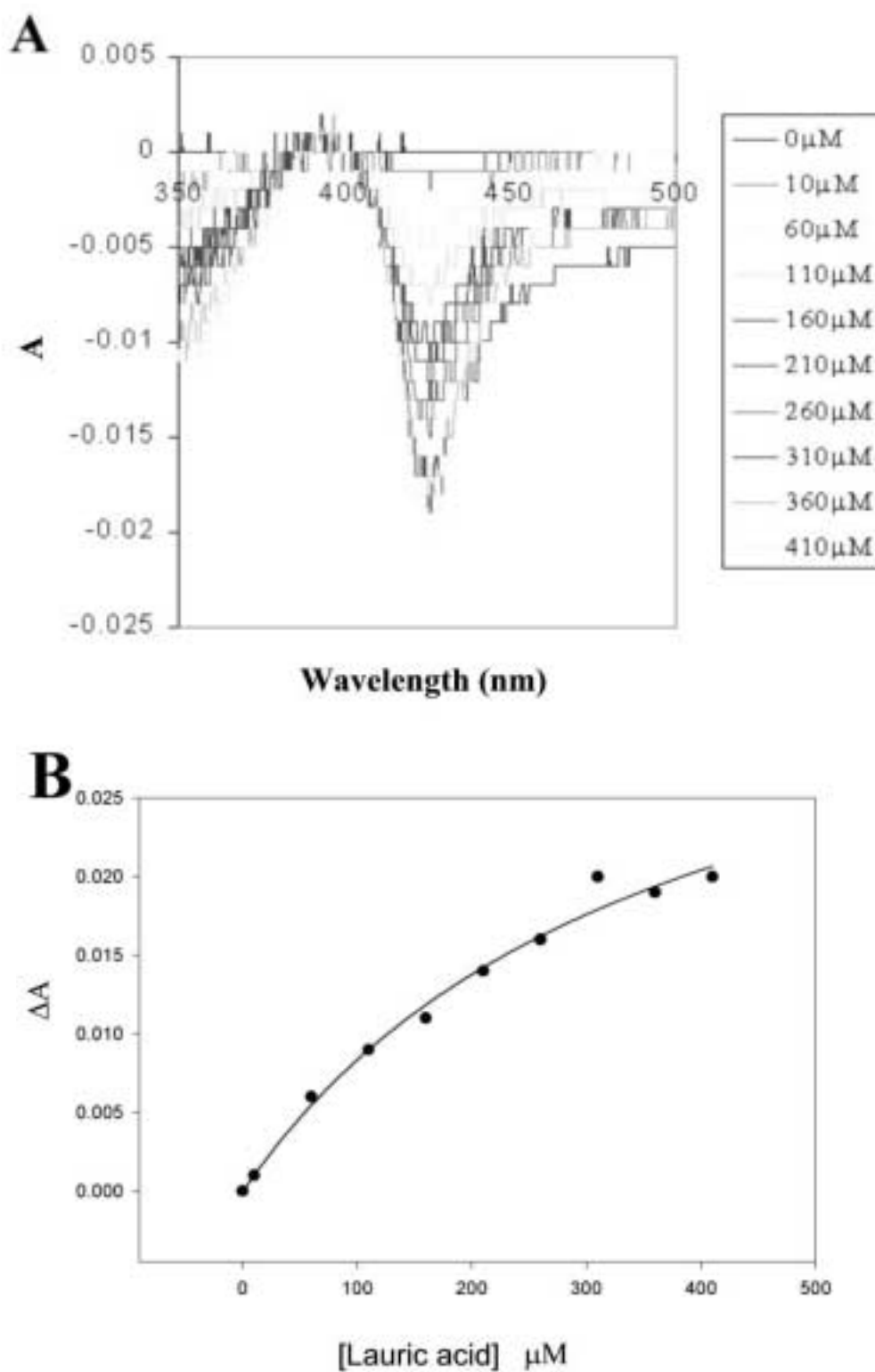


Figure 3-33. Interaction of lauric acid and R87E/K93E mutant.

(A) The difference spectrum of substrate binding. The concentration of R87E/K93E mutant was 0.55 μM. The difference spectrum was recorded as described in Materials and Methods section 2.6.1.2.

(B) Regression plot of lauric acid concentration versus ΔA. Data was analysed by SigmaPlot. K_s value was determined by fitting the equation $\Delta A = [S][E_0]/(K_s + [S])$ ($n=1$).

The difference spectrum of R87E mutant binding to dodecyltrimethylammonium bromide did not show a significant absorbance change up to 160 μ M dodecyltrimethylammonium bromide (Figure 3-34). The addition of a high concentration of dodecyltrimethylammonium bromide (210 μ M-410 μ M) to the R87E mutant resulted in a continual decrease of absorbance in the range of 350nm to 500nm, which could be caused by damage to enzyme conformation as a result of excess of detergent (dodecyltrimethylammonium bromide). These results are not consistent with specific binding of substrate, and show that the R87E mutant does not bind dodecyltrimethylammonium bromide.

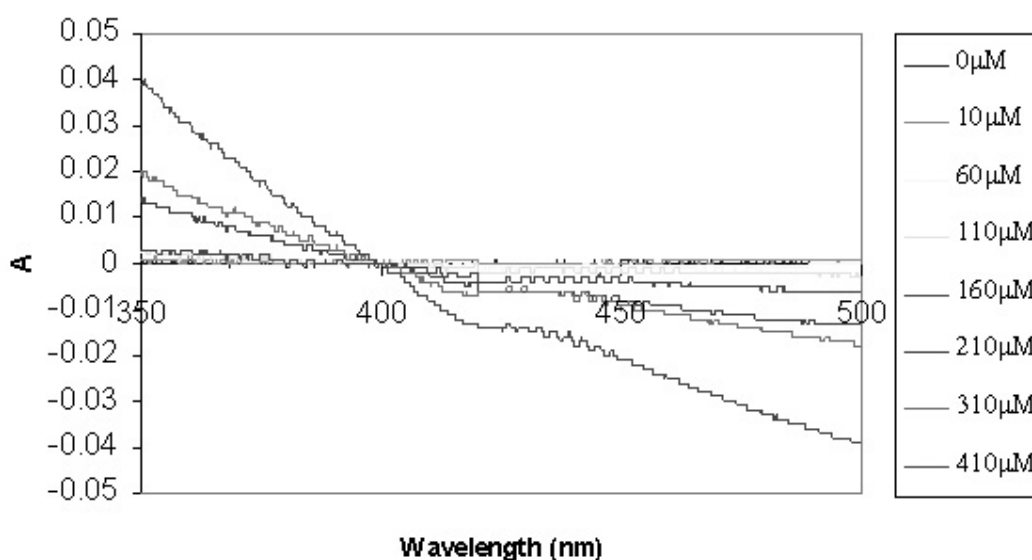


Figure 3-34. Interaction of dodecyltrimethylammonium bromide and R87E.

The difference spectrum was recorded as described in Materials and Methods section 2.6.1.2. The concentration of enzyme was 0.33 μ M.

The difference spectrum of R87E/K93E double mutant binding to dodecyltrimethylammonium bromide was similar to that of K93E mutant. The trough at approximate 420nm was observed but no obvious peak was formed at 390nm (Figure 3-35). The absorbance change did not reach maximum with the concentration range of 0-410 μ M dodecyltrimethylammonium bromide. Owing to possible damage to the

conformation of the enzyme caused by adding excessive dodecyltrimethylammonium bromide, concentrations of dodecyltrimethylammonium bromide higher than 410 μ M were not used. The regression plot shows an almost straight line. The slope of line was $9.62 \times 10^{-5} \mu\text{M}^{-1} \cdot \mu\text{M}^{-1}$ P450, which is similar to the slope obtained from K93E interacting with dodecyltrimethylammonium bromide. Thus, R87E/K93E possibly binds to dodecyltrimethylammonium bromide very weakly. R87E/K93E failed to metabolise dodecyltrimethylammonium bromide (unpublished, V. E. Holmes, School of Pharmaceutical Sciences, University of Nottingham). This activity assay was consistent with the substrate binding assay result.

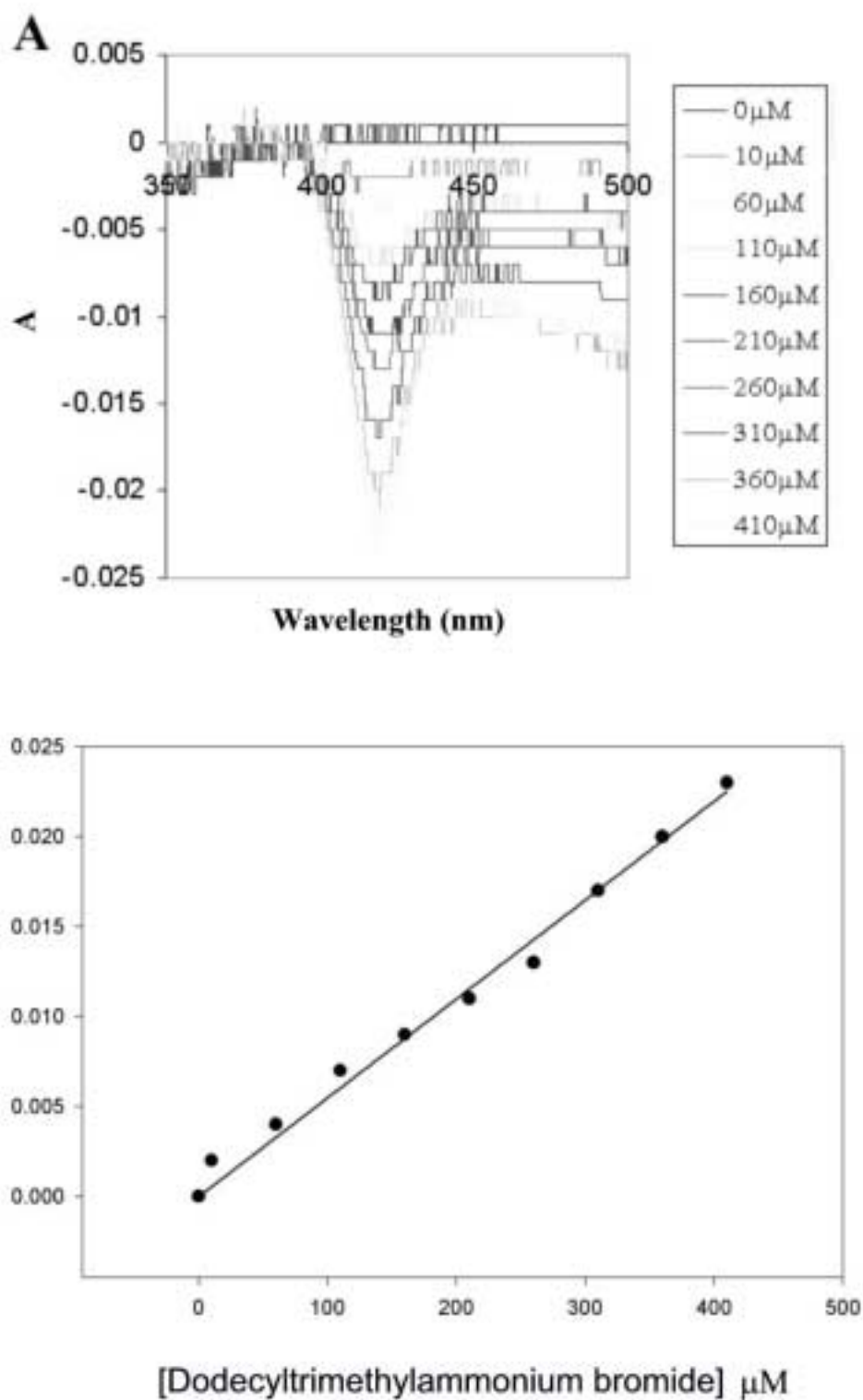


Figure 3-35. Interaction of dodecyltrimethylammonium bromide and R87E/K93E.
(A) The difference spectrum of substrate binding. The concentration of R87E/K93E mutant was 0.55 μM . The difference spectrum was recorded as described in Materials and Methods section 2.6.1.2.
(B) Regression plot of dodecyltrimethylammonium bromide concentration versus ΔA . Data was analysed by SigmaPlot (n=1).

Owing to the failure to observe any activity in R87E and R87E/K93E mutants, the alternative mutation at 87 was examined. The CYP4As alignment (Figure 3-20) shows there is a neutral residue W in the corresponding position of CYP4A4. It was proposed that a change of residue from R87 to W would not completely destroy the P450 activity, as CYP4A4 remained functional. Therefore, the R87W/K93E mutant was designed to examine the function of R87 residue.

3.4.1.2.2 R87W/K93E mutant

The R87W/K93E mutant was constructed by GeneEditor Kits as described in Materials and Methods section 2.7.1. The DNA sequence was confirmed by double-strand sequencing as shown below.

R87W/K93E:

```
GCCTTTCCTTGGTGGTTCTGGGGATCCGAAGCTTACTTAATT
A F P W W F W G S E A Y L I
```

Figure 3-36. DNA Sequence of R87W/K93E and deduced amino acids.

The mutation was bold; the novel *Bam*H I and *Hind* III sites were underlined.

After expression and purification, homogenous protein was obtained (Figure 3-30). The expression level was 74nmol/l. The CO-difference spectrum of the R87W/K93E showed a typical P450 spectrum, but a small amount of P420 was evident (Figure 3-37).

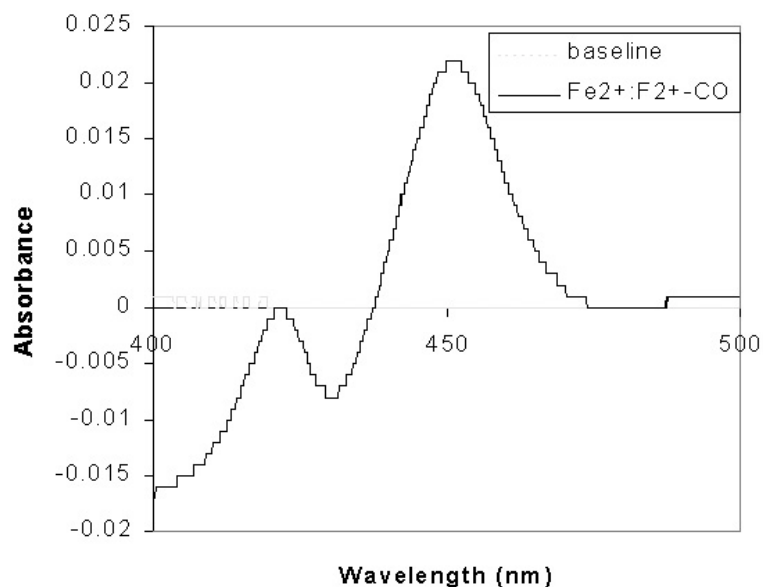


Figure 3-37. The CO-difference spectrum of R87W/K93E.

The concentration of protein was $0.23\mu\text{M}$. The difference spectrum was recorded as described in Materials and Methods section 2.6.1.1.

The difference spectrum of R87W/K93E mutant binding to lauric acid is shown in Figure 3-38. The pattern of R87W/K93E mutant binding to lauric acid (Type I difference spectrum) was similar to that of R87E/K93E mutant. The K_s value ($724\mu\text{M}$) from regression is inherently inaccurate, since the maximal value at steady state was not obtained. However, this K_s value still suggests that lauric acid bound poorly to R87W/K93E when compared with the K_s of lauric binding to CYP4A1.

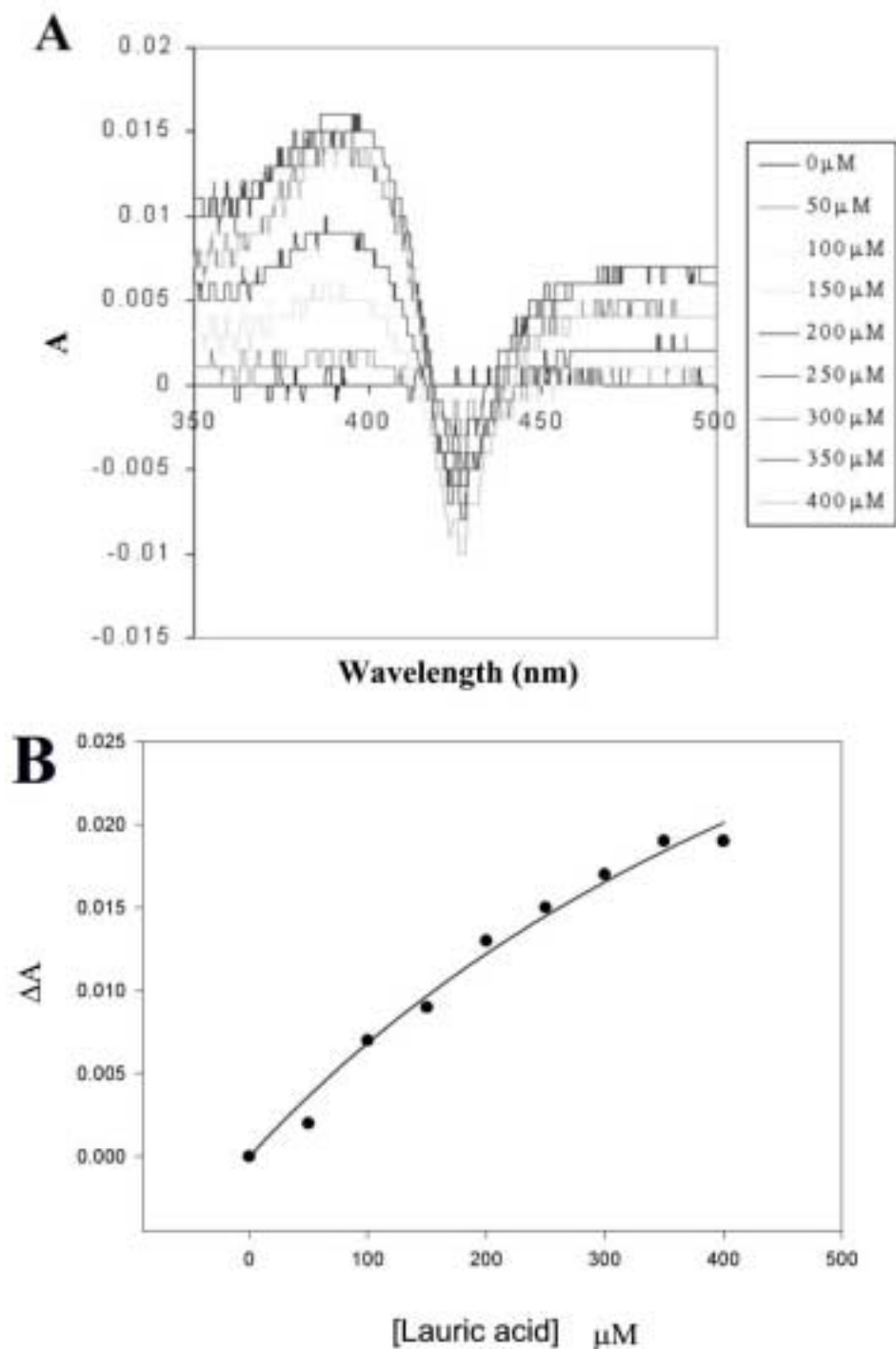


Figure 3-38. Interaction of lauric acid and R87W/K93E.

(A) The difference spectrum of substrate binding. The concentration of R87E/K93E mutant was $0.44\mu\text{M}$. The difference spectrum was recorded as described in Materials and Methods section 2.6.1.2.

(B) The regression plot of lauric acid concentration versus ΔA . Data was analysed by SigmaPlot. K_s value was determined by fitting the equation $\Delta A = [S][E_0]/(K_s + [S])$ ($n=1$).

The difference spectrum of R87W/K93E mutant binding to dodecyltrimethylammonium bromide (Figure 3-39) was similar to that of K93E and R87E/K93E. There was a trough at 420nm but no peak appeared at 390nm. The highest concentration of dodecyltrimethylammonium was used up to 300 μ M, because the R87W/K93E sample became cloudy when higher concentrations of amine compound were added. The regression of ΔA versus the concentration of dodecyltrimethylammonium bromide showed a nearly linear relationship. The slope of the line was $13.2 \times 10^{-5} \mu\text{M}^{-1} \cdot \mu\text{M}^{-1}$ P450, which is close to data obtained from K93E and R87E/K93E binding to dodecyltrimethylammonium bromide. Therefore, R87W/K93E possibly bound the amine compound weakly. The activity of R87W/K93E will be further examined.

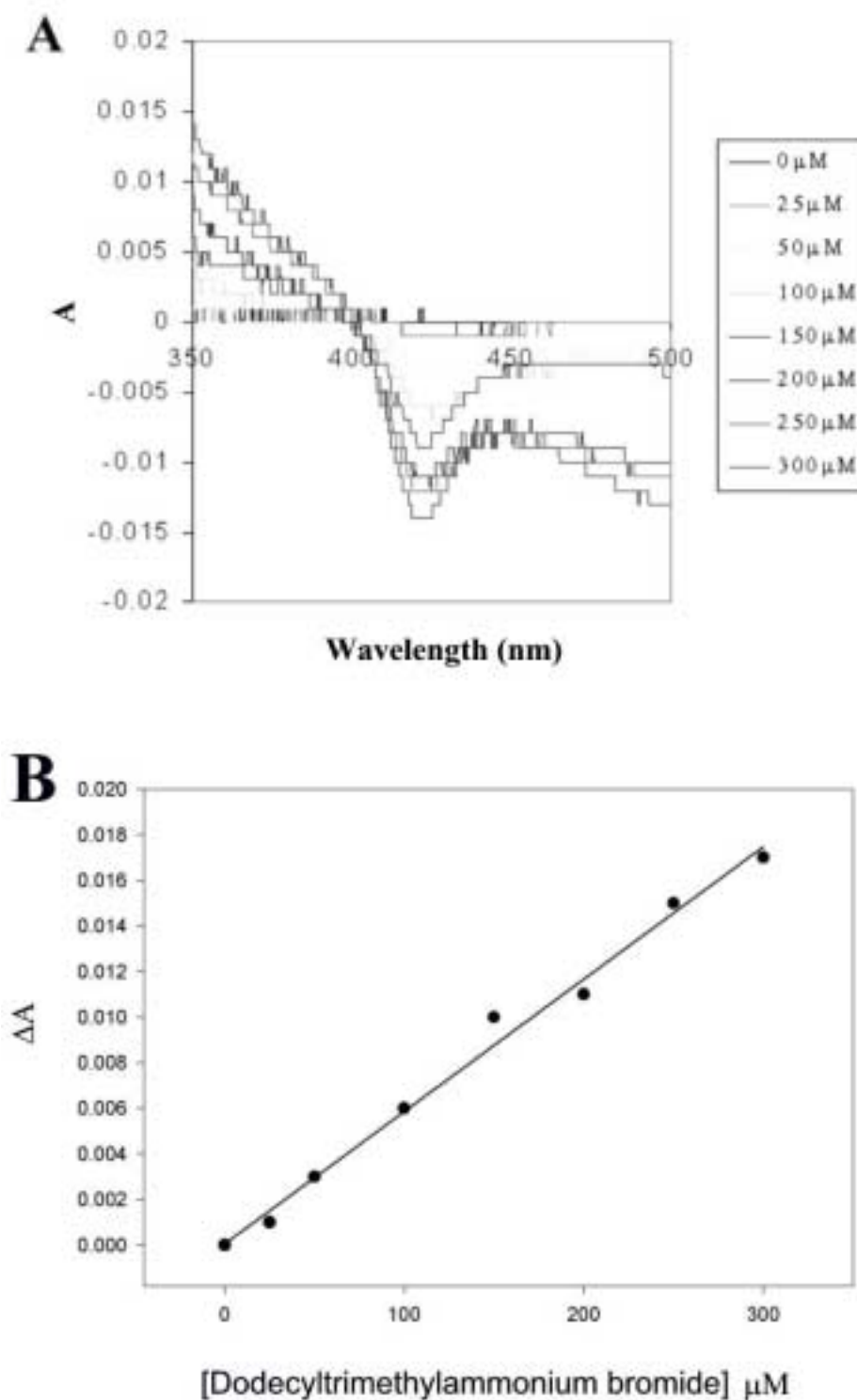


Figure 3-39. Interaction of dodecyltrimethylammonium bromide and R87W/K93E.

(A) The difference spectrum of substrate binding. The concentration of R87E/K93E mutant was 0.44 μM . The difference spectrum was recorded as described in Materials and Methods section 2.6.1.2.

(B) The regression plot of dodecyltrimethylammonium bromide concentration versus ΔA . Data was analysed by SigmaPlot (n=1).

All K_s data are summarised in the Table 3-9. For lauric acid binding, the K_s value of K93E is approximate three times higher than that of CYP4A1 but the change of K_s is smaller than expected for electrostatic repulsion between K93 and lauric acid. K_s values of R87E, R87E/K93E and R87W/K93E are much higher than that of CYP4A1, which showed the low affinity of lauric acid for these mutants. CYP4A1 and R87E do not bind to dodecyltrimethylammonium bromide, but K93E, R87E/K93E and R87W/K93E possibly have weak contact with amine compound.

	Lauric acid	Dodecyltrimethylammonium bromide
CYP4A1	9.7 μ M	Not binding ^a
K93E	32 μ M	Linear (no saturation) ^b
R87E	544 μ M	Not binding ^a
R87E/K93E	370 μ M	Linear (no saturation) ^b
R87W/K93E	724 μ M	Linear (no saturation) ^b

a. The absorbance did not change in the applied concentration range of substrate.

b. ΔA continually changed with increase of concentration of substrate. The regression curve was close to a straight line.

Table 3-9. Binding of substrate to R87E, R87E/K93E and R87W/K93E.

Lauric acid and dodecyltrimethylammonium bromide were used as the substrate. All enzymes are in 20mM potassium phosphate buffer (pH 7.5) with 20% glycerol. The concentrations of R87E, R87E/K93E and R87W/K93E were 0.33 μ M, 0.55 μ M and 0.44 μ M, respectively. The difference spectra with and without substrates were recorded as described in Materials and Methods section 2.6.1.2. The K_s values (μ M) were obtained by nonlinear regression as described in Materials and Methods section 2.6.1.2.

In summary, R87E shows drastically increased K_s for lauric acid, and no specific interaction with amine compound. R87E/K93E shows a similar K_s as for interaction of R87E with lauric acid, but also a weak binding to amine compound was observed in R87E/K93E. R87W/K93E has very high K_s value for lauric acid, and also shows weak contact with amine compound. Therefore, the change of R to E at position 87 possibly causes to structural distortion of the substrate-binding site, and the replacement of R by W results in low affinity to lauric acid. The combination of R87 mutation with K93E results in weak contact between mutants and amine compound,

which is possibly caused by K93E mutation. In a conclusion, R87 is important to keep the function of P450, but it is not clear if it contributes to binding of substrate.

3.4.1.3 N116

In view of the failure to identify a key residue for interaction with substrate, alternative residues were investigated. The structural study of CYPBM3 suggested that Ser72, which aligns to N116 in CYP4A1, could interact with the polar head of palmitoleic acid (Chang and Loew, 1999a). The model of CYP4A11 also suggested that H117 residue, which is equivalent to N116 in CYP4A1, was one of the residues in the substrate-binding channel (Chang and Loew, 1999b). The study in CYP4A3 and CYP4A2 suggested that Ser-Gly-Ile in CYP4A3 were involved in substrate contact (Hoch *et al.*, 2000). The alignment of CYP4A proteins showed the corresponding position of S114 in CYP4A3 was N116 in CYP4A1 (Figure 3-40). Therefore, N116 might play a similar role in CYP4A1. Moreover, alignment among CYP4A proteins shows N116 in CYP4A1 aligns primarily with basic residues in other CYP4As; such as R in CYP4A5 and 4A7, and H in 4A8 and 4A11 (Figure 3-40), which can potentially form ion-pairs with fatty acids.

The model of CYP4A1 suggests that N116 is located in the substrate-binding channel and faces the K93 residue (Figure 3-41). The amide group in asparagine could also interact with carboxyl of fatty acids. As a result, it was proposed that the substrate might initially dock at the K93 residue, then shift to N116.

Therefore, N116 is another potential candidate for substrate binding. We designed the N116E and N116E/K93E mutants, which carry the negative charge E at position 116, to investigate the function of N116 in CYP4A1.

	108	116	124
CYP4A1_RAT :	LGRSDPKANGVYRL	<u>L</u>	LAP
CYP4A2_RAT :	LGRSDPKP---	YQ	SLAP
CYP4A3_RAT :	LGRSDPKASGIYQ	<u>L</u>	FLAP
CYP4A4_RAB :	LGRSDPKAPRNYKL	M	T
CYP4A5_RAB :	LGRSDPKSRGSYTF	V	AP
CYP4A6_RAB :	LGRSDPKAQGSYR	F	LAP
CYP4A7_RAB :	LGRSDPKARVSYS	F	LAP
CYP4A8_RAT :	LGRSDPKAHGSYR	F	LAP
CYP4A11_HU :	LGRSDPKSHGSYR	<u>L</u>	FLAP
CYPBM3 :	ESRFDKNLSQALK	F	VRD

Figure 3-40. Alignment of CYP4A proteins.

Alignment was created by pileup program and displayed by GeneDoc program. The conserved region is shown by different shades. The black shade is 100% identity, the deep gray shade is 80% identity and the light gray shade is 60% identity. The similar residues are considered to be identity. N116 in CYP4A1, S114 in CYP4A3 and H117 in CYP4A11 are underlined.

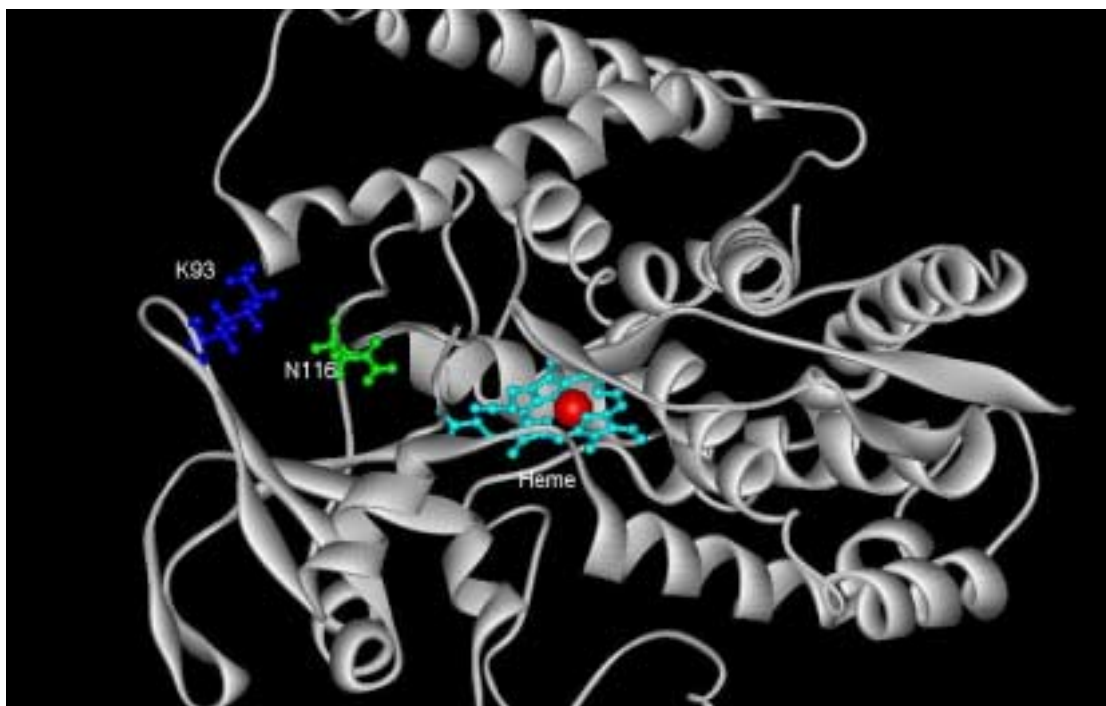


Figure 3-41. The position of N116 in CYP4A1 model.

The N116 residue is green. The K93 residue is blue. The heme group in CYP4A1 is light blue. The iron in the heme is red.

The N116E and N116E/K93E mutants were constructed by GeneEditor Kits as described in Materials and Methods section 2.7.1. The DNA sequence was confirmed by double-strand sequencing as shown below.

N116E:

ATGAAGGTGATTCTCGGGCGATCGGATCCAAAGGCC**GAA**GGCGTC
M K V I L G R S D P K A **E** G V

N116E/K93E:

TGGGGATCC**GAA**GCCTACTTAATTGTCTATGACCCTGACTACATGAAGGTGATTCTC
W G S **E** A Y L I V Y D P D Y M K V I L
93

GGGCGATCAGATCCAAAGGCC**GAA**GGCGTCTACAGATTGCTAGCTCCATGGATC
G R S D P K A **E** G V Y R L L A P W I
116

Figure 3-42. DNA sequence of N116E and N116E/K93E and deduced amino acids.

The mutations are bold; the novel *BamH I* and *Nco I* are underlined.

The N116E mutant was expressed and purified as described in Materials and Methods section 2.6.2.3 for CYP4A1. The expression level of N116E was 69nmol/l. The purified N116E mutant showed a single band on SDS-PAGE and a typical P450 spectrum (Figure 3-43). The expression level of N116E/K93E in JM109 was low (30nmol/l). After microsome preparation and solubilisation, little P450 (4 nmol for 1 litre culture) remained. Therefore, N116E/K93E was not further purified and investigated for its activity and substrate binding ability.

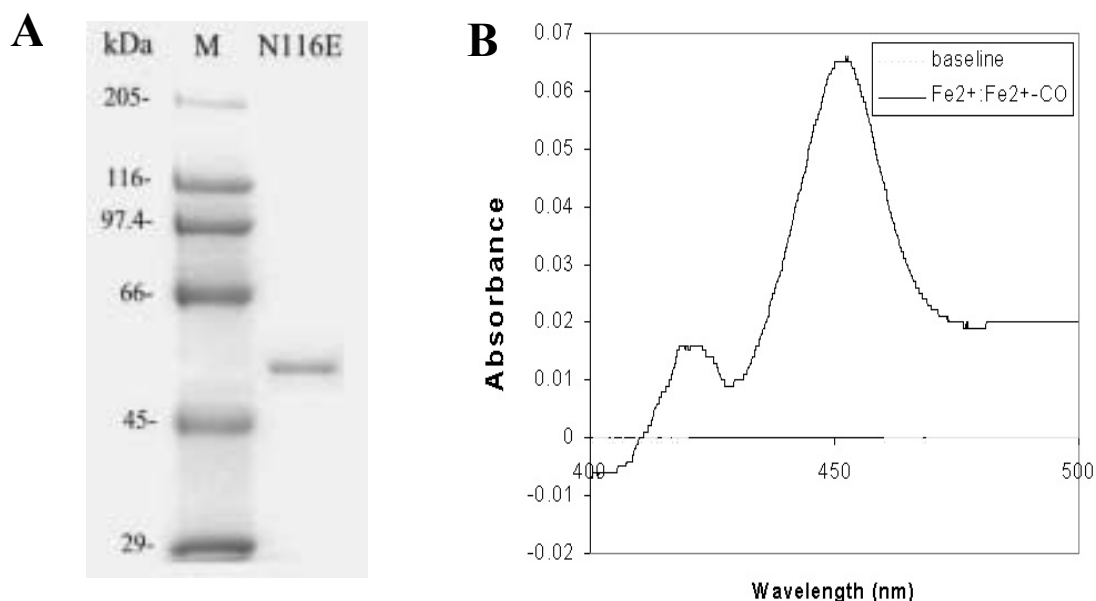


Figure 3-43. The purified N116E mutant protein.

(A) Purified N116E mutant on SDS-PAGE. 3pmol N116E was loaded in 10% polyacrylamide gel and detected by coomassie blue. The position of protein marker (kDa) was indicated. M= Marker. **(B) $\text{Fe}^{2+} : \text{Fe}^{2+}\text{-CO}$ difference spectrum of N116 mutant.** The concentration of enzyme was 0.48 μM . The difference spectrum was recorded as described in Materials and Methods section 2.6.1.1.

The N116E mutant was able to bind to lauric acid well. The difference spectrum was a Type I spectrum (Figure 3-44). The K_s value of N116E binding to lauric acid was close to that obtained from interaction of CYP4A1 with lauric acid (Table 3-10). The N116E mutant failed to bind to the amine compound (Figure 3-45) as no major change of absorbance was observed; the same observation being made with CYP4A1. Therefore, substrate-binding assay suggests that substrate affinity and specificity of N116E mutant is similar to those of wild type CYP4A1. The activity of N116E is being examined.

	Lauric acid	Dodecyltrimethylammonium bromide
N116E	8 μM	Not binding ^a
CYP4A1	9.7 μM	Not binding ^a

a. The absorbance did not change in the applied concentration range of substrate.

Table 3-10. Binding of substrate to N116E and CYP4A1.

The concentration of N116E and CYP4A1 were 0.77 μM and 0.44 μM , respectively. The difference spectra were recorded as described in Materials and Methods section 2.6.1.2. The K_s values (μM) were obtained by nonlinear regression as described in Materials and Methods section 2.6.1.2.

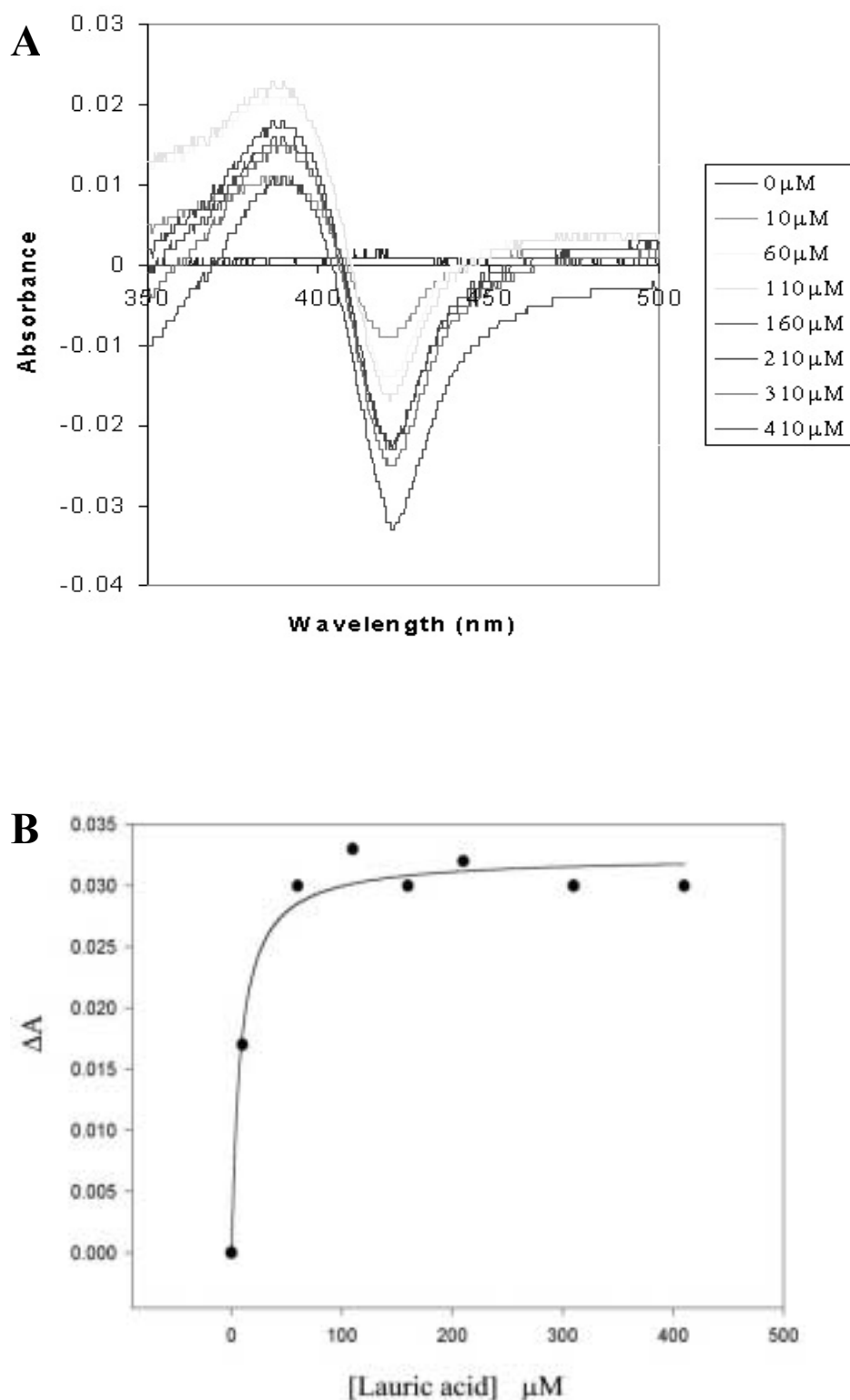


Figure 3-44. Interaction of N116E and lauric acid.

(A) The difference spectrum of substrate binding. The concentration was $0.77\mu\text{M}$. The difference spectrum was recorded as described in Materials and Methods section 2.6.1.2. **(B) The regression plot of lauric acid concentration versus ΔA .** Data was analysed by SigmaPlot. K_s value was determined by fitting the equation $\Delta A = [S][E_0]/(K_s + [S])$ ($n=1$).

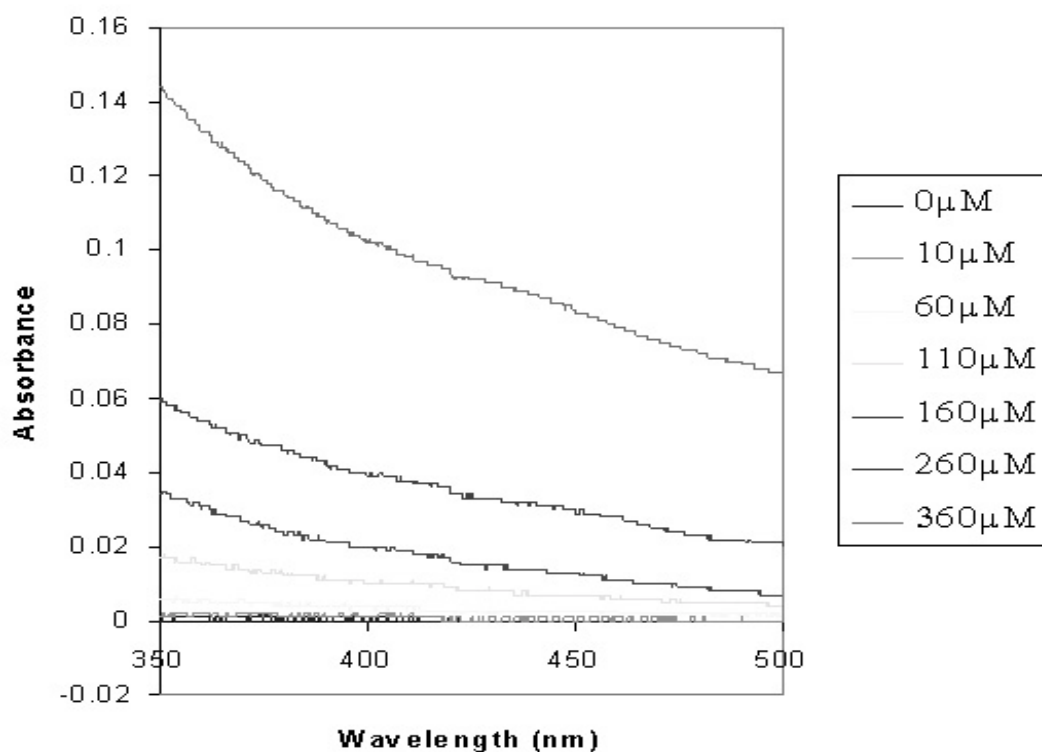


Figure 3-45. Interaction of N116E and dodecyltrimethylammonium bromide.

The concentration of enzyme was $0.77\mu\text{M}$. The difference spectrum was recorded as described in Materials and Methods section 2.6.1.2.

3.4.2 The C-helix region in CYP4A1

The C-helix region in CYP4A1 consists of 21 amino acids from G135 to K155, according to the structure of CYP102 (Ravichandran *et al.*, 1993). The alignment of CYP4 proteins showed this region to be highly conserved (Figure 3-46). The model of CYP4A1 suggests that the C-helix is close to, and putatively makes contact with the heme group in CYP4A1. Moreover, there are many positive charged residues in the C-helix that could form part of the positive surface of CYP4A1. Therefore, the C-helix could play a role in the interaction between P450 and electron donors, such as cytochrome P450 reductase and cytochrome b5, which carry the negative charge on the surface. However, the function of this region is still not well understood.

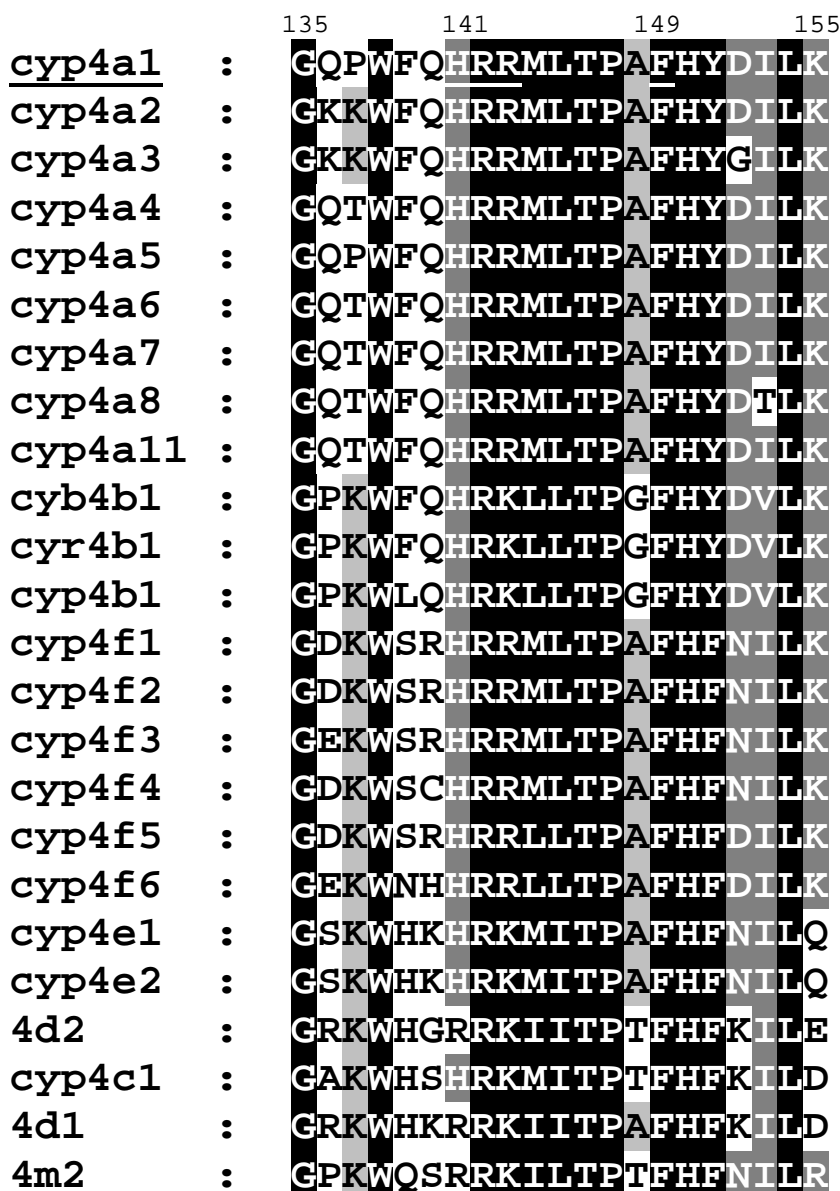


Figure 3-46. Alignment of the C-helix region in CYP4 proteins.

Alignment was created by pileup program and displayed by GeneDoc program. The conserved region is shown by different shades. The black shade is 100% identity, the deep gray shade is 80% identity and the light gray shade is 60% identity. The similar residues are considered to be identity. H141, R142, R143 and F149 residues in CYP4A1 are underlined.

3.4.2.1 H141

H141 is located at the beginning of C-helix. The model of CYP4A1 showed that H141 is very close to two acidic residues: D309 and E313 in the I-helix (Figure 3-47). Therefore, H141 could form an ion-pair with D309 and E313. This contact between H141 in C-helix and two residues including D309 and E313 in I-helix could

contribute to stabilisation of the structure of CYP4A1 and provide a potential pathway for transferring electron from redox partners to CYP4A1. To explore the role of H141, three mutants including H141R, H141F and H141L were designed.

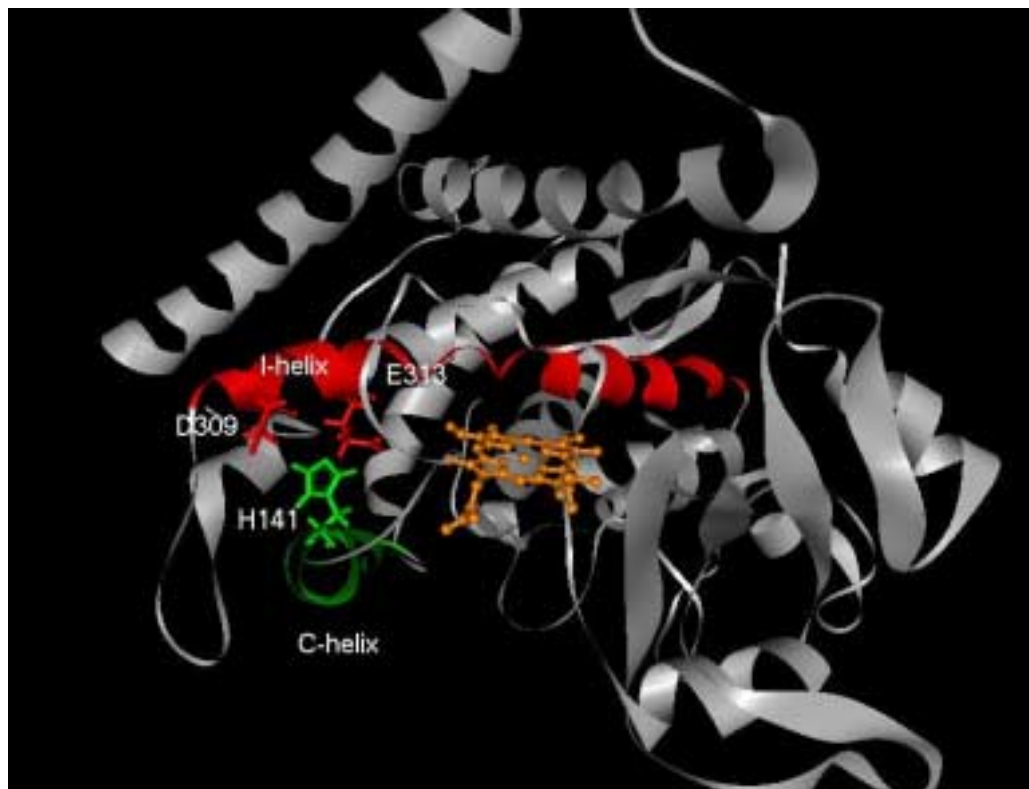


Figure 3-47. The position of H141 in the model of CYP4A1.

The C-helix of CYP4A1 is green and the I-helix is red. H141 residue (green) is very close to D309 and E313 (red).

In H141R mutant, the H residue was replaced by the residue R, which still carries the positive charge but does not contain the aromatic group. Conversely, in H141F mutant, the basic residue H was replaced by the residue F, which does not have positive charge but the keeps the aromatic structure. The H141L mutant changed positively charged residue H to hydrophobic residue L. All three mutants were constructed by GeneEditor Kits as described in Materials and Methods section 2.7.1, and expressed in JM109 as described in Materials and Methods section 2.6.2.3 for CYP4A1. The sequences of mutation were confirmed by double-strand sequencing as shown below.

H141R:
 GGACAACCGTGGTTCCAG**CGT**CGGCGAATGCTAACCCCAGCCTTCCAC
 G Q P W F Q **R** R R M L T P A F H

H141L:
 GGACAACCGTGGTTCCAG**CTG**CGGCGAATGCTAACCCCAGCCTTCCAC
 G Q P W F Q **L** R R M L T P A F H

H141F:
 GGACAACCATGGTTCCAG**TTT**CGGCGAATGCTAACCCCAGCCTTCCAC
 G Q P W F Q **F** R R M L T P A F H

Figure 3-48. DNA sequences of H141R, H141L and H141F and deduced amino acids.
 The mutations are shown as in bold; the novel *Nco I* site is underlined.

The expression levels were 17nmol/l for H141F, 38nmol/l for H141L and 62nmol/l for H141R. After purification, the homogenous proteins of the three mutants were observed (Figure 3-49). All of them showed the typical P450 spectra (Figure 3-50, 51, 52). The purified proteins were stored in 20mM potassium phosphate buffer (pH 7.4), 20% glycerol at -80°C until future use.

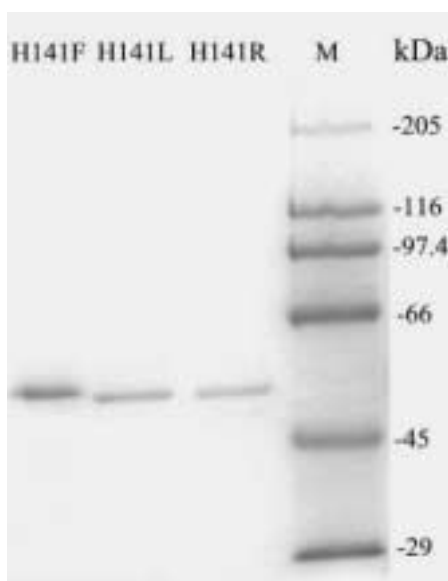


Figure 3-49. The purified H141R, H141F and H141L proteins.

3pmol of H141R, 5pmol of H141L and 9pmol of H141F were loaded on SDS-PAGE. The proteins were separated by 10% polyacrylamide gel and detected by coomassie blue. The protein marker was indicated (M=Marker, the unit was kDa).

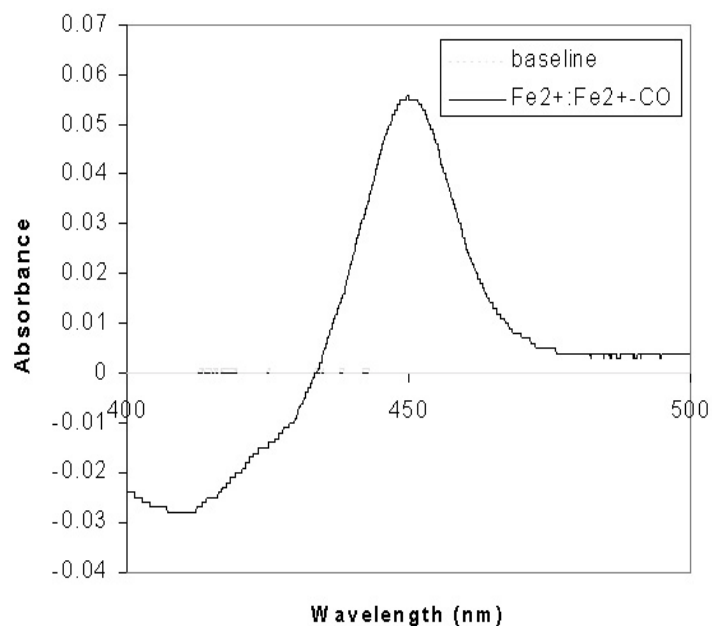


Figure 3-50. The CO-difference spectrum of purified H141R mutant.

The Fe^{2+} : Fe^{2+} -CO difference spectrum was recorded as described in Materials and Methods section 2.6.1.1. The concentration of enzyme was $0.56\mu\text{M}$.

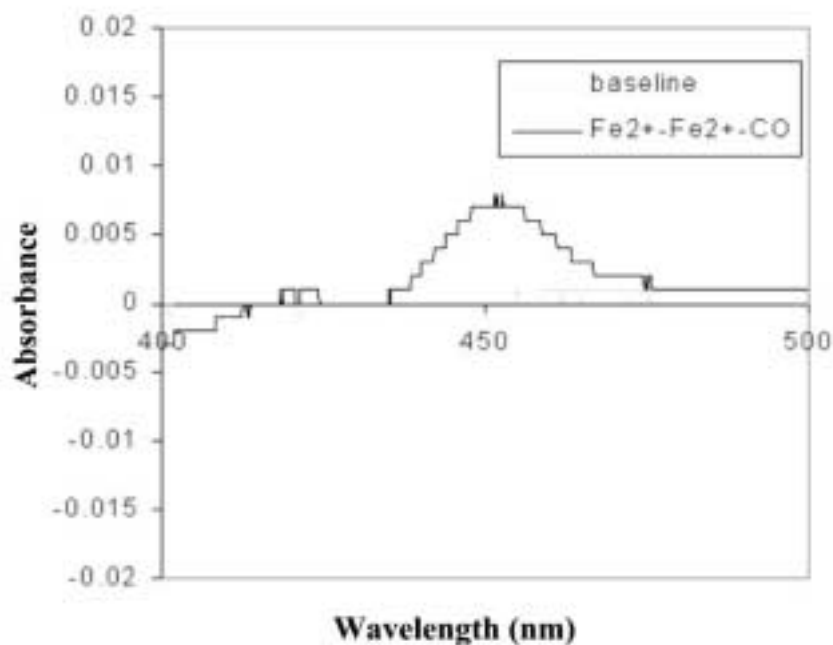


Figure 3-51. The CO-difference spectrum of purified H141F.

The Fe^{2+} : Fe^{2+} -CO difference spectrum was recorded as described in Materials and Methods section 2.6.1.1. The concentration of H141F was $0.08\mu\text{M}$.

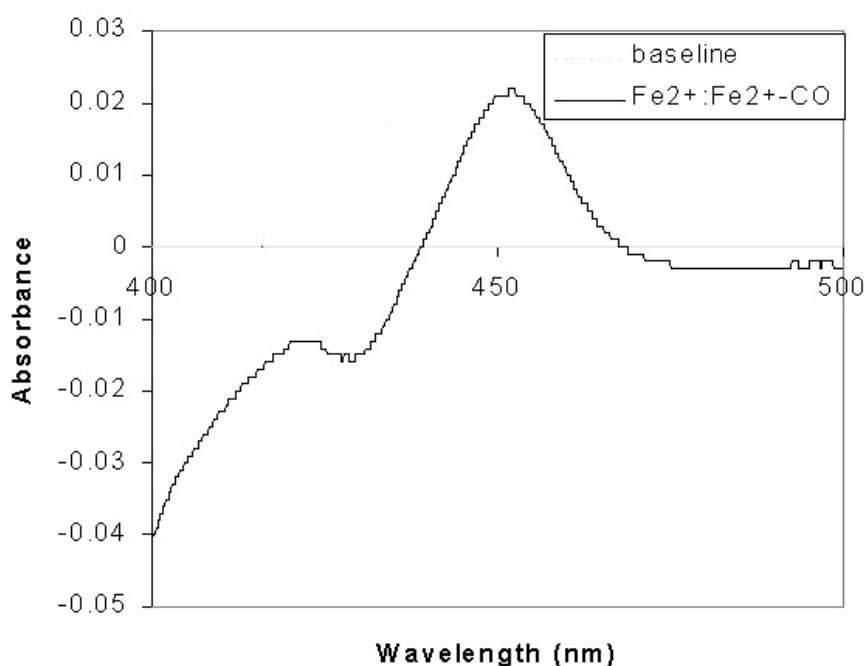


Figure 3-52. The CO-difference spectrum of purified H141L.

The $\text{Fe}^{2+} : \text{Fe}^{2+}\text{-CO}$ difference spectrum was recorded as described in Materials and Methods section 2.6.1.1. The concentration of H141L was $0.21\mu\text{M}$.

The activity of the three mutants was examined. The preliminary results showed that the activity of H141R was similar to wild type, but the activity of H141L and H141F kept only approximately 10~20% lauric acid ω -hydroxylation activity of wild type (unpublished, V. E. Holmes, Pharmaceutical Sciences, University of Nottingham). Therefore, the positive charge at 141 was important to keep the activity of P450.

3.4.2.2 F149

The residue F149 is located at the end of C-helix. The model of CYP4A1 shows that F149 is close to F317 in I-helix (Figure 3-53). Therefore, I-helix might interact with the C-helix through these two residues. To investigate the function of F149, two mutants, F149Y and F149I were constructed. In F149Y mutant, the polar residue tyrosine replaced the hydrophobic residue phenylalanine. As a result, the aromatic

structure is kept but the hydroxyl group at tyrosine makes the residue at 149 become hydrophilic. In F149I mutant, the hydrophobic character is kept because of the hydrophobic residue isoleucine, but the aromatic structure is eliminated.

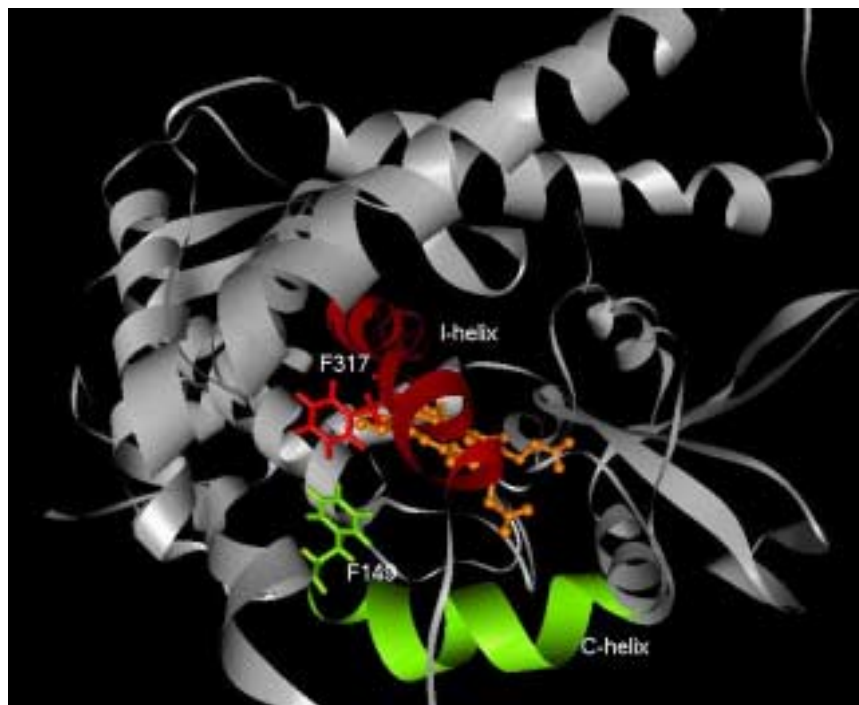


Figure 3-53. The F149 residue in the model of CYP4A1.

The F149 residue (green) in C-helix is close to the F317 residue (red) in I-helix. The C-helix and I-helix are green and red, respectively. The heme group in CYP4A1 is orange.

All mutants were constructed by GeneEditor Kits. The sequences of the mutations were confirmed by double-strand sequencing as shown below.

F149Y:

ATGCTAACCCCAGCC**AT**CCACTATGATATCCTGAAA
M L T P A **F** H Y D I L K

F149I:

ATGCTAACCCCAGC**CTA**CCACTATGATATCCTGAAA
M L T P A **I** H Y D I L K

Figure 3-54. DNA Sequences of F149Y and F149I and deduced amino acids.

The mutations are shown as in bold; the novel *EcoR* V sites are underlined.

The typical expression level of F149Y was 30nmol/l. The F149Y protein was purified to homogeneity as shown in Figure 3-55. The process of purification could

not remove P420. The spectrum of purified F149Y protein showed that the main maximum absorption was at 420nm and the peak at 450nm was very low (Figure 3-56).

The preliminary result showed that the activity of F149Y was approximate 30-40% of that of the wild type (unpublished, V. E. Holmes, Pharmaceutical Sciences, University of Nottingham). Therefore, the polar group at the position 149 could decrease P450 activity.

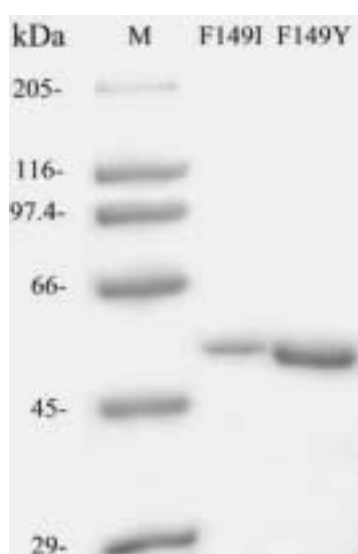


Figure 3-55. The purified F149I and F149Y protein.

5pmol of F149Y and 5 μ g of F149I were loaded on 10% SDS-PAGE and detected by coomassie blue. The protein marker was indicated (M=Marker, the mass unit is kDa).

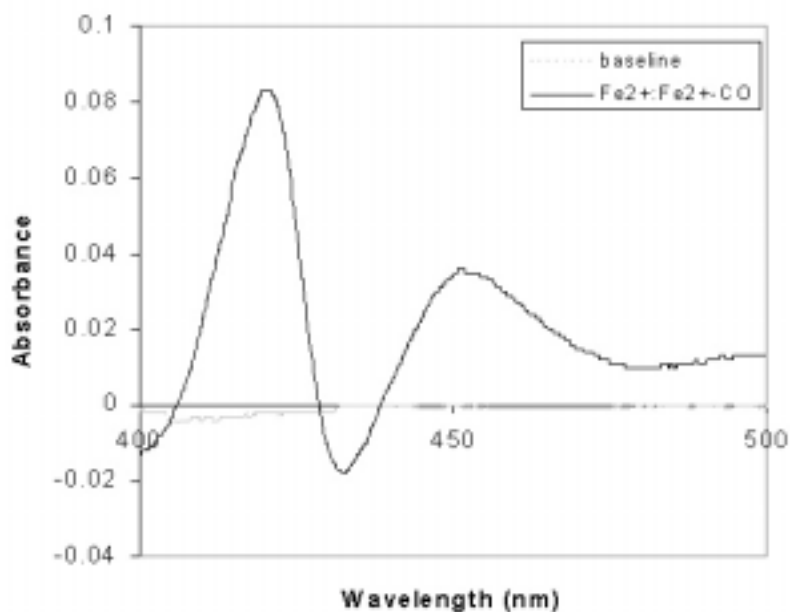


Figure 3-56. The CO-difference spectrum of F149Y.

The Fe^{2+} : Fe^{2+} -CO difference spectrum was recorded as described in Materials and Methods section 2.6.1.1. The concentration of enzyme was $0.27\mu\text{M}$.

After the F149I mutant was expressed in *E.coli*, no P450 could be detected in bacteria (Data not shown). After cells were sonicated, little P450 was found. The protein was purified to homogeneity as shown in Figure 3-55. The purified F149I protein contains almost no P450 (Figure 3-57). The activity of F149I mutant was not examined owing to insufficient P450 spectral activity. Therefore, the aromatic structure at 149 is necessary to keep the function of P450.

In summary, the aromatic group at position 149 is critical for P450 function; the hydrophilic group at this position can diminish P450 activity. Both aromatic and hydrophobic environments are required at position 149 of CYP4A1.

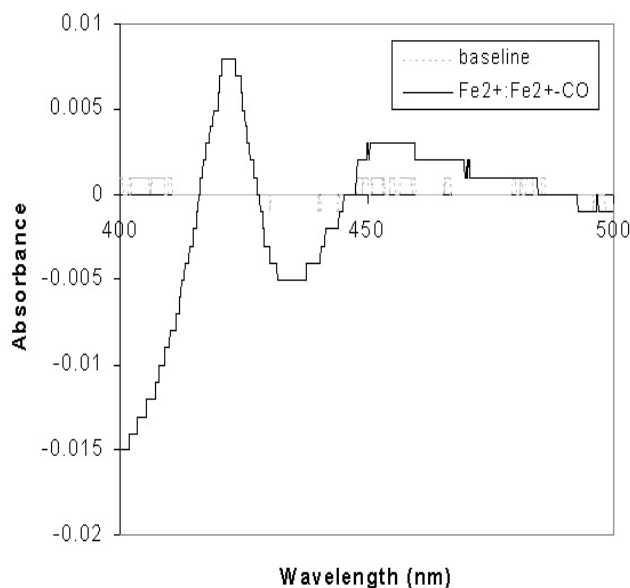


Figure 3-57. The CO-difference spectrum of F149L.

The Fe^{2+} : Fe^{2+} -CO difference spectrum was recorded as described in Materials and Methods section 2.6.1.1.

3.4.2.3 R142 and R143

The CYP4A1 model shows that R142 and R143 extend to the outer space (Figure 3-58). Both R142 and R143 carry positive charges. Therefore, these residues form part of the positively charged surface on CYP4A1.

The study of other P450s suggests the positively charged surface could interact with redox partners such as cytochrome P450 reductase and cytochrome b5 that carry negative charge on the surface (Omata *et al.* 1994; Bridges *et al.* 1998; Schenkman and Jansson 1999; Omata *et al.* 2000). Therefore, R142 and R143 could play a role in binding to redox partners. Two mutants, R142A and R143A were designed by replacing the positively charged arginine to the neutral residue, alanine.



Figure 3-58. The position of R142 and R143 in CYP4A1 model.

R142 and R143 residues are green and extend to outwards. The C-helix is green and I-helix is red. The heme group in CYP4A1 is orange.

The mutants were constructed by GeneEditor Kits as described in Materials and Methods section 2.7.1. The sequences of mutant were confirmed by double-strand sequencing as shown below.

R142A:

GGACAACCCATGGTTCCAGCAC**GCT**CGAATGCTAACCCAGCCTTCCAC
 G Q P W F Q H **A** R M L T P A F H

R143A:

GGACAACCCATGGTTCCAGCACCG**GCT**ATGCTAACCCAGCCTTCCAC
 G Q P W F Q H R **A** M L T P A F H

Figure 3-59. DNA Sequences of R142A and R143A and deduced amino acids.

The mutations are showed as the bold; the novel *Nco* I site is underlined.

The expression level of R142A and R143A mutants was low. The typical levels of expression were 13nmol/l for R142A and 26nmol/l for R143A. R142A mutant was not further purified as insufficient P450 was obtained. The R143A mutant was

purified to homogeneity (Figure 3-60-A). The R143A mutant showed the typical P450 difference spectrum (Figure 3-60-B). However, a large quantity of P420 was observed in this spectrum.

The preliminary result showed that the activity of R143A mutant was only approximately 10% of that of the wild type (unpublished, V. E. Holmes, Pharmaceutical Sciences, University of Nottingham). Therefore, the positive charge at 142 and 143 is important to keep normal P450 function. The decreased activity of R143A might result from insufficient contact between the CYP4A1 and the electron donor.

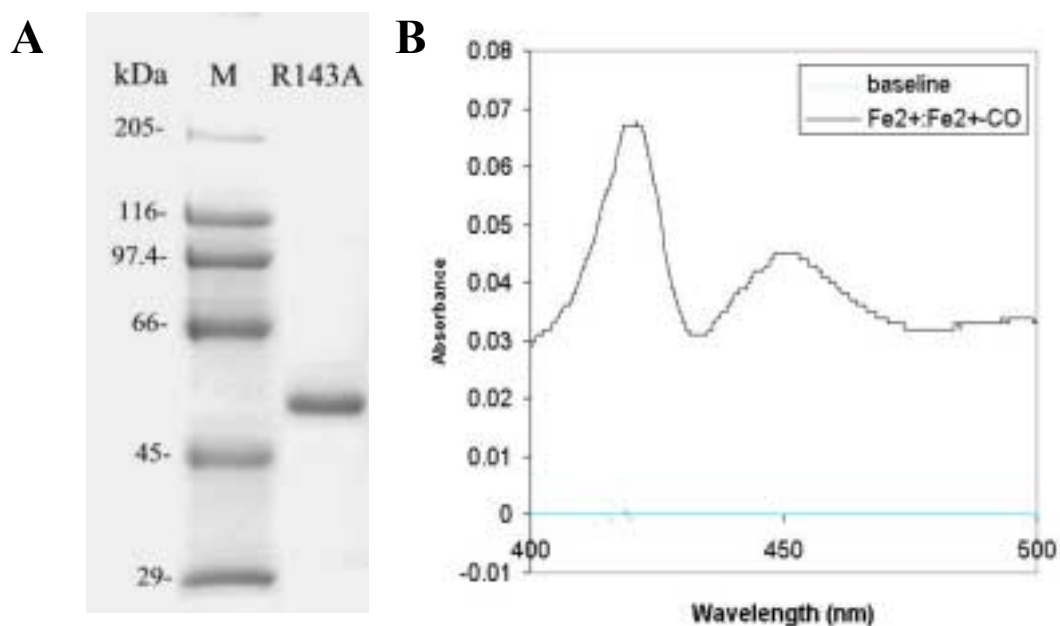


Figure 3-60. The R143A mutant protein.

(A) Purified R143A mutant on SDS-PAGE. 15pmol of R143A was loaded on 10% polyacrylamide gel and detected by coomassie blue. The position of protein marker (kDa) was indicated (M= Marker). **(B) Fe²⁺: Fe²⁺-CO difference spectrum of R143A mutant.** The concentration of enzyme was 0.14 μ M. The difference spectrum was recorded as described in Materials and Methods section 2.6.1.1.

4 Discussion

4.1 Expression of cytochrome b5

In order to reconstitute CYP4A1 activity *in vitro*, it was necessary to obtain enough pure and functional cytochrome b5 and cytochrome P450 reductase (CPR). A heterologous expression system was established to express cytochrome b5 and CPR.

Human cytochrome b5 was expressed in *E.coli* using a T7 expression system. In order to maximally express cytochrome b5, a series of conditions were optimised.

BL21(DE3)pLysS and HMS174(DE3)pLysS were examined as the host strains. They contain the λ DE3 lysogen, which provides T7 RNA polymerase to induce expression of the target protein; and the plasmid pLysS, which produces T7 lysozyme to inhibit T7 RNA polymerase produced at basal levels in the host (Studier *et al.* 1990). Thus, leaky expression would be reduced, which could be toxic to the host bacteria because membrane-bound cytochrome b5 could disturb the normal function of membrane. BL21 strain is deficient in *lon* and *ompT* proteases and therefore it has advantages for expression of some heterologous protein (Studier *et al.* 1990). However, my experience was that the expression of cytochrome b5 in BL21(DE3)pLysS was variable (data not shown). HMS174(DE3)pLysS was more suitable to express cytochrome b5 due to high-level expression and consistent reproducibility (Figure 3-4). This may be because the HMS174 strain is *recA*⁻, which may help to stabilise the DE3 prophage, unlike the BL21 strain that has *recA*⁺ background.

Terrific broth with rare salt was the best medium to express functional cytochrome b5 in HMS174(DE3)pLysS (Figure 3-4). It has been shown that terrific broth was also good for expression of cytochrome P450 in *E.coli* (Barnes 1996). This is

possibly because terrific broth is a rich media, in which bacteria grow better. Terrific broth also contains phosphate buffer, which can help to stabilise the culture pH around 7, and glycerol, which is ready to be used as carbon source (Barnes 1996).

Other reports suggest that the concentration of IPTG affects expression of cytochrome b5 in the T7 system (Holmans *et al.* 1994). Lower concentrations of IPTG were preferred, due to reduction of heterologous protein aggregates (Holmans *et al.* 1994). However, we did not observe that the concentration of IPTG (from 0.1mM to 1mM) had any obvious effect on the expression of cytochrome b5 (Figure 3-5). Even 1mM IPTG still induced the expression of functional cytochrome b5 (Figure 3-5). In our cytochrome b5 expression system, T7 lysozyme, which is produced by the pLysS plasmid in the host strain, inhibits T7 polymerase to reduce leaky expression. As a result, T7 polymerase present at a relatively low level, and so T7 promoter would not be very active even in the presence of high concentration of IPTG. Therefore, this system may not be very sensitive to the concentration of IPTG. The T7 system reported by Holmans *et al.* (1994) is different from our system; they did not use the plasmid pLysS. Thus, their system had a strong T7 promoter and as a result would be more easily affected by the concentration of IPTG (Holmans *et al.* 1994).

The optimal induction temperature was 27°C for expression of cytochrome b5 (Figure 3-6), differing from a previous report, which found expression of cytochrome b5 at above 25°C would form inclusion bodies (Holmans *et al.* 1994). The different effect of induction temperature observed between the current study and the previous report might also be caused by pLysS plasmid in the host strain, which reduces the T7 polymerase level, and possibly weakens the T7 promoter.

Expression level reached a peak after 24 hours induction, and longer induction time did not improve expression level (Figure 3-5). This was consistent with other reports using the T7 system to express cytochrome b5 (Holmans *et al.* 1994; Mulrooney and Waskell 2000).

Under optimal conditions, up to 265nmol of cytochrome b5 was expressed in 1 litre medium. Compared with other reports (Table 4-1), which also used T7 system to express mammalian cytochrome b5, this level was relatively low.

Table 4-1. Expression of cytochrome b5 in the different systems.

References	Holmans, shet <i>et al</i> , 1994	Mulrooney and Waskell <i>et al</i> , 2000	Current study
Level	1200-2000nmol/l	820mg/l	100-265nmol/l
Plasmid	pT7-7	pLW01	pRSET
Host strain	BL21(DE3)FT ^Q	C41(DE3)	HMS174(DE3)pLysS
Medium	TB	TB	TB
Induction time	24 hours	16-20 hours	24 hours
IPTG	0.1mM	0.01mM	0.1mM
Induction temperature	24°C	37°C	27°C

We compared our expression conditions with other references (Holmans *et al.* 1994; Mulrooney and Waskell 2000). All plasmids carried the T7 promoter. However, the host strains had different characters. Holmans *et al.* (1994) used a strain that had the *lac* repressor gene, *lacI*. As a result, T7 RNA polymerase was tightly switched off in the absence of IPTG because this gene is located downstream of the *lacUV5* promoter. Thus, the basal level of T7 RNA polymerase could be controlled, but the T7 promoter would still be strong as long as T7 polymerase was induced.

We used the pLysS plasmid included in the host strain, which produces an inhibitor of T7 polymerase to control leaky expression. However, the strength of the T7 promoter also became weaker (Studier *et al.* 1990). Moreover, it was reported by

Holmans *et al.* (1994) that pLysS could be lethal to the host strain during expression of cytochrome b5. Although we did not find the presence of pLysS to be fatal to the host bacteria during expression, there might have been a toxic effect of pLysS, which could also reduce expression level of cytochrome b5. Therefore, the expression level of cytochrome b5 was lower in the host containing pLysS plasmid.

More recently, mutants of BL21(DE3) were developed, including C41(DE3) and C43(DE3), which are specially beneficial for expression of membrane protein (Miroux and Walker 1996). It was believed that these mutants produced either deficient or less T7 RNA polymerase (Miroux and Walker 1996). As a result, the toxic effect of accumulating RNA on the host bacteria, which was caused by strong T7 RNA polymerase, could be reduced (Miroux and Walker 1996). Rabbit cytochrome b5 was expressed in C41(DE3) at a high level using T7 system (Mulrooney and Waskell 2000). Interestingly, the induction temperature in this system was 37°C (Mulrooney and Waskell 2000), which is much higher than other reports (Holmans *et al.* 1994) including our experiments. This is possibly due to the fact that the T7 promoter is less active in C41(DE3). We also used C41(DE3) to express human cytochrome b5. The expression level increased approximately 2 fold (data not shown). The advantage of using C41(DE3) to express membrane protein was confirmed.

It was reported that as much as 3000nmol/l rat cytochrome b5 was expressed in *E.coli* using pCWori⁺ plasmid (Chudaev and Usanov 1997), which is commonly used for expression of cytochrome P450. Therefore, other plasmids, which have a weaker promoter, might benefit expression of cytochrome b5 in *E.coli*.

T7 lysozyme produced by pLysS can not only inhibit the T7 RNA polymerase but also lyse the *E.coli* cell wall (Studier *et al.* 1990). As a result, simply freezing and thawing can help extract the target protein (Studier *et al.* 1990). However, freezing and thawing was not very efficient at lysing cells in our study (Table 3-1). It was necessary to combine this treatment with sonication (Table 3-1 and Table 3-2).

The efficiency of sonication depended on duration. Longer sonication times increased cell lysis but there was the risk of degradation of cytochrome b5. Thus, it is important to control the strength of sonication in order to obtain high recovery of cytochrome b5. The recovery of membrane-bound cytochrome b5 (33%) in our experiment (Table 3-3) was similar to the previous report (36%) (Holmans *et al.* 1994).

The His tag provided an easy way to purify cytochrome b5. Complex processes such as anion exchange and hydrophobic chromatography could be avoided. However, the recovery of cytochrome b5 was very low after the nickel affinity chromatography. Later, we found that binding of solubilised CYP4A1- (His)₆ protein to the nickel column was much better after protein storing buffer was exchanged for fresh buffer by a size exclusion PD-10 column. We proposed that the storing buffer after membrane protein solubilisation might contain histidine or other low molecular weight compounds, which competed with histidine tag protein binding to the nickel resin. As a result, the recovery by nickel affinity chromatography was low. Therefore, buffer exchange before purification may help to improve the recovery of cytochrome b5 purification.

Interestingly, when less detergent was used to solubilise membrane-bound cytochrome b5, the purification recovery increased (Table 3-4). This shows that the

amount of detergent used for cytochrome b5 solubilisation may also affect the recovery of cytochrome b5 purification.

In conclusion, functional human cytochrome b5 was expressed in *E.coli*. After purification, pure and spectrally functional cytochrome b5 was obtained (Figure 3-7 and 3-8). These purified cytochrome b5 was used in reconstitution of CYP4A1 activity.

4.2 Expression of CPR

Human cytochrome P450 reductase was expressed in *E.coli* using plasmid pB55, with human CPR cDNA fused to the *pelB* leader sequence in pB55. The initial study showed that expression of CPR in *E.coli* led to serious degradation of CPR (Porter *et al.* 1987); therefore the signal peptide, OmpA, was utilised to transport CPR into periplasmic space to avoid proteolysis (Shen *et al.* 1989). In this project, *pelB* was supposed to play a similar role to OmpA because *pelB* is also a signal peptide.

The recombinant CPR expressed in JM109 showed cytochrome c reduction activity (Table 3-5). This meant that the recombinant CPR was functional. After affinity purification by 2', 5'-ADP agarose, there were two bands of approximate molecular weight 66,000Da and 78,000Da, on SDS-PAGE. The high molecular weight corresponded to intact CPR. According to previous studies, the low molecular weight band was likely to result from the proteolysis of CPR (Porter *et al.* 1987). The purified CPR retained strong cytochrome c reduction activity, and was used for reconstitution of CYP4A1 activity *in vitro*.

4.3 Expression of CYP4A1

OmpA is a membrane protein in *E.coli*, which contains 346 amino acids, the first 21 of which make up the transmembrane signal region (MKKTAIAIAVAIAGFATVAQAA) (Movva *et al.* 1980). The signal peptide of OmpA was fused to CYP4A1 to express P450 in *E.coli*. A six-histidine tag was introduced in the fusion protein to help purification.

Several factors including the host strain, the concentration of IPTG, induction time, and induction temperature were examined for maximal expression of OmpA.4A1.HT. The optimal conditions (Section 3.3.1.4) were similar to a previous study for expression of cytochrome P450 in *E.coli*. (Barnes 1996). The effect of δ -ALA was also investigated. The supplement of δ -ALA was found to enhance the expression of OmpA.4A1.HT (Figure 3-14). However, a previous report showed that expression of OmpA-3A4 was not improved by the addition of δ -ALA (Pritchard *et al.* 1997). δ -ALA is the precursor of heme, which might explain enhancement in expression of P450s. However, when P450s are expressed at high level, heme may not be the limiting factor and as a result, the additional δ -ALA would not improve the expression level. The effect of δ -ALA could differ for expression of different P450s. In a previous report, the same OmpA-fusion strategy was used to express CYP3A4, 2A6 and 2E1 (Pritchard *et al.* 1997). All expression levels, except for CYP2E1, were higher than N-terminally modified versions (Pritchard *et al.* 1997). However, the expression level of OmpA.4A1.HT fusion was 60-100nmol in one litre of media under optimal conditions, similar to the expression level of modified N-terminal CYP4A1 (Figure 3-15). Therefore, although functional OmpA-CYP4A1 was successfully expressed in *E.coli*, OmpA-fusion did not improve the expression level

of CYP4A1. The reason why expression level of different P450s shows such variation needs further investigation.

Previous studies showed that buffer, detergent and the concentration of protein could affect solubilisation of membrane protein (Hjelmeland 1990). Phosphate buffer is well known for its ability to aid in solubilisation of membrane protein (Hjelmeland 1990), and so it was chosen for solubilisation of CYP4A1 in this project.

Non-ionic surfactants such as Emulgen 913 are widely used for extracting P450s from membranes. Interestingly, we found that the combination of Emulgen 913 and sodium cholate, which is an ionic detergent, improved the recovery of the P450 after solubilisation (Table 3-6). This might be because the ionic detergent could interact with the charged surface of P450, enhancing the solubility of P450. Thus, detergents with different properties were used together.

Higher concentrations of protein can improve solubilisation of P450 from the microsome (Hjelmeland 1990). When the membrane protein concentration was higher than 1mg/ml, better recovery was obtained (Hjelmeland 1990). Therefore, the microsome protein concentration was kept at more than 1 mg/ml in this experiment.

After CYP4A1 was purified by Ni²⁺ chelate affinity chromatography, the protein showed a single band on the SDS-PAGE (Figure 3-16A). This meant that CYP4A1 was homogenous. The purified CYP4A1 had a typical P450 carbon monoxide binding spectrum and little P420 was detected (Figure 3-16B). Therefore, pure and functional CYP4A1 was obtained.

The specific content of purified OmpA.4A1.HT (2.2 nmol/mg protein) was found to be lower than the theoretical value (16.4 nmol/mg protein, based on a molecular weight of OmpA.4A1.HT of 60.8kDa), which meant that a considerable amount of

P450 lost spectral activity during purification. A similar result was observed during purification of [His]₆-CYP2D6-Δ25 (Kempf *et al.* 1995). The authors proposed that imidazole, which was used to elute P450 from nickel column, could compete with carbon monoxide to bind with heme and therefore the content of P450 could be underestimated (Kempf *et al.* 1995).

Dierks *et al.* (1998) reported that imidazole could bind to CYP4A1 and induce a difference spectrum that had a peak around 425nm. The K_s value of CYP4A1 binding to imidazole was 1.4±0.1mM, determined by the difference spectrum (Dierks *et al.* 1998a). During purification of CYP4A1, the concentration of imidazole in the buffer (5-750mM) was much higher than the K_s value. Therefore, imidazole could bind to CYP4A1 and possibly occupy the heme iron site in CYP4A1. Although the purified CYP4A1 was desalted using a PD-10 column, there may still been some tightly bound imidazole in CYP4A1. This could affect the binding of carbon monoxide to P450 and as a result, the content of P450 could be undervalued.

Another reason for low specific content of CYP4A1 could be the loss of heme during purification. It was reported that 30% of heme, in the *E.coli* expressed CYP4A1, was covalently bound and 70% heme was in free form (Hoch and Ortiz De Montellano 2001). When CYP4A1- (His)₆ bound to the nickel column, some free heme may have been washed out by the washing buffer, resulting in some CYP4A1 losing the heme.

Therefore, the functional recombinant CYP4A1 was successfully expressed in *E.coli*. CYP4A1 protein was purified to be homogenous by nickel chelate chromatography and the purified protein had the typical P450 spectrum (Figure 3-16). These CYP4A1 proteins were used for substrate-binding and activity assays.

4.4 Structure-function relationships of CYP4A1

4.4.1 Substrate binding sites

Site-directed mutagenesis was used to examine residues in CYP4A1, which could bind substrate. We tried to distinguish mutants, which only affected substrate-binding patterns from other mutations, which diminished CYP4A1 catalytic activity because of other reasons, such as disturbing the tertiary structure of the enzyme. Therefore, mutants were designed, which are supposed to change the substrate specificity from fatty acid to fatty amine.

4.4.1.1 K93

A model of CYP4A1 was built to help to investigate structure-function relationships in CYP4A1 (unpublished, C. A. Laughton, University of Nottingham). This model suggests that the basic residue K93, located at the entrance of the substrate-binding channel, is a substrate-binding residue (Figure 3-21). The alignment of CYP4A proteins also showed that K or R, which carry a positive charge; often appear at a similar position in other CYP4A members (Figure 3-20). Moreover, R47 in CYPBM3, which is equivalent to K93 in CYP4A1, was identified as a crucial residue for substrate binding (Graham-Lorence *et al.* 1997; Oliver *et al.* 1997; Noble *et al.* 1999). Therefore, we proposed that K93 could possibly form an ion-pair with the carboxyl group of a fatty acid substrate, and then would play an important role in substrate contact.

In order to examine this hypothesis, we changed the positively charged residue K93 to the negatively charged residue E by site-directed mutagenesis and proposed that the K93E mutant would change the substrate specificity from fatty acid to fatty

amine. This was because K93E would form ion-pair with the amine compound that carries a positive charge, but not with fatty acid, which carries the same negative charge as the residue E.

The substrate affinity of K93E mutant was investigated, and compared with wild type. Two kinds of substrate: lauric acid and dodecyltrimethylammonium bromide, which carry negative and positive charge respectively, were used in the experiments. Addition of lauric acid to CYP4A1 and K93E induced a Type I difference spectra (Figure 3-24A and 3-25A). For lauric acid, the K_s value of K93E ($32\mu\text{M}$) was approximately three times higher than that of CYP4A1 ($9.7\mu\text{M}$), but the change was less than expected. The expected electrostatic repulsion between the carboxyl groups in lauric and glutamic acid should have produced a bigger difference in K_s . For dodecyltrimethylammonium bromide, no difference spectrum was observed during titration of the substrate in CYP4A1 (Figure 3-26). However, the difference spectrum of K93E showed a trough at approximate 420nm but no peak at 390nm (Figure 3-27A). This change in the difference spectrum could not be an artefact because CYP4A1 did not show a similar pattern. The K_s value could not be determined because the regression curve was linear in the range of 0-410 μM of amine compound. This linear pattern was consistent with the initial region of the regression curve (0-100 μM lauric acid) obtained from CYP4A1 binding to lauric acid (Figure 3-25B). The maximal change of absorbance caused by titration of amine compound in K93E was approximately half (Figure 3-27B) that caused by titration of lauric acid in CYP4A1 (Figure 3-24B). Higher concentrations of amine compound were not used in this experiment due to the fact that a large amount of detergent would destroy the

enzyme tertiary structure. Therefore, this difference spectrum suggested that there was a weak interaction between K93E and dodecyltrimethylammonium bromide.

Our hypothesis predicted that K93E would bind to fatty amine compound because the ion-pair could form between the negatively charged glutamic acid and the positively charged dodecyltrimethylammonium bromide. This contact was detected by a substrate-binding assay, but the interaction between K93E and fatty amine compound was weaker than expected.

In summary, K93E mutant results in an increase of K_s for lauric acid and the weak binding to fatty amine compound, but the change of K to E did not greatly affect substrate-specificity.

Our previous hypothesis suggested that K93E would change substrate-specificity from fatty acid to fatty amine compound. Our results clearly showed that change of K93 to E in CYP4A1 slightly decreased the affinity against lauric acid and produced a weak interaction with fatty amine compound. Therefore, K93 in CYP4A1 could be related to substrate contact, but is not the principle substrate binding residue. Other residues in CYP4A1 may work together with K93 and determine the substrate binding.

4.4.1.2 R87

Because K93 was not identified as the determinative residue for substrate binding, we then investigated other residues that could be involved in substrate binding. The model of CYP4A1 suggested R87 to be located on the opposite side of K93 but also in the mouth of substrate channel (Figure 3-28). Moreover, R87 carries a positive charge, which could potentially form an ion-pair with substrate. Therefore, we designed a series of mutants to examine the role of R87.

Firstly, R87 mutant was replaced by the residue E. Substrate specificity of R87E was investigated. Titration of lauric acid induced in a Type I substrate-binding difference spectrum (Figure 3-32). The K_s value of R87E binding to lauric acid ($544\mu\text{M}$) was much higher than that of CYP4A1 binding to lauric acid ($9.7\mu\text{M}$), showing that R87E decreased the affinity to lauric acid. No change was observed in the difference spectrum of R87E binding to dodecyltrimethylammonium bromide (Figure 3-34). Thus, R87E possibly did not bind the amine compound. The activity assay showed that R87E mutant failed to metabolise either lauric acid or amine compound (unpublished, V. E. Holmes, University of Nottingham). Since the mutation from R87 to E diminished lauric acid affinity in the absence of increased amine compound binding, this was consistent with the effect of the mutation, which had an adventitious effect on the tertiary structure of CYP4A1 in the substrate access channel; therefore, we could not assess the contribution of R87 in substrate binding from this data.

We also designed the double mutant, R87E/K93E, to examine if the combination of mutations at both R87 and K93 to E would change the substrate-binding pattern. Titration of lauric acid resulted in a Type I difference spectrum in R87E/K93E (Figure 3-33A) and the K_s value of binding lauric acid ($370\mu\text{M}$) was much higher than that of CYP4A1 binding to the same substrate ($9.7\mu\text{M}$). The difference spectrum of titration of dodecyltrimethylammonium bromide in R87E/K93E was similar to that in K93E, which showed no peak at 390nm but a trough at 420nm (Figure 3-35A). The linear relationship of ΔA against the concentration of amine compound was obtained (Figure 3-35B). This difference spectrum suggested that R87E/K93E only bound weakly to the fatty amine compound as described in section

4.4.1.1. Therefore, R87E/K93E showed low affinity to both lauric acid and amine compound, consistent with the results obtained from R87E. This could be due to the destruction of tertiary structure of CYP4A1 in the substrate access channel. Thus, the role of R87 in CYP4A1 cannot be evaluated from these data.

We then used neutral residue W to replace the basic residue R87 to further investigate the role of R87 in CYP4A1. R87W mutation is supposed to keep the P450 activity because CYP4A4 also has W in the corresponding position according to the alignment among CYP4As (Figure 3-20). We looked to see if the substrate specificity of the mutant would change when the positive charge was absent at R87 and the basic residue K93 was replaced by the acidic residue E. Thus, the double mutant R87W/K93E was constructed. Titration of lauric acid in R87W/K93E induced a Type I difference spectrum (Figure 3-38A), but the affinity to lauric acid of R87W/K93E was lower than that of wild type due to the very high K_s value (724 μ M). R87W/K93E showed weak contact to amine compound due to the similar difference spectrum of titration of dodecyltrimethylammonium bromide in R87W/K93E (Figure 3-39) as described in the section 4.4.1.1. These results suggested that the change of R87 to W decreased the affinity to lauric acid because K93E single mutant did not dramatically affect the substrate affinity, but R87W/K93E did not shift the substrate specificity from lauric acid to the amine compound. This can be explained by the fact that W could not form an ion-pair with amine and K93E only bound the amine weakly. However, we could not distinguish the reduction of fatty acid affinity in R87W/K93E resulted from the poor binding of substrate, or destruction of tertiary structure at the entrance of substrate-binding channel. A further activity assay of R87W/K93E may help to find the answer.

Therefore, R87 is important to keep the function of P450 but it is not clear if R87 residue is directly involved in the substrate binding.

4.4.1.3 N116

N116 is located behind the K93 in the model of CYP4A1 (Figure 3-41). We hypothesised that the substrate might initially interact with K93, then shift to N116. Therefore, N116 could be another candidate for substrate binding.

We designed the N116E and N116E/K93E mutants to investigate the function of N116. We failed to obtain the purified functional N116E/K93E mutant, owing to low level of expression and few P450 in microsome (section 3.4.1.3). Therefore, only N116E mutant was examined.

The substrate binding assay showed that the K_s value of N116E binding to lauric acid ($8\mu\text{M}$) was similar to that of CYP4A1 ($9.7\mu\text{M}$), and titration of dodecyltrimethyl-ammonium bromide did not cause the change of difference spectrum (Figure 3-45), the same observation as seen with CYP4A1. These results suggested that the mutation in N116 did not affect substrate-binding pattern, and that N116 was probably not involved in substrate binding.

We investigated the role of three residues including K93, R87 and N116 in CYP4A1 for substrate binding. Our results showed that the K93 residue is involved in binding substrate but that it does not determine the substrate binding. Also, R87 is important for maintaining the normal P450 activity but we cannot assess the substrate-binding ability of R87 due to the fact that E mutation at R87 resulted in the non-functional enzyme; and that N116 is probably not involved in substrate contact.

K93 in CYP4A1 is equivalent to K91T in CYP4A3. In a previous report, the K91T mutant of CYP4A3 completely lost catalytic activity and the titration of lauric acid

and myristic acid did not cause a spin state change (Hoch *et al.* 2000a). The authors did not describe the reason why the CYP4A3-K91T mutant lost the activity in their study. There are two possibilities that could have caused activity loss of CYP4A3-K91T mutant. The first possibility was that the K91T mutant failed to bind substrate. The second possibility was that the mutation deconstructs the tertiary structure of the substrate-binding channel. Our results suggested that the K93E mutant still bound lauric acid well and kept significant activity. Therefore, we propose that the activity loss of CYP4A3-K91T mutant was possibly caused by the second reason.

In CYP4A7, there is a natural E residue in the position corresponding to that of K93 in CYP4A1. However, CYP4A7 can bind and metabolise lauric acid well (Loughran *et al.* 2000). This seems to be consistent with our observation from K93E mutant.

The position of R47 in CYPBM3 is equivalent to K93 in CYP4A1. Although R47 in CYPBM3 was a critical residue for substrate binding; there is argument about the role of R47 in CYPBM3. In the crystal structure of CYPBM3, R47 residue could not be well defined (Ravichandran *et al.* 1993). The authors suggested that the position of R47 could be flexible (Ravichandran *et al.* 1993). The crystal structure of CYPBM3 with palmitoleic acid and N-palmitoylglycine revealed that the distance between R47 and the carboxyl group of substrates was longer than efficient electrostatic interaction range (Li and Poulos 1997; Haines *et al.* 2001). The authors proposed that the role of R47 in substrate binding could be flexible and transient (Li and Poulos 1997; Haines *et al.* 2001). Although the R47 mutants showed decreased affinity for some substrates of BM3 (Graham-Lorence *et al.* 1997; Oliver *et al.* 1997; Noble *et al.* 1999), it was recently reported that R47A mutant had a higher turnover than the wild type for lauric acid oxidation. Also, the K_s of R47A only increased 3.7

fold for arachidonic acid and 4.9 fold for palmitoleic acid (Coward *et al.* 2001), which is similar to our observation in K93E binding to lauric acid. Therefore, K93 in CYP4A1 may also be flexible. It may it might initially form a temporary intermediate with the substrate, the substrate would then shift to (an) other binding site(s). Other residues in CYP4A1 could determine substrate binding.

R90 in CYP4A7 is the equivalent to R87 in CYP4A1 in the alignment of CYP4A proteins (Figure 3-20). In a previous study, R90W mutant of CYP4A7 showed a decrease of catalytic activity against laurate and arachidonate but a slight increase of PGE₁ activity (Loughran *et al.* 2000). Our substrate-binding assay suggested that the affinity of R87W/K93E to lauric acid was reduced, which is consistent with the observation in CYP4A7-R90W mutant.

Owing to failure of identifying the key substrate binding residues, it remains in question what residue(s) is (are) crucial for substrate binding. The study in CYPBM3 suggested that Y51 plays an important role in substrate binding. The hydrogen bond could be formed between Y51 and carboxyl group in the fatty acid. Y95 in CYP4A1 is similar to Y51 in CYPBM3. The CYP4A1 model showed that Y95 is also located at the entrance of the substrate channel; it is close to K93 but behind K93. Therefore, the position of Y95 is suitable to bind substrate.

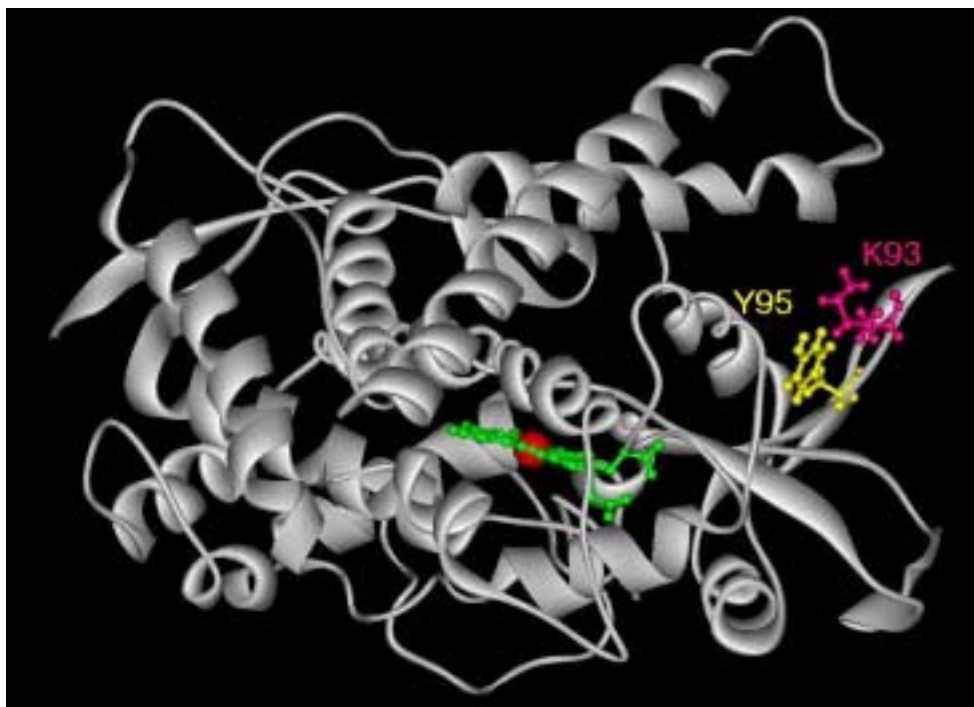


Figure 4-1. Y95 residue in CYP4A1 model.

The Y95 residue is yellow; the K93 residue is pink. The heme group is green and the iron in the heme is red.

The alignment of the CYP4As suggested that the basic residues, which could potentially make contact with carboxyl group of fatty acid, often appear in the similar position to Y95 in CYP4A1. The two exceptions are CYP4A7 and CYP4A21, which have hydrophobic residue F and M in this position. Interestingly, CYP4A21, the new member of CYP4A subfamily, recently identified in pig, can not use lauric acid as the substrate, but it can hydroxylate chenodeoxycholic acid (Lundell *et al.* 2001). Therefore, CYP4A21 probably has different substrate recognition sites. The sites that respond to bind lauric acid could be lacking in CYP4A21. The Met90 in CYP4A21, corresponding to Y95 in CYP4A1 (Figure 4-2), might be able to explain the unique substrate specificity of CYP4A21.

	68	93 95	99
CYP4A1_rat	: DKELQQIMTCVENFPSAFPRWFWGSKAY Y LLIVY		
CYP4A2_rat	: DREFQQVLTWVEKFPGACLQWLSGSTAR V LLLY		
CYP4A3_rat	: DREFQQVLTWVEKFPGACLQWLSGSKT R VLLLY		
CYP4A4_rabbit	: DQELERIQKWVEKFPGACPWWLSGNKAR L LLVY		
CYP4A5_rabbit	: NQELQQILKWVEKFPRACPHWIGGNK V RVQLY		
CYP4A6_rabbit	: GHELQVMLKWVEKFPSACPRWLWGSRA H LLIY		
CYP4A7_rabbit	: DSELQQVLKRVEKFPSACPRWLWGSEL F LICY		
CYP4A8_rat	: DQDFQDILTRVKNFPSACPQWLWGSNV R IQVY		
CYP4A11_human	: DQELQRIQKWVETFPSACPHWLWGGK V RVQLY		
CYP4A21_pig	: ESELQPLLKRVEKYPSACARWLWGTRAM M VLVY		
		90	

Figure 4-2. Alignment of CYP4As protein sequence.

Y95 in CYP4A1 and the corresponding residues in other CYP4As are shown in bold. F96 in CYP4A7 and M90 in CYP4A21 are underlined.

Moreover, it was reported that CYP4A1 could bind methyl laurate and lauryl alcohol well (Alterman *et al.* 1995). These compounds do not carry a charge and therefore they cannot form an ion-pair with the positively charged residues in CYP4A1. However, the hydroxyl group in Y95 could possibly form a hydrogen bond with the carboxyl group in methyl laurate and hydroxyl group in lauryl alcohol. Therefore, Y95 could be another potential candidate for substrate binding.

4.4.2 The C-helix region

The C-helix is conserved in the CYP4 family according to the alignment among CYP4As (Figure 4-46), but its role is unknown. The CYP4A1 model showed that the C-helix is behind I-helix and had putative contact with the heme group (Figure 3-47). We chose four residues: H141, R142, R143 and F149 in C-helix, and examined their functions by site-directed mutagenesis.

4.4.2.1 H141

H141 is located almost at the beginning of C-helix (Figure 3-46). Histidine is a basic residue and has aromatic group. In order to examine what structural characteristic was important, we designed two mutants, H141F and H141L. These did not carry the

positive charge but H141F still had the aromatic structure. These two mutants dramatically decreased the P450 activity. Interestingly, another mutant, H141R, which kept the positive charge, had similar activity to wild type (unpublished, Holmes, University of Nottingham). Therefore, the positive charge at this position maintained the catalytic activity of CYP4A1, but aromatic structure did not.

The model of CYP4A1 suggested that basic residue H141 is very close to two acidic residues, D309 and E313, in I-helix (Figure 3-47). The ion-pair could be formed between H141 and acidic residues. This electrostatic contact could help to stabilise the tertiary structure of CYP4A1. Owing to the fact that histidine is conserved in all CYP4As, H141 possibly plays an important role in keeping P450 function.

4.4.2.2 F149

Another residue we focused on was F149, which is located at the end of the C-helix (Figure 3-46). In this study, we undertook mutagenesis to find the function of F149 in CYP4A1. After Ile replaced Phe, most of the enzyme was non-functional P420 (Figure 3-57). However, the F149Y mutant retained some activity but the activity was much lower than wild type (unpublished, Holmes, University of Nottingham). Therefore, the aromatic character was required for activity of CYP4A1.

In the CYP4A1 model, F149 in C-helix was very close to F317 in I-helix (Figure 3-53). They might interact with each other to help to stabilise the position of C-helix and I-helix. The polar hydroxy group at F149Y might reduce this interaction, and F149I could not have this interaction. As a result, F149Y has the low activity and F149 turns to non-functional P420. Therefore, F149 also contributes to the normal function of P450.

4.4.2.3 R142 and R143

There are some basic residues at C-helix, which could comprise part of positively charged surface (Figure 3-58). We designed two mutants, R142A and R143A, to eliminate the charge and then examined the activity of mutants. R142A did not yield purified enzyme due to the low expression level (12nmol/l). However, purified R143A showed a significant decrease of activity (unpublished, Holmes, University of Nottingham). The study of CYP2B4 and 2B1 suggested that the positively charged surface of P450 was related to docking negative charged redox partners including CPR and cytochrome b5 (Omata *et al.* 1994; Bridges *et al.* 1998; Omata *et al.* 2000). Some key residues, including R126 in CYP2B4 (Bridges *et al.* 1998) and R125 in CYP2B1 (Omata *et al.* 1994; Omata *et al.* 2000), have been identified. R142 and R143 in CYP4A1 correspond to the position of R125 and R126 in both 2B4 and 2B1. Therefore, it is possible that they share a common function for binding the redox partners. The low activity of R143A might be caused by the inefficient contact between CYP and redox partners.

```

          138      142                151
4A1  : WFQHRRM-LTPAFHY
2B4  : WRALRRFSLATMRDF
2B1  : WKALRRFSLATMRDF
                125

```

Figure 4-3. Alignment of 4A1 with 2B4 and 2B1.

R142 and R143 in CYP4A1 and R125 and R126 in CYP2B1 and 2B4 are underlined.

4.5 Future direction

The role of residues K93, R87 and N116 in substrate binding have been studied by site-directed mutagenesis in this project. However, it is still not very clear which residue(s) in CYP4A1 is (are) crucial for substrate-binding. Therefore, the further investigation of structure-function relationships in CYP4A1 seems to be necessary.

As described in section 4.4.1, the Y95 residue in CYP4A1 may play a role in substrate-binding, according to the CYP4A1 model, alignment among CYP4A proteins and studies in CYPBM3. Therefore, site-directed mutagenesis in Y95 may be a good start to further identify the key substrate-binding residue in CYP4A1. Furthermore, the updated CYP4A1 model may also lead to find the other potential substrate-binding residues, and then site-directed mutagenesis can help to reveal the function of these residues.

For the C-helix region in CYP4A1, it has been shown that H141, R142, R143 and F149 residues in this region are important to keep the P450 function in this study. The further experiments are necessary to elucidate the function of these residues. For example, the interactions between positively charged residues such as H141, R142 and R143 and redox partners are needed to investigate. The functions of H141 and F149 in stabilisation of CYP4A1 structure and keeping P450 spectral character are also needed to examine. These further studies may help us well understand the C-helix region in CYP4A1.

5 References

Alberts, B., D. Bray, J. Lewis, M. Raff, K. Roberts and J. D. Watson (1994).

Molecular biology of the cell. New York, Garland Publishing.

Alterman, M. A., C. S. Chaurasia, P. Lu, J. P. Hardwick and R. P. Hanzlik (1995).

"Fatty acid discrimination and omega-hydroxylation by cytochrome P450 4A1 and a cytochrome P4504A1/NADPH-P450 reductase fusion protein." *Arch Biochem Biophys* **320**(2): 289-96.

Bambal, R. B. and R. P. Hanzlik (1996a). "Active site structure and substrate specificity of cytochrome P450 4A1: steric control of ligand approach perpendicular to heme plane." *Biochem Biophys Res Commun* **219**(2): 445-9.

Bambal, R. B. and R. P. Hanzlik (1996b). "Effects of steric bulk and conformational rigidity on fatty acid omega hydroxylation by a cytochrome P450 4A1 fusion protein." *Arch Biochem Biophys* **334**(1): 59-66.

Baneyx, F. (1999). "Recombinant protein expression in Escherichia coli." *Current Opinion in Biotechnology* **10**: 411-421.

Barnes, H. J. (1996). "Maximizing expression of eukaryotic cytochrome P450s in Escherichia coli." *Methods Enzymol* **272**: 3-14.

Barnes, H. J., M. P. Arlotto and M. R. Waterman (1991). "Expression and enzymatic activity of recombinant cytochrome P450 17 alpha-hydroxylase in Escherichia coli." *Proc Natl Acad Sci U S A* **88**(13): 5597-601.

Bell, D. R., N. J. Plant, C. G. Rider, L. Na, S. Brown, I. Ateitalla, S. K. Acharya, M. H. Davies, E. Elias, N. A. Jenkins and et al. (1993). "Species-specific induction of cytochrome P-450 4A RNAs: PCR cloning of partial guinea-pig, human and mouse CYP4A cDNAs." *Biochem J* **294** (Pt 1): 173-80.

Boitier, E. and P. Beaune (1999). "Cytochromes P450 as targets to autoantibodies in immune mediated diseases." *Mol Aspects Med* **20**(1-2): 84-137.

Bridges, A., L. Gruenke, Y. T. Chang, I. A. Vakser, G. Loew and L. Waskell (1998). "Identification of the binding site on cytochrome P450 2B4 for cytochrome b5 and cytochrome P450 reductase." *J Biol Chem* **273**(27): 17036-49.

Buters, J. T., M. Shou, J. P. Hardwick, K. R. Korzekwa and F. J. Gonzalez (1995). "cDNA-directed expression of human cytochrome P450 CYP1A1 using baculovirus. Purification, dependency on NADPH-P450 oxidoreductase, and reconstitution of catalytic properties without purification." *Drug Metab Dispos* **23**(7): 696-701.

Bylund, J., M. Bylund and E. H. Oliw (2001). "cDNA cloning and expression of CYP4F12, a novel human cytochrome P450." *Biochem Biophys Res Commun* **280**(3): 892-7.

Bylund, J., N. Finnstrom and E. H. Oliw (1999). "Gene expression of a novel cytochrome P450 of the CYP4F subfamily in human seminal vesicles." *Biochem Biophys Res Commun* **261**(1): 169-74.

Bylund, J., M. Hidestrand, M. Ingelman-Sundberg and E. H. Oliw (2000). "Identification of CYP4F8 in human seminal vesicles as a prominent 19-hydroxylase of prostaglandin endoperoxides." *J Biol Chem* **275**(29): 21844-9.

Capdevila, J. H. and J. R. Falck (2001). "The CYP P450 arachidonic acid monooxygenases: from cell signaling to blood pressure regulation." *Biochem Biophys Res Commun* **285**(3): 571-6.

Capdevila, J. H., J. R. Falck and R. C. Harris (2000). "Cytochrome P450 and arachidonic acid bioactivation. Molecular and functional properties of the arachidonate monooxygenase." *J Lipid Res* **41**(2): 163-81.

Capdevila, J. H., V. Holla, C. Helvig and J. R. Falck (1999). "Microsomal cytochrome P450 and eicosanoid metabolism." *Mol Aspects Med* **20**(1-2): 42-55, 56-137.

Chang, Y. T. and G. H. Loew (1999a). "Homology modeling and substrate binding study of human CYP4A11 enzyme." *Proteins* **34**(3): 403-15.

Chang, Y. T. and G. H. Loew (1999b). "Molecular dynamics simulations of P450 BM3--examination of substrate-induced conformational change." *J Biomol Struct Dyn* **16**(6): 1189-203.

Chaurasia, C. S., M. A. Alterman, P. Lu and R. P. Hanzlik (1995). "Biochemical characterization of lauric acid omega-hydroxylation by a CYP4A1/NADPH-cytochrome P450 reductase fusion protein." *Arch Biochem Biophys* **317**(1): 161-9.

Chen, L., J. T. M. Buters, J. P. Hardwick, S. Tamura, B. W. Penman, F. J. Gonzalez and C. Crespi (1997). "Coexpression of cytochrome P4502A6 and human NADPH-P450 oxidoreductase in the baculovirus system." *Drug Metabolism and Disposition* **25**(4): 399-405.

- Chen, L. and J. P. Hardwick (1993). "Identification of a new P450 subfamily, CYP4F1, expressed in rat hepatic tumors." *Arch Biochem Biophys* **300**(1): 18-23.
- Christmas, P., S. R. Ursino, J. W. Fox and R. J. Soberman (1999). "Expression of the CYP4F3 gene. tissue-specific splicing and alternative promoters generate high and low K(m) forms of leukotriene B(4) omega-hydroxylase." *J Biol Chem* **274**(30): 21191-9.
- Chudaev, M. V. and S. A. Usanov (1997). "Expression of functionally active cytochrome b5 in Escherichia coli: isolation, purification, and use of the immobilized recombinant heme protein for affinity chromatography of electron-transfer proteins." *Biochemistry (Mosc)* **62**(4): 401-11.
- Clark, B. J. and M. R. Waterman (1991). "Heterologous expression of mammalian P450 in COS cells." *Methods Enzymol* **206**: 100-8.
- Coon, M. J., X. Ding, S. J. Pernecky and A. D. N. Vaz (1992). "Cytochrome P450 progress and predictions." *The FASEB Journal* **6**: 669-673.
- Cosme, J. and E. F. Johnson (2000). "Engineering microsomal cytochrome P450 2C5 to be a soluble, monomeric enzyme. Mutations that alter aggregation, phospholipid dependence of catalysis, and membrane binding." *J Biol Chem* **275**(4): 2545-53.
- Cowart, L. A., J. R. Falck and J. H. Capdevila (2001). "Structural determinants of active site binding affinity and metabolism by cytochrome P450 BM-3." *Arch Biochem Biophys* **387**(1): 117-24.

- Crespi, C. L. (1991). "Expression of cytochrome P450 cDNAs in human B lymphoblastoid cells: applications to toxicology and metabolite analysis." *Methods Enzymol* **206**: 123-9.
- Crespi, C. L. and V. P. Miller (1999). "The use of heterologously expressed drug metabolizing enzymes-state of the art and prospects for the future." *Pharmacology & Therapeutics* **84**: 121-131.
- Cui, X., D. R. Nelson and H. W. Strobel (2000). "A novel human cytochrome P450 4F isoform (CYP4F11): cDNA cloning, expression, and genomic structural characterization." *Genomics* **68**(2): 161-6.
- Cvrk, T. and H. W. Strobel (2001). "Role of LYS271 and LYS279 residues in the interaction of cytochrome P4501A1 with NADPH-cytochrome P450 reductase." *Arch Biochem Biophys* **385**(2): 290-300.
- Dai, R., M. R. Pincus and F. K. Friedman (2000). "Molecular modeling of mammalian cytochrome P450s." *Cell Mol Life Sci* **57**(3): 487-99.
- Dierks, E. A., S. C. Davis and P. R. Ortiz de Montellano (1998a). "Glu-320 and Asp-323 are determinants of the CYP4A1 hydroxylation regiospecificity and resistance to inactivation by 1-aminobenzotriazole." *Biochemistry* **37**(7): 1839-47.
- Dierks, E. A., Z. Zhang, E. F. Johnson and P. R. de Montellano (1998b). "The catalytic site of cytochrome P4504A11 (CYP4A11) and its L131F mutant." *J Biol Chem* **273**(36): 23055-61.
-

Doehmer, J. and F. Oesch (1991). "V79 Chinese hamster cells genetically engineered for stable expression of cytochromes P450." *Methods Enzymol* **206**: 117-23.

Domanski, T. L. and J. R. Halpert (2001). "Analysis of mammalian cytochrome P450 structure and function by site-directed mutagenesis." *Curr Drug Metab* **2**(2): 117-37.

Dong, J. and T. D. Porter (1996). "Coexpression of mammalian cytochrome P450 and reductase in Escherichia coli." *Arch Biochem Biophys* **327**(2): 254-9.

Estabrook, R. (1999). "An introduction to the cytochrome P450s." *Mol Aspects Med* **20**(1-2): 5-12, 13-137.

Farrell, G. (1999). "Effects of disease on expression and regulation of CYPs." *Mol Aspects Med* **20**(1-2): 55-70, 137.

Fernandez, J. M. and J. P. Hoeffler (1999). Selecting a suitable expression system: Considerations. *Gene expression systems*. J. P. Hoeffler, Academic Press: 3.

Fisher, C. W., D. L. Caudle, C. Martin-Wixtrom, L. C. Quattrochi, R. H. Tukey, M. R. Waterman and R. W. Estabrook (1992a). "High-level expression of functional human cytochrome P450 1A2 in Escherichia coli." *Faseb J* **6**(2): 759-64.

Fisher, C. W., M. S. Shet, D. L. Caudle, C. A. Martin-Wixtrom and R. W. Estabrook (1992b). "High-level expression in Escherichia coli of enzymatically active fusion proteins containing the domains of mammalian cytochromes P450 and NADPH-P450 reductase flavoprotein." *Proc Natl Acad Sci U S A* **89**(22): 10817-21.

Fisher, C. W., M. S. Shet and R. W. Estabrook (1996). "Construction of plasmids and expression in Escherichia coli of enzymatically active fusion proteins containing

the heme-domain of a P450 linked to NADPH-P450 reductase." *Methods Enzymol* **272**: 15-25.

Fisher, M. B., Y. M. Zheng and A. E. Rettie (1998). "Positional specificity of rabbit CYP4B1 for omega-hydroxylation of short-medium chain fatty acids and hydrocarbons." *Biochem Biophys Res Commun* **248**(2): 352-5.

Galleno, M. and A. J. Sick (1999). Baculovirus expression vector system. *Gene expression systems*. J. P. Hoeffler, Academic Press: 332-367.

Galleno, M. and A. J. Stick (1999). Baculovirus expression vector system. *Gene expression systems*. J. P. Hoeffler, Academic Press.

Gasser, R. and R. M. Philpot (1989). "Primary structures of cytochrome P-450 isozyme 5 from rabbit and rat and regulation of species-dependent expression and induction in lung and liver: identification of cytochrome P-450 gene subfamily IVB." *Mol Pharmacol* **35**(5): 617-25.

Gelboin, H. V., K. W. Krausz, F. J. Gonzalez and T. J. Yang (1999). "Inhibitory monoclonal antibodies to human cytochrome P450 enzymes: a new avenue for drug discovery." *Current Awareness* **20**: 432-438.

Gilep, A. A., O. L. Guryev, S. A. Usanov and R. W. Estabrook (2001). "Apo-cytochrome b5 as an indicator of changes in heme accessibility: preliminary studies with cytochrome P450 3A4." *J Inorg Biochem* **87**(4): 237-44.

Gillam, E. M., T. Baba, B. R. Kim, S. Ohmori and F. P. Guengerich (1993). "Expression of modified human cytochrome P450 3A4 in Escherichia coli and

purification and reconstitution of the enzyme." *Arch Biochem Biophys* **305**(1): 123-31.

Gillam, E. M., Z. Guo, M. V. Martin, C. M. Jenkins and F. P. Guengerich (1995). "Expression of cytochrome P450 2D6 in Escherichia coli, purification, and spectral and catalytic characterization." *Arch Biochem Biophys* **319**(2): 540-50.

Gonzalez, F. J., T. Aoyama and H. V. Gelboin (1991a). "Expression of mammalian cytochrome P450 using vaccinia virus." *Methods Enzymol* **206**: 85-92.

Gonzalez, F. J., S. Kimura, S. Tamura and H. V. Gelboin (1991b). "Expression of mammalian cytochrome P450 using baculovirus." *Methods Enzymol* **206**: 93-9.

Gonzalez, F. J. and K. R. Korzekwa (1995). "Cytochromes P450 expression systems." *Annu Rev Pharmacol Toxicol* **35**: 369-90.

Graham, S. E. and J. A. Peterson (1999). "How similar are P450s and what can their differences teach us?" *Arch Biochem Biophys* **369**(1): 24-9.

Graham-Lorence, S., G. Truan, J. A. Peterson, J. R. Falck, S. Wei, C. Helvig and J. H. Capdevila (1997). "An active site substitution, F87V, converts cytochrome P450 BM-3 into a regio- and stereoselective (14S,15R)-arachidonic acid epoxygenase." *J Biol Chem* **272**(2): 1127-35.

Guengerich, F. P. (1991). "Reactions and Significance of Cytochrome P-450 Enzymes." *The Journal of Biological Chemistry* **266**: 10019-10022.

Guengerich, F. P., W. R. Brian, M. A. Sari and J. T. Ross (1991). "Expression of mammalian cytochrome P450 enzymes using yeast-based vectors." *Methods Enzymol* **206**: 130-45.

Guengerich, F. P., E. M. Gillam and T. Shimada (1996). "New applications of bacterial systems to problems in toxicology." *Crit Rev Toxicol* **26**(5): 551-83.

Guengerich, F. P., N. A. Hosea, A. Parikh, L. C. Bell-Parikh, W. W. Johnson, E. M. Gillam and T. Shimada (1998). "Twenty years of biochemistry of human P450s, Purification, Expression, Mechanism, Relevance to Drugs." *Drug Metabolism and Disposition* **26**(12): 1175-1178.

Guengerich, F. P. and W. W. Johnson (1997). "Kinetics of ferric cytochrome P450 reduction by NADPH-cytochrome P450 reductase: rapid reduction in the absence of substrate and variations among cytochrome P450 systems." *Biochemistry* **36**(48): 14741-50.

Guryev, O. L., A. A. Gilep, S. A. Usanov and R. W. Estabrook (2001). "Interaction of apo-cytochrome b5 with cytochromes P4503A4 and P45017A: relevance of heme transfer reactions." *Biochemistry* **40**(16): 5018-31.

Haines, D. C., D. R. Tomchick, M. Machius and J. A. Peterson (2001). "Pivotal role of water in the mechanism of P450BM-3." *Biochemistry* **40**(45): 13456-65.

Harder, D. R., R. J. Roman and D. Gebremedhin (2000). "Molecular mechanisms controlling nutritive blood flow: role of cytochrome P450 enzymes." *Acta Physiol Scand* **168**(4): 543-9.

- Hardwick, J. P. (1991). "CYP4A subfamily: functional analysis by immunohistochemistry and in situ hybridization." *Methods Enzymol* **206**: 273-83.
- Hardwick, J. P., B. J. Song, E. Huberman and F. J. Gonzalez (1987). "Isolation, complementary DNA sequence, and regulation of rat hepatic lauric acid omega-hydroxylase (cytochrome P-450LA omega). Identification of a new cytochrome P-450 gene family." *J Biol Chem* **262**(2): 801-10.
- Hashizume, T., S. Imaoka, T. Hiroi, Y. Terauchi, T. Fujii, H. Miyazaki, T. Kamataki and Y. Funae (2001). "cDNA cloning and expression of a novel cytochrome p450 (cyp4f12) from human small intestine." *Biochem Biophys Res Commun* **280**(4): 1135-41.
- Hasler, J. A. (1999). "Pharmacogenetics of cytochromes P450." *Mol Aspects Med* **20**(1-2): 12-24, 25-137.
- Heng, Y. M., C. S. Kuo, P. S. Jones, R. Savory, R. M. Schulz, S. R. Tomlinson, T. J. Gray and D. R. Bell (1997). "A novel murine P-450 gene, Cyp4a14, is part of a cluster of Cyp4a and Cyp4b, but not of CYP4F, genes in mouse and humans." *Biochem J* **325 (Pt 3)**: 741-9.
- Henne, K. R., K. L. Kunze, Y. M. Zheng, P. Christmas, R. J. Soberman and A. E. Rettie (2001). "Covalent linkage of prosthetic heme to CYP4 family P450 enzymes." *Biochemistry* **40**(43): 12925-31.
- Hjelmeland, L. M. (1990). "Solubilization of native membrane proteins." *Methods Enzymol* **182**: 253-64.
-

Hlavica, P., M. Lehnerer and M. Eulitz (1996). "Histidine residues in rabbit liver microsomal cytochrome P-450 2B4 control electron transfer from NADPH-cytochrome P-450 reductase and cytochrome b5." *Biochem J* **318** (Pt 3): 857-62.

Hoch, U., J. R. Falck and P. R. de Montellano (2000a). "Molecular basis for the omega-regiospecificity of the CYP4A2 and CYP4A3 fatty acid hydroxylases." *J Biol Chem* **275**(35): 26952-8.

Hoch, U. and P. R. Ortiz De Montellano (2001). "Covalently linked heme in cytochrome p4504a fatty acid hydroxylases." *J Biol Chem* **276**(14): 11339-46.

Hoch, U., Z. Zhang, D. L. Kroetz and P. R. Ortiz de Montellano (2000b). "Structural determination of the substrate specificities and regioselectivities of the rat and human fatty acid omega-hydroxylases." *Arch Biochem Biophys* **373**(1): 63-71.

Holla, V. R., F. Adas, J. D. Imig, X. Zhao, E. Price, Jr., N. Olsen, W. J. Kovacs, M. A. Magnuson, D. S. Keeney, M. D. Breyer, J. R. Falck, M. R. Waterman and J. H. Capdevila (2001). "Alterations in the regulation of androgen-sensitive Cyp 4a monooxygenases cause hypertension." *Proc Natl Acad Sci U S A* **98**(9): 5211-6.

Holmans, P. L., M. S. Shet, C. A. Martin-Wixtrom, C. W. Fisher and R. W. Estabrook (1994). "The high-level expression in *Escherichia coli* of the membrane-bound form of human and rat cytochrome b5 and studies on their mechanism of function." *Arch Biochem Biophys* **312**(2): 554-65.

Hosny, G., L. J. Roman, M. H. Mostafa and B. S. Masters (1999). "Unique properties of purified, *Escherichia coli*-expressed constitutive cytochrome P4504A5." *Arch Biochem Biophys* **366**(2): 199-206.

Imaoka, S., T. Hiroi, Y. Tamura, H. Yamazaki, T. Shimada, M. Komori, M. Degawa and Y. Funae (1995). "Mutagenic activation of 3-methoxy-4-aminoazobenzene by mouse renal cytochrome P450 CYP4B1: cloning and characterization of mouse CYP4B1." *Arch Biochem Biophys* **321**(1): 255-62.

Imaoka, S., H. Ogawa, S. Kimura and F. J. Gonzalez (1993). "Complete cDNA sequence and cDNA-directed expression of CYP4A11, a fatty acid omega-hydroxylase expressed in human kidney." *DNA Cell Biol* **12**(10): 893-9.

Inoue, E., Y. Takahashi, Y. Imai and T. Kamataki (2000). "Development of bacterial expression system with high yield of CYP3A7, a human fetus-specific form of cytochrome P450." *Biochem Biophys Res Commun* **269**(2): 623-7.

Iwata, H., K. Fujita, H. Kushida, A. Suzuki, Y. Konno, K. Nakamura, A. Fujino and T. Kamataki (1998). "High catalytic activity of human cytochrome P450 co-expressed with human NADPH-cytochrome P450 reductase in *Escherichia coli*." *Biochem Pharmacol* **55**(8): 1315-25.

Jefcoate, C. R. (1978). "Measurement of substrate and inhibitor binding to microsomal cytochrome P-450 by optical-difference spectroscopy." *Methods Enzymol* **52**: 258-79.

Jenkins, C. M., I. Pikuleva and M. R. Waterman (1998). Expression of eukaryotic cytochrome P450 in *E.coli*. *Cytochrome P450s Protocols*. E. A. Shephard. Totowa, Human Press Inc. **107**: 181-193.

Jin, R., D. R. Koop, J. L. Raucy and J. M. Lasker (1998). "Role of human CYP4F2 in hepatic catabolism of the proinflammatory agent leukotriene B4." *Arch Biochem Biophys* **359**(1): 89-98.

Johnson, E. F., D. L. Walker, K. J. Griffin, J. E. Clark, R. T. Okita, A. S. Muerhoff and B. S. Masters (1990). "Cloning and expression of three rabbit kidney cDNAs encoding lauric acid omega-hydroxylases." *Biochemistry* **29**(4): 873-9.

Kaminsky, L. S. and S. D. Spivack (1999). "Cytochromes P450 and cancer." *Mol Aspects Med* **20**(1-2): 70-84, 137.

Kawashima, H., E. Kusunose, C. M. Thompson and H. W. Strobel (1997). "Protein expression, characterization, and regulation of CYP4F4 and CYP4F5 cloned from rat brain." *Arch Biochem Biophys* **347**(1): 148-54.

Kawashima, H., T. Naganuma, E. Kusunose, T. Kono, R. Yasumoto, K. Sugimura and T. Kishimoto (2000). "Human fatty acid omega-hydroxylase, CYP4A11: determination of complete genomic sequence and characterization of purified recombinant protein." *Arch Biochem Biophys* **378**(2): 333-9.

Kawashima, H. and H. W. Strobel (1995). "cDNA cloning of three new forms of rat brain cytochrome P450 belonging to the CYP4F subfamily." *Biochem Biophys Res Commun* **217**(3): 1137-44.

Kempf, A. C., U. M. Zanger and U. A. Meyer (1995). "Truncated human P450 2D6: expression in *Escherichia coli*, Ni(2+)-chelate affinity purification, and characterization of solubility and aggregation." *Arch Biochem Biophys* **321**(2): 277-88.

Kikuta, Y., E. Kusunose, K. Endo, S. Yamamoto, K. Sogawa, Y. Fujii-Kuriyama and M. Kusunose (1993). "A novel form of cytochrome P-450 family 4 in human polymorphonuclear leukocytes. cDNA cloning and expression of leukotriene B4 omega-hydroxylase." *J Biol Chem* **268**(13): 9376-80.

Kikuta, Y., E. Kusunose, M. Ito and M. Kusunose (1999a). "Purification and characterization of recombinant rat hepatic CYP4F1." *Arch Biochem Biophys* **369**(2): 193-6.

Kikuta, Y., E. Kusunose, H. Sumimoto, Y. Mizukami, K. Takeshige, T. Sakaki, Y. Yabusaki and M. Kusunose (1998). "Purification and characterization of recombinant human neutrophil leukotriene B4 omega-hydroxylase (cytochrome P450 4F3)." *Arch Biochem Biophys* **355**(2): 201-5.

Kikuta, Y., Y. Miyauchi, E. Kusunose and M. Kusunose (1999b). "Expression and molecular cloning of human liver leukotriene B4 omega-hydroxylase (CYP4F2) gene." *DNA Cell Biol* **18**(9): 723-30.

Kimura, S., N. Hanioka, E. Matsunaga and F. J. Gonzalez (1989a). "The rat clofibrate-inducible CYP4A gene subfamily. I. Complete intron and exon sequence of the CYP4A1 and CYP4A2 genes, unique exon organization, and identification of a conserved 19-bp upstream element." *DNA* **8**(7): 503-16.

Kimura, S., J. P. Hardwick, C. A. Kozak and F. J. Gonzalez (1989b). "The rat clofibrate-inducible CYP4A subfamily. II. cDNA sequence of IVA3, mapping of the Cyp4a locus to mouse chromosome 4, and coordinate and tissue-specific regulation of the CYP4A genes." *DNA* **8**(7): 517-25.

Kroetz, D. L., L. M. Huse, A. Thuresson and M. P. Grillo (1997). "Developmentally regulated expression of the CYP4A genes in the spontaneously hypertensive rat kidney." *Mol Pharmacol* **52**(3): 362-72.

Lasker, J. M., W. B. Chen, I. Wolf, B. P. Bloswick, P. D. Wilson and P. K. Powell (2000). "Formation of 20-hydroxyeicosatetraenoic acid, a vasoactive and natriuretic eicosanoid, in human kidney. Role of Cyp4F2 and Cyp4A11." *J Biol Chem* **275**(6): 4118-26.

Lee, C. A., S. H. Kadwell, T. A. Kost and C. J. Serabjit-Singh (1995). "CYP3A4 expressed by insect cells infected with a recombinant baculovirus containing both CYP3A4 and human NADPH-cytochrome P450 reductase is catalytically similar to human liver microsomal CYP3A4." *Arch Biochem Biophys* **319**(1): 157-67.

Lee, C. A., T. A. Kost and C. J. Serabjit-Singh (1996). "Recombinant baculovirus strategy for coexpression of functional human cytochrome P450 and P450 reductase." *Methods Enzymol* **272**: 86-95.

Lehnerer, M., J. Schulze, K. Achterhold, D. F. Lewis and P. Hlavica (2000). "Identification of key residues in rabbit liver microsomal cytochrome P450 2B4: importance in interactions with NADPH-cytochrome P450 reductase." *J Biochem (Tokyo)* **127**(1): 163-9.

Lewis, D. F. (1995). "Three-dimensional models of human and other mammalian microsomal P450s constructed from an alignment with P450102 (P450bm3)." *Xenobiotica* **25**(4): 333-66.

Lewis, D. F. and B. G. Lake (1995). "Molecular modelling of members of the P4502A subfamily: application to studies of enzyme specificity." *Xenobiotica* **25**(6): 585-98.

Lewis, D. F. and B. G. Lake (1999). "Molecular modelling of CYP4A subfamily members based on sequence homology with CYP102." *Xenobiotica* **29**(8): 763-81.

Lewis, D. F., B. G. Lake, M. Dickins, P. J. Eddershaw, M. H. Tarbit and P. S. Goldfarb (1999). "Molecular modelling of CYP2B6, the human CYP2B isoform, by homology with the substrate-bound CYP102 crystal structure: evaluation of CYP2B6 substrate characteristics, the cytochrome b5 binding site and comparisons with CYP2B1 and CYP2B4." *Xenobiotica* **29**(4): 361-93.

Li, H. and T. L. Poulos (1997). "The structure of the cytochrome p450BM-3 heme domain complex with the fatty acid substrate, palmitoleic acid." *Nature structural biology* **4**(2): 140-146.

Li, H. and T. L. Poulos (1999). "Fatty acid metabolism, conformational change, and electron transfer in cytochrome P-450(BM-3)." *Biochim Biophys Acta* **1441**(2-3): 141-9.

Li, Q. S., J. Ogawa, R. D. Schmid and S. Shimizu (2001a). "Residue size at position 87 of cytochrome P450 BM-3 determines its stereoselectivity in propylbenzene and 3-chlorostyrene oxidation." *FEBS Lett* **508**(2): 249-52.

Li, Q. S., J. Ogawa and S. Shimizu (2001b). "Critical role of the residue size at position 87 in H₂O₂- dependent substrate hydroxylation activity and H₂O₂

inactivation of cytochrome P450BM-3." *Biochem Biophys Res Commun* **280**(5): 1258-61.

Loughran, P. A., L. J. Roman, A. E. Aitken, R. T. Miller and B. S. Masters (2000). "Identification of unique amino acids that modulate CYP4A7 activity." *Biochemistry* **39**(49): 15110-20.

Loughran, P. A., L. J. Roman, R. T. Miller and B. S. Masters (2001). "The kinetic and spectral characterization of the E. coli-expressed mammalian CYP4A7: cytochrome b5 effects vary with substrate." *Arch Biochem Biophys* **385**(2): 311-21.

Lundell, K. (2002). "Cloning and expression of two novel pig liver and kidney fatty acid hydroxylases [cytochrome P450 (CYP)4A24 and CYP4A25]." *Biochem J* **363**(Pt 2): 297-303.

Lundell, K., R. Hansson and K. Wikvall (2001). "Cloning and expression of a pig liver taurochenodeoxycholic acid 6 α -hydroxylase (CYP4A21): a novel member of the CYP4A subfamily." *J Biol Chem* **276**(13): 9606-12.

Mansuy, D. (1998). "The great diversity of reactions catalyzed by cytochromes P450." *Comparative Biochemistry and Physiology Part C* **121**: 5-14.

Matsubara, S., S. Yamamoto, K. Sogawa, N. Yokotani, Y. Fujii-Kuriyama, M. Haniu, J. E. Shively, O. Gotoh, E. Kusunose and M. Kusunose (1987). "cDNA cloning and inducible expression during pregnancy of the mRNA for rabbit pulmonary prostaglandin omega-hydroxylase (cytochrome P-450p-2)." *J Biol Chem* **262**(27): 13366-71.

- Mauk, A. G., M. R. Mauk, G. R. Moore and S. H. Northrup (1995). "Experimental and theoretical analysis of the interaction between cytochrome c and cytochrome b5." *J Bioenerg Biomembr* **27**(3): 311-30.
- Maves, S. A., H. Yeom, M. A. McLean and S. G. Sligar (1997). "Decreased substrate affinity upon alteration of the substrate-docking region in cytochrome P450(BM-3)." *FEBS Lett* **414**(2): 213-8.
- Miroux, B. and J. E. Walker (1996). "Over-production of proteins in Escherichia coli: mutant hosts that allow synthesis of some membrane proteins and globular proteins at high levels." *J Mol Biol* **260**(3): 289-98.
- Modi, S., M. J. Paine, M. J. Sutcliffe, L. Y. Lian, W. U. Primrose, C. R. Wolf and G. C. Roberts (1996). "A model for human cytochrome P450 2D6 based on homology modeling and NMR studies of substrate binding." *Biochemistry* **35**(14): 4540-50.
- Movva, N. R., K. Nakamura and M. Inouye (1980). "Gene structure of the OmpA protein, a major surface protein of Escherichia coli required for cell-cell interaction." *J Mol Biol* **143**(3): 317-28.
- Muchmore, D. C., L. P. McIntosh, C. B. Russell, D. E. Anderson and F. W. Dahlquist (1989). "Expression and nitrogen-15 labeling of proteins for proton and nitrogen-15 nuclear magnetic resonance." *Methods Enzymol* **177**: 44-73.
- Muerhoff, A. S., K. J. Griffin and E. F. Johnson (1992). "Characterization of a rabbit gene encoding a clofibrate-inducible fatty acid omega-hydroxylase: CYP4A6." *Arch Biochem Biophys* **296**(1): 66-72.
-

Mulrooney, S. B. and L. Waskell (2000). "High-level expression in Escherichia coli and purification of the membrane-bound form of cytochrome b(5)." *Protein Expr Purif* **19**(1): 173-8.

Murray, M. (1999). "Induction and inhibition of CYPs and implications for medicine." *Mol Aspects Med* **20**(1-2): 24-33, 34-137.

Nebert, D. W. and D. R. Nelson (1991). "P450 gene nomenclature based on evolution." *Methods Enzymol* **206**: 3-11.

Nelson, D. R. (1999). "Cytochrome P450 and the individuality of species." *Arch Biochem Biophys* **369**(1): 1-10.

Nelson, D. R., L. Koymans, T. Kamataki, J. J. Stegeman, R. Feyereisen, D. J. Waxman, M. R. Waterman, O. Gotoh, M. J. Coon, R. W. Estabrook, I. C. Gunsalus and D. W. Nebert (1996). "P450 superfamily: update on new sequences, gene mapping, accession numbers and nomenclature." *Pharmacogenetics* **6**(1): 1-42.

Ngo, S., S. Kong, A. Kirlich, R. A. McKinnon and I. Stupans (2000). "Cytochrome P450 4A, peroxisomal enzymes and nicotinamide cofactors in koala liver." *Comp Biochem Physiol C Toxicol Pharmacol* **127**(3): 327-34.

Nguyen, X., M. H. Wang, K. M. Reddy, J. R. Falck and M. L. Schwartzman (1999). "Kinetic profile of the rat CYP4A isoforms: arachidonic acid metabolism and isoform-specific inhibitors." *Am J Physiol* **276**(6 Pt 2): R1691-700.

Nhamburo, P. T., F. J. Gonzalez, O. W. McBride, H. V. Gelboin and S. Kimura (1989). "Identification of a new P450 expressed in human lung: complete cDNA

sequence, cDNA-directed expression, and chromosome mapping." *Biochemistry* **28**(20): 8060-6.

Nishimoto, M., J. E. Clark and B. S. Masters (1993). "Cytochrome P450 4A4: expression in *Escherichia coli*, purification, and characterization of catalytic properties." *Biochemistry* **32**(34): 8863-70.

Noble, M. A., C. S. Miles, S. K. Chapman, D. A. Lysek, A. C. MacKay, G. A. Reid, R. P. Hanzlik and A. W. Munro (1999). "Roles of key active-site residues in flavocytochrome P450 BM3." *Biochem J* **339** (Pt 2): 371-9.

Ohgiya, S., T. Goda, T. Hoshino, T. Kamataki and K. Ishizaki (1997). "Establishment of a novel host, high-red yeast that stably expresses hamster NADPH-cytochrome P450 oxidoreductase: usefulness for examination of the function of mammalian cytochrome P450." *Arch Biochem Biophys* **343**(2): 215-24.

Okita, R. T. and J. R. Okita (2001). "Cytochrome P450 4A fatty acid omega hydroxylases." *Curr Drug Metab* **2**(3): 265-81.

Oliver, C. F., S. Modi, W. U. Primrose, L. Y. Lian and G. C. Roberts (1997). "Engineering the substrate specificity of *Bacillus megaterium* cytochrome P-450 BM3: hydroxylation of alkyl trimethylammonium compounds." *Biochem J* **327** (Pt 2): 537-44.

Omata, Y., R. Dai, S. V. Smith, R. C. Robinson and F. K. Friedman (2000). "Synthetic peptide mimics of a predicted topographical interaction surface: the cytochrome P450 2B1 recognition domain for NADPH-cytochrome P450 reductase." *J Protein Chem* **19**(1): 23-32.

Omata, Y., H. Sakamoto, R. C. Robinson, M. R. Pincus and F. K. Friedman (1994). "Interaction between cytochrome P450 2B1 and cytochrome b5: inhibition by synthetic peptides indicates a role for P450 residues Lys-122 and Arg-125." *Biochem Biophys Res Commun* **201**(3): 1090-5.

Omura, T. (1999). "Forty Years of Cytochrome P450." *Biochemical and Biophysical Research Communications* **266**: 690-698.

Omura, T. and R. Sato (1964a). "The carbon monoxide-binding pigment of liver microsomes. I. Evidence for its hemoprotein nature." *The Journal of Biological Chemistry* **239**(7): 2370-2378.

Omura, T. and R. Sato (1964b). "The carbon monoxide-binding pigment of liver microsomes. II. Solubilization, purification, and properties." *The Journal of Biological Chemistry* **239**(7): 2379-2385.

Ortiz de Montellano, P. R. (1997). Cytochrome P-450. *Molecular Toxicology*. P. D. Josephy. New York, Oxford University Press, Inc.: 209-252.

Ost, T. W., C. S. Miles, A. W. Munro, J. Murdoch, G. A. Reid and S. K. Chapman (2001a). "Phenylalanine 393 exerts thermodynamic control over the heme of flavocytochrome P450 BM3." *Biochemistry* **40**(45): 13421-9.

Ost, T. W., A. W. Munro, C. G. Mowat, P. R. Taylor, A. Pesseguiro, A. J. Fulco, A. K. Cho, M. A. Cheesman, M. D. Walkinshaw and S. K. Chapman (2001b). "Structural and spectroscopic analysis of the F393H mutant of flavocytochrome P450 BM3." *Biochemistry* **40**(45): 13430-8.

Palmer, C. N., K. J. Griffin and E. F. Johnson (1993). "Rabbit prostaglandin omega-hydroxylase (CYP4A4): gene structure and expression." *Arch Biochem Biophys* **300**(2): 670-6.

Parikh, A., E. M. Gillam and F. P. Guengerich (1997). "Drug metabolism by *Escherichia coli* expressing human cytochromes P450." *Nat Biotechnol* **15**(8): 784-8.

Patten, C. J. and P. Koch (1995). "Baculovirus expression of human P450 2E1 and cytochrome b5: spectral and catalytic properties and effect of b5 on the stoichiometry of P450 2E1-catalyzed reactions." *Arch Biochem Biophys* **317**(2): 504-13.

Pikuleva, I. and M. Waterman (1999). "Cytochromes P450 in synthesis of steroid hormones, bile acids, vitamin D3 and cholesterol." *Mol Aspects Med* **20**(1-2): 33-42, 43-37.

Pompon, D., B. Louerat, A. Bronine and P. Urban (1996). "Yeast expression of animal and plant P450s in optimized redox environments." *Methods Enzymol* **272**: 51-64.

Porter, T. D. and J. R. Larson (1991). "Expression of mammalian P450s in *Escherichia coli*." *Methods Enzymol* **206**: 108-16.

Porter, T. D., T. E. Wilson and C. B. Kasper (1987). "Expression of a functional 78,000 dalton mammalian flavoprotein, NADPH-cytochrome P-450 oxidoreductase, in *Escherichia coli*." *Arch Biochem Biophys* **254**(1): 353-67.

Powell, P. K., I. Wolf, R. Jin and J. M. Lasker (1998). "Metabolism of arachidonic acid to 20-hydroxy-5,8,11, 14-eicosatetraenoic acid by P450 enzymes in human liver: involvement of CYP4F2 and CYP4A11." *J Pharmacol Exp Ther* **285**(3): 1327-36.

Powell, P. K., I. Wolf and J. M. Lasker (1996). "Identification of CYP4A11 as the major lauric acid omega-hydroxylase in human liver microsomes." *Arch Biochem Biophys* **335**(1): 219-26.

Pritchard, M. P., R. Ossetian, D. N. Li, C. J. Henderson, B. Burchell, C. R. Wolf and T. Friedberg (1997). "A general strategy for the expression of recombinant human cytochrome P450s in Escherichia coli using bacterial signal peptides: expression of CYP3A4, CYP2A6, and CYP2E1." *Arch Biochem Biophys* **345**(2): 342-54.

R.Lemberg, J. B. (1973). *Cytochromes*. London, Academic Press Inc.

Ravichandran, K. G., S. S. Boddupalli, C. A. Hasermann, J. A. Peterson and J. Deisenhofer (1993). "Crystal structure of hemoprotein domain of P450BM-3, a prototype for microsomal P450's." *Science* **261**(5122): 731-6.

Roman, L. J., C. N. Palmer, J. E. Clark, A. S. Muerhoff, K. J. Griffin, E. F. Johnson and B. S. Masters (1993). "Expression of rabbit cytochromes P4504A which catalyze the omega-hydroxylation of arachidonic acid, fatty acids, and prostaglandins." *Arch Biochem Biophys* **307**(1): 57-65.

Sabourault, C., M. Amichot, D. Pauron, J. B. Berge, M. Lafaurie and J. P. Girard (1999). "Cloning of CYP4F7, a kidney-specific P450 in the sea bass *Dicentrarchus labrax*." *Biochem Biophys Res Commun* **258**(1): 155-61.

Sandhu, P., T. Baba and F. P. Guengerich (1993). "Expression of modified cytochrome P450 2C10 (2C9) in *Escherichia coli*, purification, and reconstitution of catalytic activity." *Arch Biochem Biophys* **306**(2): 443-50.

Saribas, A. S., L. Gruenke and L. Waskell (2001). "Overexpression and purification of the membrane-bound cytochrome P450 2B4." *Protein Expr Purif* **21**(2): 303-9.

Schenkman, J. B. and I. Jansson (1999). "Interactions between cytochrome P450 and cytochrome b5." *Drug Metab Rev* **31**(2): 351-64.

Scott, J. G. (1999). "Cytochromes P450 and insecticide resistance." *Insect Biochemistry and Molecular Biology* **29**: 757-777.

Shen, A. L., T. D. Porter, T. E. Wilson and C. B. Kasper (1989). "Structural analysis of the FMN binding domain of NADPH-cytochrome P-450 oxidoreductase by site-directed mutagenesis." *J Biol Chem* **264**(13): 7584-9.

Shet, M., C. W. Fisher, P. L. Holmans and R. W. Estabrook (1996). "The omega-hydroxylation of lauric acid: oxidation of 12-hydroxylauric acid to dodecanedioic acid by a purified recombinant fusion protein containing P450 4A1 and NADPH-P450 reductase." *Arch Biochem Biophys* **330**(1): 199-208.

Shet, M. S., C. W. Fisher and R. W. Estabrook (1997). "The function of recombinant cytochrome P450s in intact *Escherichia coli* cells: the 17 alpha-hydroxylation of progesterone and pregnenolone by P450c17." *Arch Biochem Biophys* **339**(1): 218-25.

Simpson, A. E. (1997). "The cytochrome P450 4 (CYP4) family." *Gen Pharmacol* **28**(3): 351-9.

Smith, G., M. J. Stubbins, L. W. Harris and C. R. Wolf (1998). "Molecular genetics of the human cytochrome P450 monooxygenase superfamily." *Xenobiotica* **28**(12): 1129-1165.

Soucek, P. (1999). "Expression of cytochrome P450 2A6 in Escherichia coli: purification, spectral and catalytic characterization, and preparation of polyclonal antibodies." *Arch Biochem Biophys* **370**(2): 190-200.

Stayton, P. S., T. L. Poulos and S. G. Sligar (1989). "Putidaredoxin competitively inhibits cytochrome b5-cytochrome P-450cam association: a proposed molecular model for a cytochrome P-450cam electron-transfer complex." *Biochemistry* **28**(20): 8201-5.

Stegeman, J. J. and D. R. Livingstone (1998). "Forms and functions of cytochrome P450." *Comparative Biochemistry and Physiology Part C* **121**: 1-3.

Strittmatter, P., P. Fleming, M. Connors and D. Corcoran (1978). "Purification of cytochrome b5." *Methods Enzymol* **52**: 97-101.

Strobel, H. W. and J. D. Dignam (1978). "Purification and properties of NADPH-cytochrome P-450 reductase." *Methods Enzymol* **52**: 89-96.

Stromstedt, M., S. Hayashi, P. G. Zaphiropoulos and J. A. Gustafsson (1990). "Cloning and characterization of a novel member of the cytochrome P450 subfamily IVA in rat prostate." *DNA Cell Biol* **9**(8): 569-77.

Studier, F. W., A. H. Rosenberg, J. J. Dunn and J. W. Dubendorff (1990). "Use of T7 RNA polymerase to direct expression of cloned genes." *Methods Enzymol* **185**: 60-89.

- Sueyoshi, T., L. J. Park, R. Moore, R. O. Juvonen and M. Negishi (1995). "Molecular engineering of microsomal P450 2a-4 to a stable, water-soluble enzyme." *Arch Biochem Biophys* **322**(1): 265-71.
- Tamburini, P. P., R. E. White and J. B. Schenkman (1985). "Chemical characterization of protein-protein interactions between cytochrome P-450 and cytochrome b5." *J Biol Chem* **260**(7): 4007-15.
- Truan, G. and J. A. Peterson (1998). "Thr268 in substrate binding and catalysis in P450BM-3." *Arch Biochem Biophys* **349**(1): 53-64.
- van der Weide, J. and L. S. Steijns (1999). "Cytochrome P450 enzyme system: genetic polymorphisms and impact on clinical pharmacology." *Ann Clin Biochem* **36** (Pt 6): 722-9.
- Wang, M. H., H. Guan, X. Nguyen, B. A. Zand, A. Nasjletti and M. Laniado-Schwartzman (1999). "Contribution of cytochrome P-450 4A1 and 4A2 to vascular 20-hydroxyeicosatetraenoic acid synthesis in rat kidneys." *Am J Physiol* **276**(2 Pt 2): F246-53.
- Wang, M. H., D. E. Stec, M. Balazy, V. Mastuyugin, C. S. Yang, R. J. Roman and M. L. Schwartzman (1996). "Cloning, sequencing, and cDNA-directed expression of the rat renal CYP4A2: arachidonic acid omega-hydroxylation and 11,12-epoxidation by CYP4A2 protein." *Arch Biochem Biophys* **336**(2): 240-50.
- Wang, M. H., F. Zhang, J. Marji, B. A. Zand, A. Nasjletti and M. Laniado-Schwartzman (2001). "CYP4A1 antisense oligonucleotide reduces mesenteric
-

vascular reactivity and blood pressure in SHR." *Am J Physiol Regul Integr Comp Physiol* **280**(1): R255-61.

Williams, P. A., J. Cosme, V. Sridhar, E. F. Johnson and D. E. McRee (2000a). "Mammalian microsomal cytochrome P450 monooxygenase: structural adaptations for membrane binding and functional diversity." *Mol Cell* **5**(1): 121-31.

Williams, P. A., J. Cosme, V. Sridhar, E. F. Johnson and D. E. McRee (2000b). "Microsomal cytochrome P450 2C5: comparison to microbial P450s and unique features." *J Inorg Biochem* **81**(3): 183-90.

Wu, Y., Y. Wang, C. Qian, J. Lu, E. Li, W. Wang, Y. Xie, J. Wang, D. Zhu, Z. Huang and W. Tang (2001). "Solution structure of cytochrome b(5) mutant (E44/48/56A/D60A) and its interaction with cytochrome c." *Eur J Biochem* **268**(6): 1620-30.

Yamazaki, H., W. W. Johnson, Y. F. Ueng, T. Shimada and F. P. Guengerich (1996). "Lack of electron transfer from cytochrome b5 in stimulation of catalytic activities of cytochrome P450 3A4. Characterization of a reconstituted cytochrome P450 3A4/NADPH-cytochrome P450 reductase system and studies with apo-cytochrome b5." *J Biol Chem* **271**(44): 27438-44.

Yamazaki, H., T. Shimada, M. V. Martin and F. P. Guengerich (2001). "Stimulation of cytochrome P450 reactions by apo-cytochrome b5: evidence against transfer of heme from cytochrome P450 3A4 to apo-cytochrome b5 or heme oxygenase." *J Biol Chem* **276**(33): 30885-91.

Yokotani, N., E. Kusunose, K. Sogawa, H. Kawashima, M. Kinoshita, M. Kusunose and Y. Fujii-Kuriyama (1991). "cDNA cloning and expression of the mRNA for cytochrome P-450kd which shows a fatty acid omega-hydroxylating activity." *Eur J Biochem* **196**(3): 531-6.

Yoo, M. and A. W. Steggles (1988). "The complete nucleotide sequence of human liver cytochrome b5 mRNA." *Biochem Biophys Res Commun* **156**(1): 576-80.

Zheng, Y. M., M. B. Fisher, N. Yokotani, Y. Fujii-Kuriyama and A. E. Rettie (1998). "Identification of a meander region proline residue critical for heme binding to cytochrome P450: implications for the catalytic function of human CYP4B1." *Biochemistry* **37**(37): 12847-51.